

Quantum information with Rydberg atoms

M. Saffman and T. G. Walker

Department of Physics, University of Wisconsin, 1150 University Avenue, Madison, Wisconsin 53706, USA

K. Mølmer

Lundbeck Foundation Theoretical Center for Quantum System Research, Department of Physics and Astronomy, University of Aarhus, DK-8000 Århus C, Denmark

(Published 18 August 2010)

Rydberg atoms with principal quantum number $n \gg 1$ have exaggerated atomic properties including dipole-dipole interactions that scale as n^4 and radiative lifetimes that scale as n^3 . It was proposed a decade ago to take advantage of these properties to implement quantum gates between neutral atom qubits. The availability of a strong long-range interaction that can be coherently turned on and off is an enabling resource for a wide range of quantum information tasks stretching far beyond the original gate proposal. Rydberg enabled capabilities include long-range two-qubit gates, collective encoding of multiqubit registers, implementation of robust light-atom quantum interfaces, and the potential for simulating quantum many-body physics. The advances of the last decade are reviewed, covering both theoretical and experimental aspects of Rydberg-mediated quantum information processing.

DOI: [10.1103/RevModPhys.82.2313](https://doi.org/10.1103/RevModPhys.82.2313)

PACS number(s): 03.67.–a, 32.80.Ee, 33.80.Rv, 42.50.Ct

CONTENTS

I. Introduction	2313	D. Ensemble gates and error correction	2345
A. Rydberg-mediated quantum gates	2314	1. Single qubit gates	2345
B. Rydberg coupled ensembles	2315	2. Two-qubit gates	2345
II. Rydberg Atoms and Their Interactions	2317	3. Error correction	2346
A. Properties of Rydberg atoms	2317	E. A 1000-bit collectively encoded computer	2346
B. From Förster to van der Waals	2319	F. Many-particle entanglement	2347
C. Angular dependence	2321	1. Spin squeezing	2347
D. Tuning the interaction with external fields	2322	2. GHZ states	2348
E. Three-body Förster interactions	2323	VI. Rydberg-Excited Ensembles and Quantum Optical Effects	2349
III. Rydberg Gates	2323	A. Nonlinear and quantum optics in atomic ensembles	2349
A. Blockade interaction	2323	1. Optical and electric control of transmission properties of an atomic ensemble	2349
B. Two-atom blockade gate	2324	B. Light-atom quantum interfaces with Rydberg blockade	2350
C. Alternative gate protocols	2325	1. Cooperative emission of single photons	2350
1. Interaction gates	2325	C. Quantum communication protocols	2352
2. Interference gates	2327	D. Hybrid qubit interfaces with Rydberg atoms	2353
3. Amplitude swap gates	2327	E. Rydberg atoms and alternative quantum computing paradigms	2353
4. Other approaches	2328	VII. Summary and Outlook	2354
D. Scalability of a Rydberg gate quantum computer	2328	Acknowledgments	2355
IV. Experiments	2330	References	2355
A. Experimental techniques	2330		
1. Traps for ground-state atoms	2330		
2. Traps for Rydberg atoms	2331		
B. Coherent excitation of Rydberg states	2332		
C. Two-atom blockade, two-qubit gates, and entanglement	2335		
V. Collective Effects in Rydberg Coupled Ensembles	2337		
A. Blockade scaling laws in extended samples	2337		
1. Suppression of optical Rydberg excitation	2338		
2. Blockade effects on excitation dynamics	2339		
3. Sub-Poissonian atom excitation	2340		
4. Modeling of ensemble blockade	2340		
B. Preparation of single-atom states	2341		
C. Collective qubit encoding	2342		

I. INTRODUCTION

The field of quantum information processing is currently attracting intense interest. This is fueled by the promise of applications and by rapid experimental progress. The most advanced experimental demonstrations at this time include trapped ions (Blatt and Wineland, 2008), linear optics (Kok *et al.*, 2007), superconductors (Clarke and Wilhelm, 2008; DiCarlo *et al.*, 2009), and quantum dots in semiconductors (Li *et al.*, 2003; Petta *et al.*, 2005; Barthel *et al.*, 2009). Trapped ion qubits have reached the most advanced state of sophistication

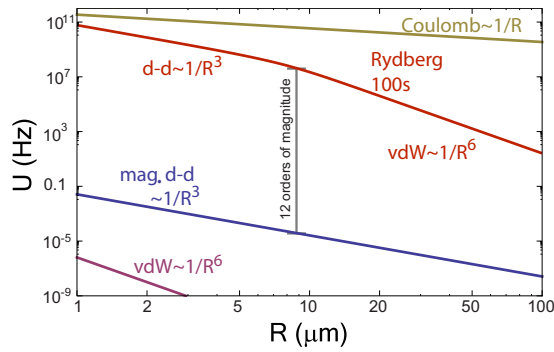


FIG. 1. (Color online) Two-body interaction strength for ground-state Rb atoms, Rb atoms excited to the 100s level, and ions.

and have been used to demonstrate high fidelity gates and small algorithms (Blatt and Wineland, 2008). Neutral atom qubits represent another promising approach (Bloch, 2008). They share many features in common with trapped ion systems including long-lived encoding of quantum information in atomic hyperfine states and the possibility of manipulating and measuring the qubit state using resonant laser pulses.

Neutral atoms distinguish themselves from ions when we consider their state dependent interaction properties, which are essential for implementing two-qubit quantum gates. Figure 1 shows the dependence of the two-particle interaction strength on separation R for singly charged ions, ground-state neutral atoms, and Rydberg atoms. The interaction of ground-state atoms is dominated by $1/R^6$ van der Waals forces at short range and $1/R^3$ magnetic dipole-dipole forces beyond about 30 nm. At spacings greater than $1 \mu\text{m}$ the interaction is weak, less than 1 Hz in frequency units, which implies that an array of neutral atom qubits can be structurally stable. On the other hand, excitation of Rb atoms to the 100s Rydberg level results in a very strong interaction that has resonant dipole-dipole character, scaling as $1/R^3$, at short distances and van der Waals character, scaling as $1/R^6$, at long distances. As will be discussed in Sec. II the characteristic length scale R_c where the Rydberg interaction changes character depends on the principal quantum number n . For the 100s state the crossover length is close to $R_c = 9.5 \mu\text{m}$, and at this length scale the ratio of the Rydberg interaction to the ground-state interaction is approximately 10^{12} .

The applicability of Rydberg atoms for quantum information processing, which is the central topic of this review, can be traced to the fact that the two-atom interaction can be turned on and off with a contrast of 12 orders of magnitude. The ability to control the interaction strength over such a wide range appears unique to the Rydberg system. We may compare this with trapped ions whose Coulomb interaction is much stronger but is always present. The strong Coulomb interaction is beneficial for implementing high fidelity gates (Benhelm *et al.*, 2008b) but the always on character of the interaction makes the task of establishing a many-qubit register ap-

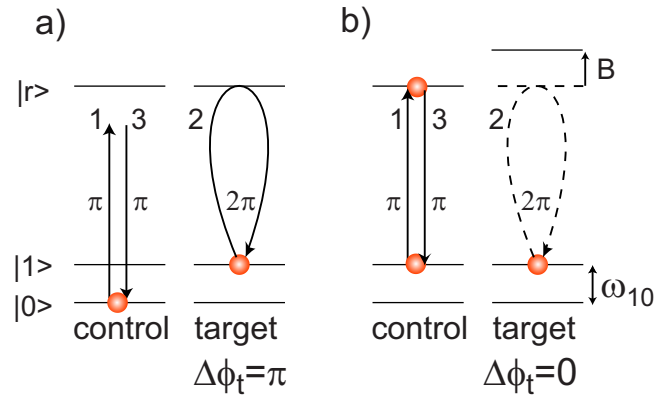


FIG. 2. (Color online) Rydberg blockade controlled phase gate operating on input states (a) $|01\rangle$ and (b) $|11\rangle$. Quantum information is stored in the basis states $|0\rangle$, $|1\rangle$ and state $|1\rangle$ is coupled to a Rydberg level $|r\rangle$ with excitation Rabi frequency Ω . The controlled phase gate is implemented with a three pulse sequence: (1) π pulse on control atom $|1\rangle \rightarrow |r\rangle$, (2) 2π pulse on target atom $|1\rangle \rightarrow |r\rangle \rightarrow |1\rangle$, and (3) π pulse on control atom $|r\rangle \rightarrow |1\rangle$. (a) The case where the control atom starts in $|0\rangle$ and is not Rydberg excited so there is no blockade. (b) The case where the control atom is in $|1\rangle$ which is Rydberg excited leading to blockade of the target atom excitation.

pear more difficult than it may be for an array of weakly interacting neutral atoms. Several approaches to scalability in trapped ion systems are being explored including the development of complex multizone trap technologies (Seidelin *et al.*, 2006) and anharmonic traps (Lin *et al.*, 2009). We note that some of the attractive features of Rydberg-mediated interactions may also be applicable to trapped ion systems (Müller *et al.*, 2008).

A. Rydberg-mediated quantum gates

The idea of using dipolar Rydberg interactions for neutral atom quantum gates was introduced in 2000 (Jaksch *et al.*, 2000) and quickly extended to a mesoscopic regime of many-atom ensemble qubits (Lukin *et al.*, 2001). The basic idea of the Rydberg blockade two-qubit gate is shown in Fig. 2. When the initial two-atom state is $|01\rangle$ [Fig. 2(a)] the control atom is not coupled to the Rydberg level and the target atom picks up a π phase shift. When the initial state is $|11\rangle$ both atoms are coupled to the Rydberg level. In the ideal case when the two-atom “blockade” shift B due to the Rydberg interaction is large compared to the excitation Rabi frequency Ω , excitation of the target atom is blocked and it picks up no phase shift. The evolution matrix expressed in the computational basis $\{|00\rangle, |01\rangle, |10\rangle, |11\rangle\}$ is

$$U = \begin{pmatrix} 1 & 0 & 0 & 0 \\ 0 & -1 & 0 & 0 \\ 0 & 0 & -1 & 0 \\ 0 & 0 & 0 & -1 \end{pmatrix}, \quad (1)$$

which is a controlled-Z (C_Z) gate. As is well known (Nielsen and Chuang, 2000) the C_Z gate can be readily

converted into a controlled-NOT (CNOT) gate by including $\pi/2$ rotations between $|0\rangle \leftrightarrow |1\rangle$ on the target atom before and after the interaction. The CNOT gate together with single-qubit operations form a set of universal gates for quantum computing (Nielsen and Chuang, 2000).

If the Rydberg levels $|r\rangle$ were stable, the approach of Fig. 2 would enable gates with arbitrarily high fidelity. Rydberg states of real atoms have a finite lifetime τ due to radiative decay. This leads to a tradeoff between fast excitation which minimizes spontaneous emission and slow excitation which maximizes blockade effectiveness. We show in Sec. IV.C that the minimum error E of the blockade gate scales as (Saffman and Walker, 2005a) $E \sim 1/(\mathcal{B}\tau)^{2/3}$ and also analyze the performance of several alternative Rydberg-based gate protocols. We show that a demonstration of gates with errors below $E=0.001$ appears to be a realistic goal.

The blockade concept, while not the only means of performing Rydberg-mediated quantum information processing, is attractive for several reasons. First, the gate fidelity is to first order independent of the blockade shift in the limit of large shifts. It is therefore not necessary to control the value of the blockade shift, beyond ensuring that it is sufficiently large. Second, the fidelity of the entanglement protocol depends only weakly on the center of mass atomic motion so that sub-Doppler temperatures at the level of $\sim 50 \mu\text{K}$ are sufficient for a high fidelity quantum gate (Saffman and Walker, 2005a). Undesired entanglement with external motional degrees of freedom is thereby suppressed. Third, the interactions are of sufficiently long range to allow gates between optically resolvable atoms without having to physically move them from place to place.

Numerous alternative proposals exist for two-atom quantum gates including short-range dipolar interactions (Brennen *et al.*, 1999), ground-state collisions (Jaksch *et al.*, 1999), coupling of atoms to photons (Pellizzari *et al.*, 1995), magnetic dipole-dipole interactions (You and Chapman, 2000), optically controlled dipolar interactions (Lukin and Hemmer, 2000), and gates with delocalized qubits (Mompert *et al.*, 2003). Many-particle entanglement mediated by collisional interactions has been observed in optical lattice based experiments (Mandel *et al.*, 2003; Anderlini *et al.*, 2007), but to date only the Rydberg interaction has been successfully applied to demonstration of a quantum gate between two neutral atoms. We note that the Rydberg blockade gate is inherently optimized for MHz-rate gate operations, a significant advantage compared to alternative neutral atom quantum gate proposals.

In experiments described in Sec. IV it is shown that coherent excitation and deexcitation of single ground-state atoms to Rydberg levels is feasible (Johnson *et al.*, 2008) and that Rydberg blockade can be observed between two atoms in spatially separated volumes (Gaëtan *et al.*, 2009; Urban, Johnson, *et al.*, 2009). The most recent experiments in Madison and Palaiseau (Isenhower *et al.*, 2010; Wilk *et al.*, 2010) have shown that the blockade interaction can be used to implement a two-qubit CNOT gate and to create entanglement between pairs of

atoms. As discussed in Sec. IV.C these initial demonstrations generated relatively weak entanglement and suffered from excess atom loss. Nevertheless it is realistic to expect significant improvements in the next few years, as experimental techniques are further refined.

In this review we focus on phenomena that involve quantum states stored in ground hyperfine levels of cold trapped atoms. Interactions between atoms rely on transient excitation of atom pairs to low angular momentum Rydberg states using laser fields. There is never any long term storage of information in the Rydberg levels. There is also an alternative approach to coherent quantum dynamics that utilizes strong coupling between Rydberg atoms and microwave photons inside high finesse resonators (Raimond *et al.*, 2001; Walther *et al.*, 2006). In this cavity quantum electrodynamics (CQED) approach relatively long-lived microwave cavity fields may be thought of as qubits, with moving atoms serving both to couple the qubits and to control the preparation of nonclassical field states (Bernu *et al.*, 2008). Direct interaction between the atoms is never invoked.

A series of experiments elucidating the interaction between single atoms and single photons (Guerlin *et al.*, 2007) and leading to the creation of two-atom entanglement (Hagley *et al.*, 1997) have been performed using so-called “circular” Rydberg states with maximal magnetic quantum number $|m|=n-1$. These states have radiative lifetimes that are close to 1000 times longer than low angular momentum states of the same n . The long coherence times together with the large dipole moments between states of neighboring n have enabled creation of atom-photon entanglement by shooting Rydberg atoms through microwave cavities. Introducing several atoms sequentially allows atom-photon entanglement to be mapped onto atom-atom entanglement (Hagley *et al.*, 1997) despite the fact that the atoms have no direct interaction.

The Rydberg CQED approach is quite complementary to the approach based on trapped atoms we focus on in this review. In the CQED experiments the stationary qubits are microwave field states, and two-qubit interactions are mediated by strong coupling between microwave fields and long-lived circular Rydberg states. In contrast the trapped atom approach uses long-lived hyperfine qubits and direct interaction of relatively short-lived Rydberg states to mediate the coupling between hyperfine qubits. Nevertheless it is quite possible that future developments will lead to a synthesis of elements of both approaches. There are ideas for trapping the circular states (Hyafil *et al.*, 2004) which, if combined with the direct interaction approach, could lead to excellent gate fidelities due to the very large values of τ .

B. Rydberg coupled ensembles

The blockade gate of Fig. 2 operates between two individual atoms. However, Lukin *et al.* (2001) showed that this can be directly extended to ensemble qubits, each consisting of N atoms. The extension relies on the concept of collective Rydberg blockade whereby excitation

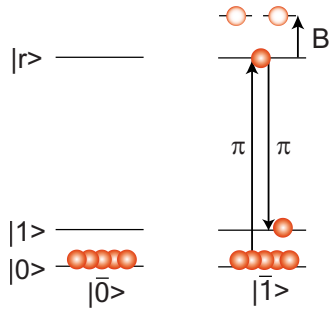


FIG. 3. (Color online) Ensemble qubits and rotations between the logical basis states $\{|\bar{0}\rangle, |\bar{1}\rangle\}$. Double excitation of the state $|1\rangle$ is prevented by the two-atom shift B .

of a single atom to a Rydberg state can block the subsequent excitation of not just one but a large number of atoms within the surrounding volume. As shown in Fig. 3 the blockade effect allows us to manipulate ensemble qubits in a straightforward manner. We define an N atom logical 0 by $|\bar{0}\rangle = \prod_{i=1}^N |0_i\rangle$ and a logical 1 by the symmetric singly excited state $|\bar{1}\rangle = \frac{1}{\sqrt{N}} \sum_{i=1}^N |0 \cdots 1_i \cdots 0\rangle$. Single-qubit rotations in the logical basis $\{|\bar{0}\rangle, |\bar{1}\rangle\}$ are performed with sequential two-photon transitions via the Rydberg level $|r\rangle$ as shown in Fig. 3. Provided the blockade shift B is sufficiently large double excitation is prevented and we have a closed two-level system with the collectively enhanced Rabi frequency $\Omega_N = \sqrt{N}\Omega$. Two-qubit gates can then be performed between two ensemble qubits or between a single atom and an ensemble qubit in a fashion that is completely analogous to the single-atom protocol of Fig. 2. It is also possible to create higher-order collective excitation of the state $|1\rangle$ using sequential pulses with tailored Rabi frequencies coupling $|0\rangle \rightarrow |r\rangle$ and $|r\rangle \rightarrow |1\rangle$. Such states are of interest for the generation of multiphoton wave packets (Lukin *et al.*, 2001; Nielsen and Mølmer, 2010).

A requirement for the validity of the ensemble qubit picture is that a blockade interaction is present for all atoms in the ensemble (Lukin *et al.*, 2001). The probability of unwanted double excitation is determined by the off-resonant excitation to the doubly excited states that are shifted by an amount B due to the blockade effect. In the limit of strong blockade, the probability of double excitation is

$$P_2 = \frac{N-1}{N} \frac{\Omega_N^2}{2B^2}, \quad (2)$$

where the blockade shift is (Walker and Saffman, 2008)

$$\frac{1}{B^2} = \frac{2}{N(N-1)} \sum_{\varphi} \sum_{i < j} \frac{|\kappa_{\varphi ij}|^2}{\Delta_{\varphi ij}^2}. \quad (3)$$

Since there are generally a number of possible doubly excited states $|\varphi\rangle$ for atoms i and j , Eq. (2) depends on the dipole-dipole energy shift $\Delta_{\varphi ij}$ of each state, and on the associated Rabi coupling for exciting a pair of atoms to state $|\varphi\rangle$, parametrized by the dimensionless factor

$\kappa_{\varphi ij}$. Equation (3) shows that the blockade shift is dominated by the weakest possible atom-atom interactions; in an electrical circuit analogy the blockade shift can be thought of as an impedance B^2 that is formed by a parallel network of individual impedances, each of size $\sim (N^2/2)[\sum_{i < j} |\kappa_{\varphi ij}|^2 / \Delta_{\varphi ij}^2]^{-1}$. Weak blockade on any atom-pair state $|\varphi\rangle$ permits efficient two-atom excitation and acts to short circuit the effectiveness of the blockade process. A detailed accounting for the multitude of doubly excited states and their interactions is therefore crucial to achieving a strong N atom blockade. We review the relevant Rydberg physics in Sec. II and derive Eqs. (2) and (3) in Sec. III.A.

The powerful idea of Rydberg blockade has led to a large amount of theoretical and experimental work and has been further developed far beyond the original proposals (Jaksch *et al.*, 2000; Lukin *et al.*, 2001). Promising ideas exist for such disparate tasks as deterministic single-atom loading (Saffman and Walker, 2002), spin squeezing of atomic ensembles (Bouchoule and Mølmer, 2002), collective encoding of many-qubit registers (Brion, Mølmer, and Saffman, 2007; Saffman and Mølmer, 2008), nonlocal gates by coupling to microwave resonators (Sørensen *et al.*, 2004; Petrosyan and Fleischhauer, 2008), and long-distance entanglement and quantum communication (Saffman and Walker, 2002, 2005b; Pedersen and Mølmer, 2009). Rydberg blockade has also been proposed as a means of generating many-particle entanglement (Unanyan and Fleischhauer, 2002; Møller *et al.*, 2008; Müller *et al.*, 2009; Saffman and Mølmer, 2009) as well as a basis for dissipative quantum many-body simulations (Weimer *et al.*, 2010).

The difficulty of achieving perfect blockade has stimulated renewed theoretical interest in the classical problem of the structure and strength of the dipole-dipole interaction between atoms in excited states (Gallagher, 1994; Gallagher and Pillet, 2008). Recent work has elucidated the transition from a near-resonant $1/R^3$ Förster interaction (Förster, 1948) at short range to a long range $1/R^6$ van der Waals interaction (Protsenko *et al.*, 2002; Li *et al.*, 2005; Walker and Saffman, 2005). In addition it was found that pairs of atoms can couple to noninteracting “Förster zero states” which evade the Rydberg blockade (Walker and Saffman, 2005, 2008) unless special care is taken in the choice of atomic states and relative orientation. However, the physics of Rydberg blockade turns out to be subtle and contains some unexpected twists. For example, recent work showed (Pohl and Beraman, 2009) that the addition of a third atom can create a noninteracting zero state that can be accessed by a weak three-photon excitation even when the two-photon excitation is well blocked (see Sec. II.E). Advances in the theoretical description of Rydberg blockade in many-atom samples are reviewed in Sec. V.

In parallel with the theoretical developments there has been a great deal of experimental activity in the field. Experiments performed in the early 1980s with atomic beams provided the first direct observations of many-body Rydberg interaction effects (Raimond *et al.*, 1981; Safinya *et al.*, 1981; Gallagher *et al.*, 1982). Using

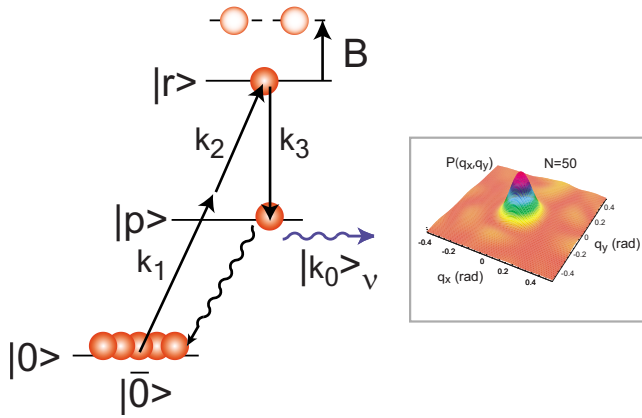


FIG. 4. (Color online) Preparation of the symmetric singly excited state (4). Radiative decay of this state produces a photon in the phase matched direction \mathbf{k}_0 as shown in the inset for $N=50$ atoms. Adapted from Saffman and Walker, 2002.

modern cold atom techniques a number of recent experiments have reported the observation of excitation suppression due to Rydberg interactions in small dense samples (Singer *et al.*, 2004; Tong *et al.*, 2004; Cubel Liebisch *et al.*, 2005; Afrousheh *et al.*, 2006; Vogt *et al.*, 2006; van Ditzhuijzen *et al.*, 2008) and collective effects in coherent excitation (Cubel *et al.*, 2005; Heidemann *et al.*, 2007, 2008; Raitzsch *et al.*, 2008; Reetz-Lamour, Amthor, *et al.*, 2008; Reetz-Lamour, Deiglmayr, *et al.*, 2008). Other recent work has explored novel quantum and nonlinear optical effects due to interaction of light with Rydberg excited samples including superradiance (Wang *et al.*, 2007; Day *et al.*, 2008), electromagnetically induced transparency (Mohapatra *et al.*, 2007; Bason *et al.*, 2008; Weatherill *et al.*, 2008; Pritchard *et al.*, 2009), and four-wave mixing (Brekke *et al.*, 2008). These experiments, reviewed in Secs. V and VI, have shown the existence of long-range Rydberg interactions, and in some cases signatures of blockade, but have not yet reached the strong blockade regime of only a single atomic excitation that is crucial for quantum information applications of ensemble qubits.

Part of the current interest in Rydberg coupled ensembles stems from their use for creating a light-atom quantum interface and long-distance entanglement. It was recognized early on that Rydberg blockade could be used to deterministically create symmetric entangled states with unit excitation (Lukin *et al.*, 2001) and with controllable emission characteristics (Saffman and Walker, 2002). The basic idea is shown in Fig. 4 where a multiphoton excitation is used to prepare an ensemble in the state

$$|\Psi_0\rangle = \frac{1}{\sqrt{N}} \sum_{j=1}^N e^{i\mathbf{k}_0 \cdot \mathbf{r}_j} |p_j\rangle \otimes |0\rangle_\nu. \quad (4)$$

Here $|p_j\rangle \equiv |0 \cdots p_j \cdots 0\rangle$ is shorthand for the state with atom j at position \mathbf{r}_j excited, the other atoms in their ground state $|0\rangle$, and $|0\rangle_\nu$ is the vacuum state of the photon field. This state, containing a single excitation collectively shared among the atoms, with a position-

dependent complex phase is prepared with three laser fields. The first two with wave vectors $\mathbf{k}_1, \mathbf{k}_2$ drive a resonant excitation into a Rydberg state, where the blockade interaction prevents transfer of more than a single atom. A resonant π pulse with wave vector \mathbf{k}_3 hereafter drives the atomic excitation into the excited state $|p\rangle$, producing the state (4) with $\mathbf{k}_0 = \mathbf{k}_1 + \mathbf{k}_2 - \mathbf{k}_3$. As discussed in Sec. VI spontaneous decay of this state preferentially creates

$$|\Psi\rangle = |\bar{0}\rangle \otimes |\mathbf{k}_0\rangle_\nu, \quad (5)$$

with all atoms in the ground state and a photon emitted at the phase-matched wave vector \mathbf{k}_0 .

The use of Rydberg blockade is significant since it would provide deterministic ensemble preparation and single-photon generation without the requirement of a deterministic single-photon source which is otherwise needed to remove the probabilistic character of non-blockade based schemes (Duan *et al.*, 2001). In Sec. VI we discuss the use of Rydberg-mediated light-atom interfaces for applications such as single photon on demand generation and entanglement generation between remote ensembles (Saffman and Walker, 2005b; Pedersen and Mølmer, 2009).

In the remainder of this review we expand upon the topics discussed above, presenting a comprehensive picture of the current theoretical and experimental state of the field of Rydberg-mediated quantum information processing. We conclude in Sec. VII with a summary and outlook for the future.

II. RYDBERG ATOMS AND THEIR INTERACTIONS

As described in the Introduction, the success of blockade for quantum manipulation of atoms at large distances depends on the interactions between the atoms in their Rydberg states. In this section we review the relevant Rydberg physics. Here and in the rest of the paper apart from Sec. VE, we exclusively discuss the situation for the heavy alkali atoms Rb and Cs. The alkalis in general are the most convenient elements for laser cooling, and the heavy alkalis are best suited for qubit encoding due to the large hyperfine splittings in the excited manifolds of the first resonance lines, which facilitates qubit measurements by light scattering.

A. Properties of Rydberg atoms

The properties of Rydberg atoms are reviewed in several books (Stebbins and Dunning, 1983; Gallagher, 1994) and also in some recent reviews (Choi *et al.*, 2007; Gallagher and Pillet, 2008). We consider here those elements of most importance for current blockade experiments, emphasizing low angular momentum states that are readily accessible via optical excitation from the atomic ground state. In the absence of perturbing fields, the energy levels are represented by quantum numbers n, l, s , and j denoting the traditional principal, orbital

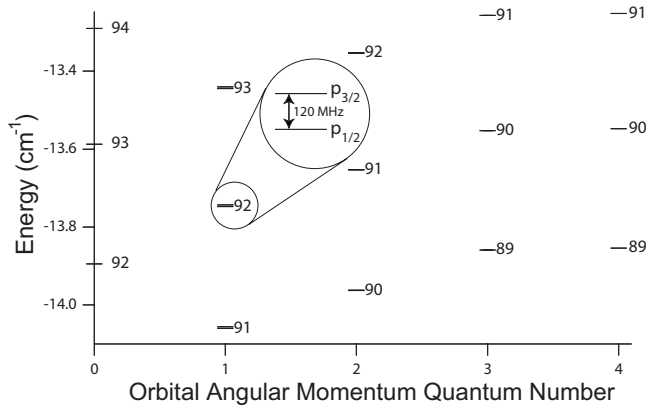


FIG. 5. Energy levels of Rb Rydberg states near $n=90$.

angular momentum, spin angular momentum, and total angular momentum quantum numbers. The energy levels are accurately represented by

$$E_{nlj} = -\frac{\text{Ry}}{[n - \delta_{lj}(n)]^2}, \quad (6)$$

where $\text{Ry} = 109\,737.315\,685\text{ cm}^{-1}$ is the Rydberg constant and the quantum defect $\delta_{lj}(n)$ is a slowly varying function of the principal quantum number. The quantum defect is closely related to the scattering phase shift for low energy electron-ion scattering (Fano and Rau, 1986). With the exception of low-lying s states, hyperfine interactions are generally negligible.

High fidelity entanglement at large interatomic separations necessarily involves MHz scale operations due to the finite lifetime of Rydberg levels. Viewed at MHz resolution, the fine-structure splitting is large in the p and d states of the heavy alkalis up to $n=100$, while the f state fine-structure levels are resolved below about $n=50$. A portion of the Rb Rydberg energy level structure around $n=90$ is shown in Fig. 5. The energy level structure of Rb and Cs has recently been discussed by Walker and Saffman (2008).

The wave functions of Rydberg states $|nljm_j\rangle = P_{nl}(r)|ljm_j\rangle/r$ can be conveniently calculated from quantum-defect theory (Seaton, 1958) using hypergeometric functions available in most numerical libraries. The radial matrix elements

$$\langle r \rangle_{nl}^{n'l'} = \int r P_{n'l'}(r) P_{nl}(r) dr \quad (7)$$

are of particular importance because they govern the interaction of the Rydberg atoms with both external and internal electric fields that shift the atomic energy levels. These matrix elements can be calculated by numerical integration of the quantum-defect wave functions by numerical integration directly from model potentials (Marinescu *et al.*, 1994) or, perhaps most conveniently, using analytical formulas derived by a semiclassical WKB analysis (Kaulakys, 1995).

The radial matrix elements for dipole allowed transitions with $l' = l \pm 1$ between states with $n \gg 1$ are dominated by transitions between the states with the closest

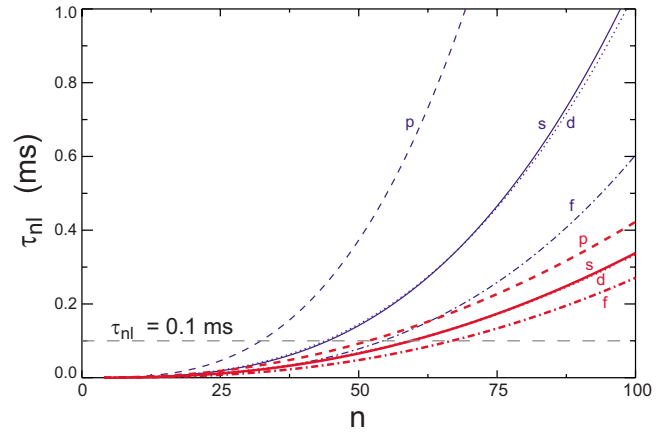


FIG. 6. (Color online) Excited-state lifetimes due to radiative decay for $T=0$ and $T=300\text{ K}$ for s , p , d , and f states of Rb. From Saffman and Walker, 2005a.

eigenenergies and hence similar radial wave functions. These largest matrix elements are generally of order $(0.5-1.5)n^2 a_0$, with a_0 the Bohr radius. For example, the matrix elements from $nl=90d$ to $(91p, 92p, 89f, 88f)$ in Rb are $(1.3, 0.76, 1.3, 0.80)n^2 a_0$; the matrix elements to all other states are less than $0.17n^2 a_0$. Thus in most situations the electric field shifts (for small fields) and the interatomic potentials can be understood by focusing on the effects of the two (for s states) or four neighboring $l \pm 1$ energy levels.

The radiative and blackbody lifetimes of the low angular momentum Rydberg states (Gallagher, 1994) set fundamental limits on the fidelity of coherent operations. If the 0 K lifetime is $\tau_{nl}^{(0)}$, the finite temperature lifetime is

$$\frac{1}{\tau_{nl}} = \frac{1}{\tau_{nl}^{(0)}} + \frac{1}{\tau_{nl}^{(\text{bb})}}, \quad (8)$$

where $\tau_{nl}^{(\text{bb})}$ is the finite temperature blackbody contribution. The 0 K radiative lifetime can be parametrized by (Gounand, 1979)

$$\tau_{nl}^{(0)} = \tau_l^{(0)} (n^*)^{\alpha_l}, \quad (9)$$

with constants enumerated by Gallagher (1994). For all the alkalis $\alpha_l \approx 3$. For large n the blackbody rate can be given as (Gallagher, 1994)

$$\frac{1}{\tau_{nl}^{(\text{bb})}} = \frac{4\alpha^3 k_B T}{3\hbar n^2}, \quad (10)$$

where α is the fine-structure constant. Equation (10) includes transitions to continuum states so that it accounts for blackbody induced photoionization. Both blackbody transfer and ionization have recently been considered by Beterov *et al.* (2007, 2009). Figure 6 shows the radiative lifetime for low- l states of Rb. We see that for $n > 50$ the s , p , d , and f states have lifetimes greater than about $50\ \mu\text{s}$ at room temperature. Thus, for high fidelity Rydberg manipulations, it is necessary to use MHz-scale operations.

The large dipole matrix elements also imply that Rydberg states are extremely sensitive to small low-frequency electric fields. This may be a problem or a feature for coherent optical manipulation. On the one hand, this sensitivity requires that electric fields be well controlled to avoid frequency fluctuations. On the other hand, it also makes it possible to tune the strength and angular dependence of Rydberg-Rydberg interactions using such fields.

For small dc electric fields E such that the dipole couplings $e\langle r \rangle E$ are much less than the energy difference ΔE of the nearest opposite parity state, the Stark effect is quadratic and the shift is at most of order $-(e\langle r \rangle E)^2/\Delta E \sim \hbar^6 n^7 E^2/m^3 e^6$. In fact the shift is often substantially smaller than this due to partial cancellation of states with equal and opposite ΔE , as can be inferred from Fig. 5, that tend to cause shifts in opposite directions. Even so, the electric field stability required to hold Stark shifts below 1 MHz is typically of order $0.01(100/n)^{7/2}$ V/cm.

In higher electric fields, mixing of opposite parity states gives the atom an electric dipole moment of order $n^2 e a_0$ and hence a linear Stark effect. This may be desirable to get the strongest possible Rydberg-Rydberg interactions (see Sec. II.D), but stability requirements become more problematic, about $10^{-4}(100/n)^2$ V/cm for a 1 MHz shift.

The response of Rydberg atoms to optical frequency fields is primarily through ac Stark shifts (see Sec. IV.A.2) and photoionization. Since the Rydberg electron spends the vast majority of its time far from the ionic core, to a good approximation it is a free electron, and in a high-frequency field it therefore feels a repulsive force from the ponderomotive potential (Dutta *et al.*, 2000). While inside the core, however, it can absorb a photon, resulting in photoionization. In the mK deep optical traps that have been used to date for blockade-based quantum operations, the photoionization rates can approach $10^5/s$ (Saffman and Walker, 2005a; Johnson *et al.*, 2008). A discussion of photoionization, including the wavelength dependence, has been presented by Potvliege and Adams (2006).

B. From Förster to van der Waals

Successful Rydberg-mediated entanglement of atoms is only possible due to the large interatomic potentials that arise from the large dipole moments of Rydberg atoms. As described below, the Rydberg blockade concept requires that the Rydberg-Rydberg interaction be much stronger than the Rabi coupling of the Rydberg atoms. When this condition, to be quantified below, is satisfied, the entanglement produced is insensitive to first order in the Rydberg-Rydberg interaction. Thus the strength of the interaction does not have to be precisely controlled. This in turn lessens the requirements on atomic position and temperature control.

Due to the extreme electric field sensitivities of Rydberg states, if possible it is desirable to get the strongest

possible interactions in the absence of applied fields. In this section we discuss the properties of dipole-dipole interactions between Rydberg atoms in this limit. This limit has been discussed in several recent papers (Flannery *et al.*, 2005; Singer *et al.*, 2005; Walker and Saffman, 2005, 2008; Stanojevic *et al.*, 2006, 2008; Reinhard *et al.*, 2007).

At interatomic distances $R \gg n^2 a_0$ separating two Rydberg atoms **A** and **B**, the leading electrostatic interaction is the dipole-dipole interaction

$$V_{\text{dd}} = \frac{e^2}{R^3} (\mathbf{a} \cdot \mathbf{b} - 3 \mathbf{a} \cdot \hat{\mathbf{R}} \hat{\mathbf{R}} \cdot \mathbf{b}), \quad (11)$$

where **a** and **b** are the positions of the two Rydberg electrons measured from their respective nuclei. At such large distances, overlap between the atoms can be neglected.

In most realizations of blockade, the two atoms are excited by light to the same fine-structure level so that the two-atom state for $R = \infty$ can be written

$$|\psi_2\rangle = |\psi_A \psi_B\rangle = |\psi_{nlj} \psi_{nlj}\rangle \quad (12)$$

and the dipole-dipole interactions experienced by atoms in this state are of primary interest.¹ In the absence of external fields, this state has a degeneracy of $(2j+1)^2$, where j is the total electronic angular momentum. The dipole-dipole interaction causes transitions to other two-atom states where the angular momentum quantum numbers of each electron obey the usual dipole selection rules, namely, $l_a, l_b = l \pm 1$, $j_a, j_b = j \pm 0, 1$. Including continuum states, there are an infinite number of such states, but in practice the dipole-dipole interaction is dominated by a small number of the closest two-atom states of this type. To illustrate, Fig. 7 shows the energy level structure centered around the $|60p_{3/2}60p_{3/2}\rangle$ state of Rb at zero relative energy. If we restrict changes in the principal quantum numbers to at most ± 8 , there are 18 two-atom states within ± 4 GHz of the initial state. Despite the large number of states the interactions are strongly dominated by coupling between $|60p_{3/2}60p_{3/2}\rangle$ and $|60s_{1/2}61s_{1/2}\rangle$. This is because the energy difference is small and the dipole matrix elements are largest. Other states with larger offsets in the principal quantum numbers have much smaller dipole matrix elements (Walker and Saffman, 2008) and do not play a significant role. The cluster of $|p_j p_j\rangle$ states near -2 GHz will only affect the $|60s_{1/2}61s_{1/2}\rangle$ weakly and thus have only a small indirect effect on the $|60p_{3/2}60p_{3/2}\rangle$ energy. To an excellent approximation, the long-range behavior of the $|60p_{3/2}60p_{3/2}\rangle$ states is dominated by interactions with $|60s_{1/2}61s_{1/2}\rangle$.

Thus we can consider the long-range interaction between Rydberg atoms as arising predominantly from two coupled channels $nlj+nlj$ and $n_a l_a j_a + n_b l_b j_b$ with an en-

¹There are, however, cases where excitation of pairs with the same l, j but different n can lead to stronger interactions (Han and Gallagher, 2009).

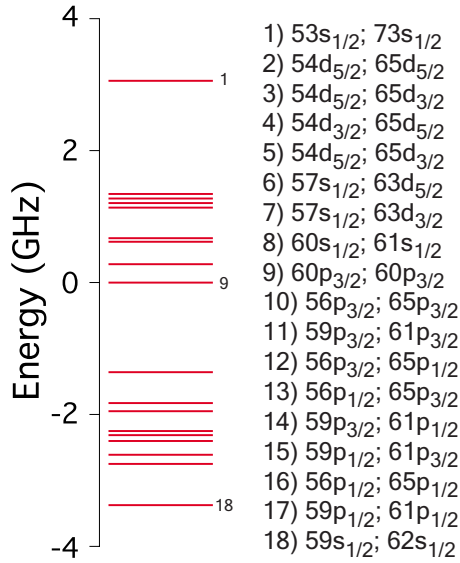


FIG. 7. (Color online) Two-atom energy levels connected to the $|60p_{3/2}60p_{3/2}\rangle$ state by the dipole-dipole interaction.

ergy defect $\delta = E(n_a l_a j_a) + E(n_b l_b j_b) - 2E(nl j)$. Note that for the purposes of blockade we are not interested in actual population transfer between the channels (which would be detrimental), but rather in the energy shift of the $nl j + nl j$ levels due to the interaction with the $n_a l_a j_a + n_b l_b j_b$ manifold of states.

In this two-level approximation, the corresponding Förster eigenstates are linear combinations of states from the different channels (Walker and Saffman, 2008). Representing the $nl j + nl j$ components of the wave function as $|\varphi\rangle$ and the $n_a l_a j_a + n_b l_b j_b$ components as $|\chi\rangle$, the time-independent Schrödinger equation describing the dipole-dipole interaction is

$$\begin{pmatrix} \delta \cdot I_\chi & V_{\text{dd}} \\ V_{\text{dd}}^\dagger & 0 \cdot I_\varphi \end{pmatrix} \begin{pmatrix} |\chi\rangle \\ |\varphi\rangle \end{pmatrix} = \Delta \begin{pmatrix} |\chi\rangle \\ |\varphi\rangle \end{pmatrix}. \quad (13)$$

Here V_{dd} is a $\tilde{2}(2j_a+1)(2j_b+1) \times (2j+1)^2$ operator,² while I_χ and I_φ are identity matrices on the $\tilde{2}(2j_a+1)(2j_b+1)$ and $(2j+1)^2$ dimensional Hilbert subspaces of the $|\chi\rangle$ and $|\varphi\rangle$ wave function components, respectively. Solving for $|\chi\rangle$ as

$$|\chi\rangle = \frac{V_{\text{dd}}}{\Delta - \delta} |\varphi\rangle$$

and substituting this into the second row of Eq. (13) leads to the nonlinear eigenvalue equation for $|\varphi\rangle$:

$$\frac{V_{\text{dd}}^\dagger V_{\text{dd}}}{\Delta - \delta} |\varphi\rangle = \Delta |\varphi\rangle. \quad (14)$$

The solutions of this equation are determined uniquely by eigenvalues and eigenvectors of the matrix $V_{\text{dd}}^\dagger V_{\text{dd}}$. Since all matrix elements of this operator share matrix

² $\tilde{2}=1$ if $(n_a, l_a, j_a) = (n_b, l_b, j_b)$ and $\tilde{2}=2$ otherwise.

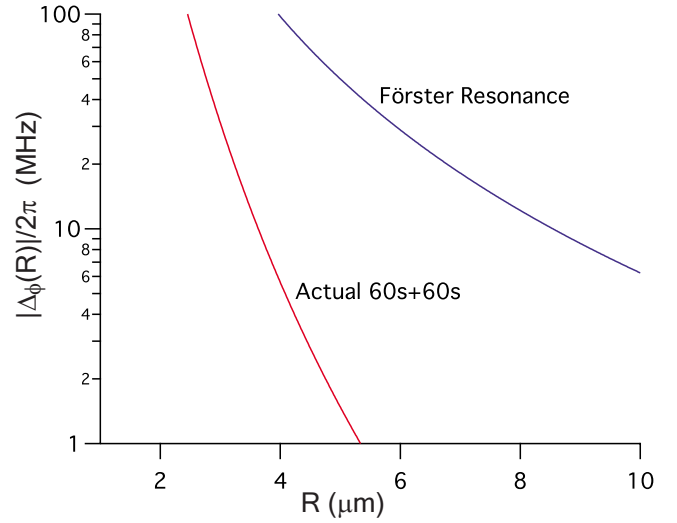


FIG. 8. (Color online) Dipole-dipole interactions for two 60s Rb atoms are significantly reduced from the resonant Förster case ($\delta=0$) for real Rb atoms with $\delta \neq 0$.

elements, $C_3 = e^2 \langle r \rangle_{n_l}^{n_l a} \langle r \rangle_{n_l}^{n_l b}$ and a $1/R^6$ dependence on interatomic distance, it is natural to parametrize these van der Waals eigenstates with eigenvalues D_φ which in most cases lie between 0 and 1 by

$$V_{\text{dd}}^\dagger V_{\text{dd}} |\varphi\rangle = \frac{C_3^2}{R^6} D_\varphi |\varphi\rangle. \quad (15)$$

Inserting these solutions, we can proceed and solve Eq. (14) for the Förster energy eigenvalues Δ ,

$$\Delta_\varphi(R) = \frac{\delta}{2} - \text{sgn}(\delta) \sqrt{\frac{\delta^2}{4} + \frac{C_3^2}{R^6} D_\varphi}, \quad (16)$$

which constitute the R -dependent potential curves between the atoms, correlating asymptotically to the $nl j + nl j$ eigenstates for large R . These are the states coupled to the qubit states by the laser fields and for which we are interested in the energy shifts due to the Rydberg-Rydberg interaction.

It is convenient to define a crossover distance R_c via $\delta = C_3 \sqrt{D_\varphi} / R_c^3$ that denotes the region where the energies transition from the van der Waals to the resonant form. At large distances $R \gg R_c$, the energy shift is of the classic van der Waals form $\Delta_\varphi \approx C_3^2 D_\varphi / \delta R^6$. At small distances, $R \ll R_c$, the two channels are effectively degenerate and the energy is

$$\Delta_\varphi \approx -\text{sgn}(\delta) C_3 \sqrt{D_\varphi} / R^3. \quad (17)$$

This gives the largest possible interaction energy between two nonoverlapping Rydberg atoms. A plot of the interaction energy for a pair of 60s Rb atoms ($\delta = 1.7$ GHz) is shown in Fig. 8, along with the hypothetical interaction energy for $\delta=0$. The nonzero energy defect results in a substantial reduction in the interaction energy for the actual case.

The van der Waals interaction typically scales as n^{11} (Boisseau *et al.*, 2002; Singer, Reetz-Lamour, *et al.*, 2005;

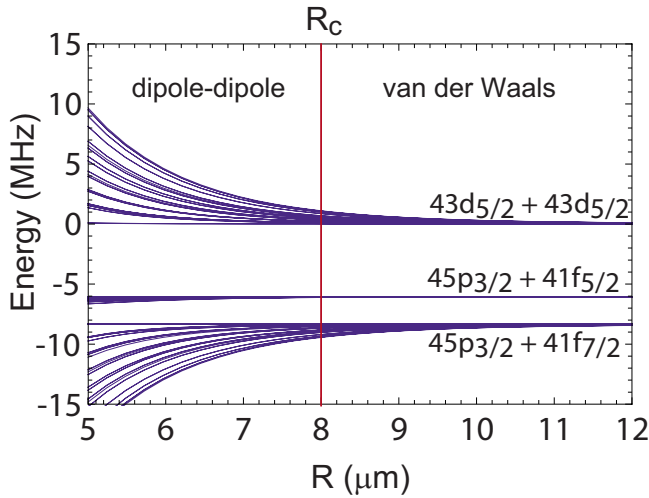


FIG. 9. (Color online) Interaction potentials for $43d_{5/2} + 43d_{5/2}$ Rb Rydberg atoms. The cutoff radius R_c represents the distance scale for the transition from resonant dipole-dipole to van der Waals behavior.

Walker and Saffman, 2008), except in cases where the quantum defects give nearly zero Förster defect for special values of n (Walker and Saffman, 2008). Thus it is generally advantageous to work at as high a principal quantum number as is practical. The resonant Förster interaction scales only as n^4 , so for high principal quantum numbers, often around $n=100$, the atoms are in the resonant limit at 5–10 μm distances.

Due to the Zeeman degeneracies of the states at zero external field, there is typically a range of values \mathcal{D}_φ for any given set of angular momenta. In fact, for most channels there are one or more Förster-zero states with $\mathcal{D}_\varphi=0$ (Walker and Saffman, 2005, 2008). It turns out that Förster-zeros exist for all single channels except those with $j_a=j_b=j+1$, with j the angular momentum of the initial states. Since Förster-zero states can usually be excited by the lasers, they allow doubly excited states to be resonantly populated so that the blockade will not work. Even when multiple channels are considered, there is often one or more states with nearly zero van der Waals interaction. As an example, we show in Fig. 9 the potential energies for the interaction channel $43d_{5/2} + 43d_{5/2} \rightarrow 45p_{3/2} + 41f_{5/2,7/2}$ in Rb, which has extremely small energy defects of $\delta=-6.0, -8.3$ MHz for $j_{41f}=5/2, 7/2$ and so might be normally expected to have promising blockade characteristics (Reinhard *et al.*, 2007; Walker and Saffman, 2008). The two ($j=5/2, 7/2$) f states break the conditions for the existence of Förster-zero states. Nevertheless, there are states with extremely small \mathcal{D}_φ , resulting in poor blockade. In Fig. 9 these states are the nearly flat ones that correlate to $43d_{5/2} + 43d_{5/2}$ at large R .

It is important to point out that s states generally do not have Förster zeros; in the limit of small fine-structure splitting in the p levels the Förster eigenenergies are degenerate, with $\mathcal{D}_\varphi=4/3$. These states are therefore natural choices for blockade experiments. Un-

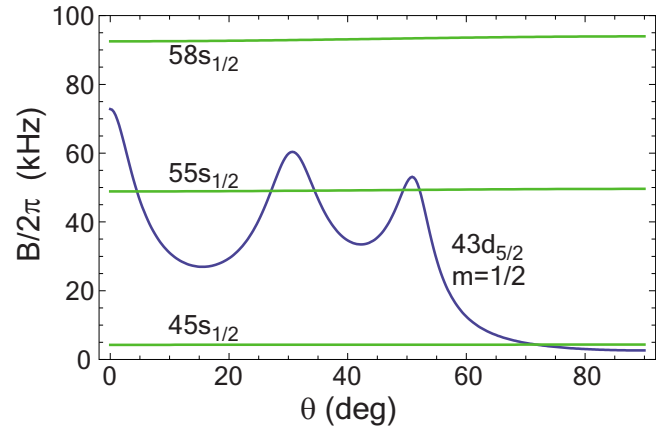


FIG. 10. (Color online) Angular dependence of blockade shift for $43d_{5/2}, m=1/2, 45s_{1/2}, 55s_{1/2},$ and $58s_{1/2}$ at $R=10 \mu\text{m}$ with θ the angle between the molecular axis and \hat{z} .

fortunately, excitation Rabi frequencies from the low-lying p states are typically a factor of 3 smaller than for d states in Rb. This and other technical reasons led to the choice of d states for several recent experiments (Johnson *et al.*, 2008; Gaëtan *et al.*, 2009; Urban, Johnson, *et al.*, 2009).

C. Angular dependence

The critical measure of the interaction strength for Rydberg blockade is the blockade shift of Eq. (3). In zero external field, rotational invariance requires that the Förster eigenenergies $\Delta_{\varphi ij}$ depend only on the distance R_{ij} between atoms i and j , but the coupling of the corresponding eigenstates to the excitation light $\kappa_{\varphi ij}$ depends on the angle between the interatomic axis and light polarization. A typical three-dimensional (3D) distribution of atoms includes pairs with arbitrary relative orientations so that laser fields with laboratory fixed polarizations will generally couple to all possible two-atom eigenstates, including those with weak interactions. The blockade shift is an inverse-square average of the interaction strengths and so is particularly sensitive to states with small Δ_φ . For reduced-dimension geometries such as long cylinders, the effects of small Δ_φ may be mitigated by polarization choices that also give small $\kappa_{\varphi ij}$. However, in a spherical sample the atoms will have random orientations and the blockade strength will be dominated by those orientations with the weakest blockade shifts. These points are discussed by Walker and Saffman (2008).

Examples of angular dependences of the blockade shifts are given in Fig. 10. Excitation by \hat{z} -polarized light has been assumed. For pairs of s -state atoms, the blockade is nearly spherically symmetric (the weak departure from spherical symmetry is due to the fine-structure splitting of the p states), while for $43d_{5/2}$ atom pairs there is a considerable variation with angle. The small Förster defect of $43d_{5/2}$ produces a much stronger, albeit anisotropic, interaction for most angles than the nearby

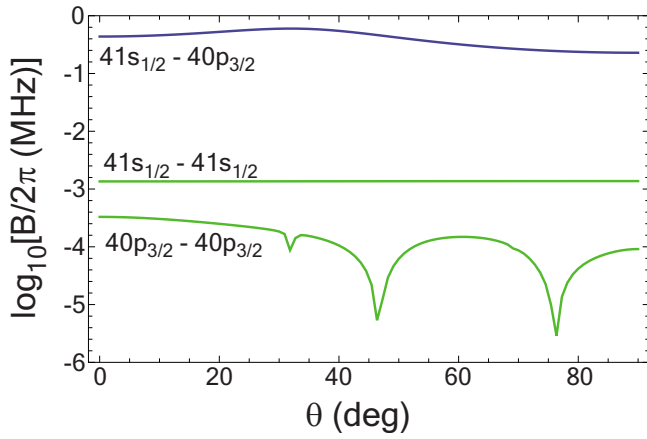


FIG. 11. (Color online) Comparison of the blockade shift B at $R=10 \mu\text{m}$ for interacting Rb $41s_{1/2}-40p_{3/2}$ atoms as compared to van der Waals blockade for two $41s_{1/2}$ or $40p_{3/2}$ atoms. All atoms have magnetic quantum number $m=1/2$.

in energy $45s_{1/2}$ state. In order to obtain a comparable isotropic interaction strength it is necessary to use a $55s_{1/2}$ or higher state.

Rydberg atoms in states with l differing by 1 experience the dipole-dipole interaction in first order so the interaction scales with distance as $1/R^3$. This case was observed spectroscopically by [Afrousheh et al. \(2004, 2006\)](#). The van der Waals interaction between states of the same l is much weaker at long range, scaling as $1/R^6$. The use of this interaction asymmetry for efficient creation of multiparticle entanglement was proposed by [Saffman and Mølmer \(2009\)](#) (see Sec. V.F.2). An example of the blockade shifts for $s+p_{3/2}$ states, including a comparison to the van der Waals case, is shown in Fig. 11. We see that the asymmetry is more than two orders of magnitude over the full angular range.

D. Tuning the interaction with external fields

The interactions between the Rydberg atoms are generally sensitive to the application of external magnetic and electric fields. An extreme case occurs when an electric field is applied of sufficient strength to mix states of different parity. The atoms then acquire a permanent electric dipole moment $\langle \mathbf{d} \rangle$, and the dipole-dipole interaction to first order becomes

$$V_{\text{dd}} = \frac{1}{R^3} (\langle \mathbf{d} \rangle^2 - 3 \langle \mathbf{d} \rangle \cdot \hat{\mathbf{R}} \hat{\mathbf{R}} \cdot \langle \mathbf{d} \rangle). \quad (18)$$

Since the dipole moments are usually of order $n^2 e a_0$, this is a very strong but anisotropic interaction that may work well for blocking anisotropic samples. A weakness of this situation is that the atomic energy levels are also sensitive to electric field fluctuations that may inhomogeneously broaden the Rydberg excitation line.

In other cases, it is possible to use electric fields to tune certain Zeeman states into a Förster resonance to give dipole-dipole interactions of order $n^4 e^2 a_0^2 / R^3$. This is illustrated in the early experiment of [Anderson et al.](#)

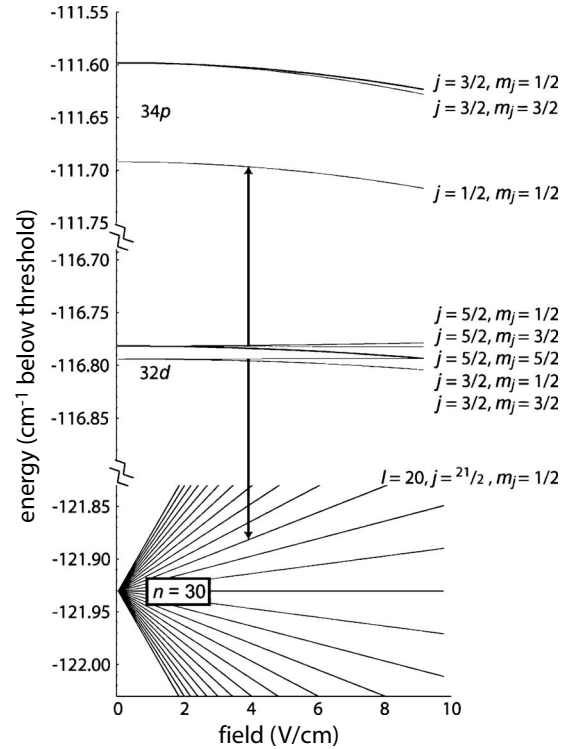


FIG. 12. Tuning of Förster resonances with an electric field. From [Carroll et al., 2004](#).

(1998), more recently by [Vogt et al. \(2007\)](#), and discussed in the recent review of [Gallagher and Pillet \(2008\)](#). Again, this generally results in a strong but anisotropic blockade shift. Resonant transfer between spatially separated samples was observed and studied by [Tauschinsky et al. \(2008\)](#) and [van Ditzhuijzen et al. \(2008, 2009\)](#), and simulated by [Carroll et al. \(2009\)](#). Double-resonance spectroscopy was used by [Reinhard et al. \(2008\)](#) to directly observe the difference between van der Waals and resonant dipole-dipole interactions. The effects of dc electric fields on Rydberg-Rydberg interactions are treated by [Schwettmann et al. \(2006\)](#).

A possible way to dc field-enhance dipole-dipole interactions while minimizing field broadening of the optical resonance is illustrated by [Carroll et al. \(2004, 2006\)](#). They used relatively field insensitive $32d$ states for optical excitation, while coupling to a field-sensitive Förster resonance. This is shown in Fig. 12. By exciting a long narrow tube of atoms, they also observed the angular dependence of the interaction.

Another tool for tuning the atom-atom interactions with external fields is to use resonant or near-resonant microwave fields. For example, [Bohlouli-Zanjani et al. \(2007\)](#) used the ac-Stark shift from near-resonant microwaves to tune the near Förster resonance between Rb $43d_{5/2}$ atoms shown in Fig. 9, enhancing energy-transfer collision rates. They then demonstrated resonant $f-g$ microwave coupling to accomplish the same purpose ([Petruș et al., 2008](#)). As with the [Carroll et al. \(2004\)](#) experiment, this coupling has a relatively small effect on the energies of the initial d states.

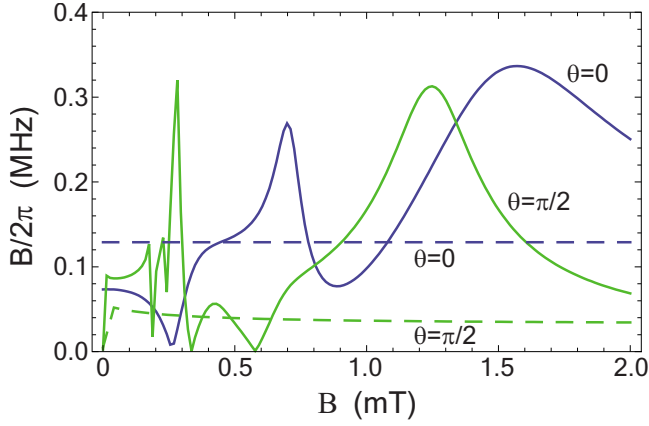


FIG. 13. (Color online) Blockade interaction of Rb $43d_{5/2}$ states as a function of the magnetic field applied along the quantization axis and $R=10 \mu\text{m}$. The solid (dashed) lines are for excitation of $m=1/2$ ($5/2$) states and θ is the angle between the applied field and the molecular axis.

Modest magnetic fields can also strongly affect the Rydberg-Rydberg interactions by breaking the Zeeman degeneracy that produces Förster zeros. An example is given in Fig. 13, which shows the blockade shifts of the $43d_{5/2}+43d_{5/2}$ states as a function of magnetic field. The states with maximal magnetic quantum number $m=5/2$ are quite insensitive to magnetic fields since there is only one combination of Zeeman levels with the same total $M=m+m=5$. On the other hand, the $m=1/2$ states are strongly dependent on magnetic field since it breaks the degeneracy between the $M=1$ Zeeman pairs $(1/2, 1/2)$, $(-1/2, 3/2)$, and $(-3/2, 5/2)$. The extent to which the laser excited states couple to the molecular eigenstates is also angle dependent, hence the different behavior seen for $\theta=0$ and $\pi/2$. Magnetic field effects were demonstrated experimentally by Afrousheh *et al.* (2006) who used a small magnetic field to reduce resonant dipole-dipole interactions. Conversely Urban, Johnson, *et al.* (2009) used a magnetic field in a well-controlled geometry to increase the interaction strength.

E. Three-body Förster interactions

It might be expected that under conditions of strong blockade for atom pairs, three-atom states would be further off-resonance. However, Pohl and Berman (2009) showed that for three two-level atoms interacting via the Förster mechanism there are triply excited states that are noninteracting. This “breaks” the blockade in the sense that resonant two-photon transitions can occur between the singly excited state and the triply excited state. However, the two-photon Rabi coupling to the triply excited states is via the doubly excited state that is off-resonance by $1/\Delta_{\text{dd}}$. Thus the probability of three-atom excitation is of order $\Omega^2/\Delta_{\text{dd}}^2$, similar to the blockade error of Eqs. (2) and (3) that will be considered in the next section.

III. RYDBERG GATES

In this section we discuss a variety of approaches to implementing neutral atom gates with Rydberg interactions. Prior to discussing the various protocols we provide a derivation of the blockade shift of Eq. (3) following the analysis of Walker and Saffman (2008). The original blockade gate of Jaksch *et al.* (2000) is then examined in Sec. III.B followed by consideration of alternative approaches in Sec. III.C. We restrict our attention to gates that operate between single-atom qubits. These primitives will find use for ensemble and collective gates and as building blocks for many particle entanglement protocols in Secs. V.C, V.D, and V.F. Since the Rydberg interaction is long ranged (see Fig. 1), it is natural to ask what the limit is on the number of qubits in a fully connected register. We compare the limits as a function of the space dimensionality of the qubit array in Sec. III.D.

A. Blockade interaction

Consider a cloud of N atoms with internal ground states $|g\rangle$ and Rydberg states $|\gamma\rangle$ with g, γ shorthand for the full set of quantum numbers needed to specify the states. We are interested in the situation where blockade is active and assume that at most two atoms can be simultaneously excited to a Rydberg state. Thus the atomic cloud can be in the possible states

$$|g\rangle, |\gamma k\rangle, \text{ and } |\varphi kl\rangle, \quad (19)$$

representing all the atoms in the ground state, the k th atom in the singly excited Rydberg state γ , and the k th and l th atoms in the doubly excited Rydberg state φ respectively. The label φ denotes eigenstates of the Förster Hamiltonian of Eq. (14): $H_F|\varphi kl\rangle = \Delta_{\varphi kl}|\varphi kl\rangle$.

The light-atom coupling at atom k is described by an electric dipole Hamiltonian \mathcal{H}_k and an excitation Rabi frequency $\Omega_{\gamma k} = (2/\hbar)\langle\gamma k|\mathcal{H}_k|g\rangle$. We define an N -atom collective Rabi frequency by

$$\Omega_N = \sqrt{\sum_{\gamma k} |\Omega_{\gamma k}|^2} = \sqrt{N}\Omega, \quad (20)$$

where Ω is the rms single-atom Rabi frequency averaged over all atoms in the ensemble. With this definition we can write a normalized singly excited state as

$$|s\rangle = \sum_{\gamma k} \frac{\Omega_{\gamma k}}{\Omega_N} |\gamma k\rangle,$$

and the wave function for the N -atom ensemble as

$$|\psi\rangle = c_g|g\rangle + c_s|s\rangle + \sum_{\varphi, k < l} c_{\varphi kl} |\varphi kl\rangle. \quad (21)$$

This expression is valid to first order in $|\Omega/B|$, where B is the blockade shift defined in Eq. (3).

Using the above definitions, the Schrödinger equations for the ground, symmetric singly excited state, and the doubly excited states are

$$i\dot{c}_g = \frac{\Omega_N^*}{2} c_s, \quad (22a)$$

$$i\dot{c}_s = \frac{\Omega_N}{2} c_g + \frac{\Omega_N^*}{N} \sum_{\varphi, k < l} \kappa_{\varphi kl}^* c_{\varphi kl}, \quad (22b)$$

$$i\dot{c}_{\varphi kl} = \Delta_{\varphi kl} c_{\varphi kl} + \frac{\Omega_N}{N} \kappa_{\varphi kl} c_s. \quad (22c)$$

Here the overlap amplitudes between the optically excited states and the Förster eigenstates are given by $\kappa_{\varphi kl} = (4/\hbar^2 \Omega^2) \langle \varphi kl | \mathcal{H}_k \mathcal{H}_l | g \rangle$.

We are now ready to calculate the effectiveness of Rydberg blockade. Assume we start in the ground state $|\psi\rangle = |g\rangle$ and apply a π pulse: $\Omega_N t = \pi$. With the assumption that there is a strong blockade, the doubly excited amplitudes are small and $c_s(t) \approx 1$. Making an adiabatic approximation to Eq. (22c) we get

$$c_{\varphi kl} = -\frac{\Omega_N \kappa_{\varphi kl}}{N \Delta_{\varphi kl}} c_s,$$

and the probability of double excitation is

$$P_2 = \sum_{\varphi, k < l} |c_{\varphi kl}|^2 = \frac{|\Omega_N|^2}{N^2} \sum_{\varphi, k < l} \left| \frac{\kappa_{\varphi kl}}{\Delta_{\varphi kl}} \right|^2. \quad (23)$$

It is critical to note that, given relatively even excitation of the two-atom Rydberg states, it is an average of $1/\Delta_{\varphi kl}^2$ that determines the blockade effectiveness. This means that Rydberg-Rydberg states with small interaction shifts are much more strongly weighted than those with large energy shifts. We define a mean blockade shift B via

$$\frac{1}{B^2} = \frac{2}{N(N-1)} \sum_{\varphi, k < l} \frac{|\kappa_{\varphi kl}|^2}{\Delta_{\varphi kl}^2}. \quad (24)$$

Then the probability of double excitation becomes

$$P_2 = \frac{N-1}{N} \frac{|\Omega_N|^2}{2B^2}. \quad (25)$$

This shows that for fixed Ω_N , the frequency of the *collective* oscillation, the probability of double excitation is virtually independent of the number of atoms in the ensemble.

It is important to keep in mind that the blockade shift B depends on the polarization of the excitation light as well as the Zeeman structure of the states $|g\rangle, |\varphi kl\rangle$ through the overlap factor $\kappa_{\varphi kl}$. We do not explicitly indicate these dependences in order to avoid a proliferation of subscripts. Explicit examples of the angular dependence have been given in Sec. II.C.

B. Two-atom blockade gate

As discussed in connection with Fig. 2 Rydberg gates are intrinsically prone to errors due to the finite lifetime of the Rydberg levels that are used. In the strong blockade limit ($B \gg \Omega$), the gate fidelity is high, and we can

estimate the errors by adding the contributions from the physically distinct processes of spontaneous emission from Rydberg states and state rotation errors, which are primarily due to imperfect blockade. We note that the gate error depends on the input state applied to the gate. Referring to Fig. 2 the state $|00\rangle$ experiences relatively small errors since Rydberg excitation is off-resonance by a detuning ω_{10} . For hyperfine encoded qubits ω_{10} is typically several GHz as opposed to the few MHz of Ω and B . On the other hand, the state $|11\rangle$ leads to the largest errors since both atoms are Rydberg excited and subject to spontaneous decay. In this section and the following one, we base our analysis on “square pulse” excitation schemes. The possibility of improving on the error limits we find using shaped or composite pulses remains an open question.

An average gate error was defined by Saffman and Walker (2005a) by simply averaging over the four possible two-atom inputs. The dominant errors come from imperfect blockade in step 2 with error $E_{bl} \sim \Omega^2/B^2$ and spontaneous emission of the control or target atom with error $E_{se} \sim 1/\Omega\tau$, where τ is the Rydberg state spontaneous lifetime. Keeping track of the numerical prefactors, neglecting higher order terms in $\Omega/B, B/\omega_{10}$, and averaging over the input states, we find the gate error³

$$E \approx \frac{7\pi}{4\Omega\tau} \left(1 + \frac{\Omega^2}{\omega_{10}^2} + \frac{\Omega^2}{7B^2} \right) + \frac{\Omega^2}{8B^2} \left(1 + 6 \frac{B^2}{\omega_{10}^2} \right). \quad (26)$$

The first term proportional to $1/\tau$ gives the spontaneous emission error and the second term gives the probability of an atom populating the Rydberg level at the end of the gate. These expressions assume piecewise continuous pulses. Other assumptions, such as pulses with phase jumps (Qian *et al.*, 2009), lead to different coefficients, but it is still the ratio of the effective bandwidth of the excitation to the blockade strength that governs the magnitude of the errors.

In the limit of $\omega_{10} \gg (B, \Omega)$ we can extract a simple expression for the optimum Rabi frequency which minimizes the error

$$\Omega_{opt} = (7\pi)^{1/3} \frac{B^{2/3}}{\tau^{1/3}}. \quad (27)$$

Setting $\Omega \rightarrow \Omega_{opt}$ leads to a minimum averaged gate error of

$$E_{min} = \frac{3(7\pi)^{2/3}}{8} \frac{1}{(B\tau)^{2/3}}. \quad (28)$$

The gate error for excitation to ^{87}Rb ns states is shown in Fig. 14 for $50 \leq n \leq 200$ as a function of the two-atom separation R . Despite the use of finite lifetime Rydberg states the interaction is strong enough to allow for fast excitation pulses which keep the total error small. We see that gate errors below 0.001, which corresponds to recent theoretical estimates (Knill, 2005; Ali-

³Equations (26)–(28) correct some algebraic errors in Table V and Eq. (38) of Saffman and Walker (2005a).

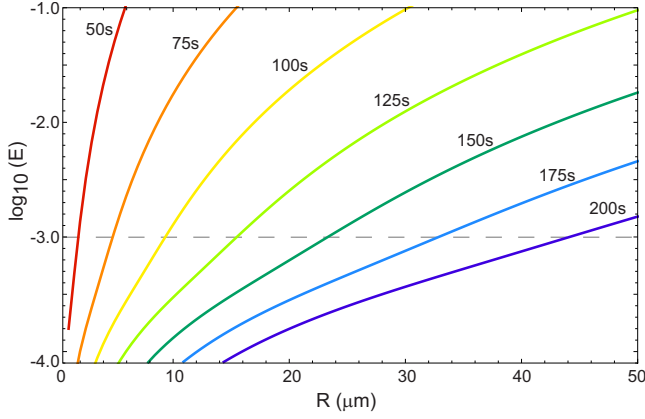


FIG. 14. (Color online) Intrinsic blockade gate error from Eq. (26) for ^{87}Rb ns states. The lifetimes for $n=50$ – 200 were calculated from Eq. (8) to be $\tau=(70,180,340,570,860,1200,1600)\ \mu\text{s}$.

feris and Preskill, 2009) for the fault tolerant threshold in a scalable quantum computer, can be achieved over a large range of interatomic separations. At relatively low excitation of $n=50$, an error of 0.001 requires $R\sim 1\ \mu\text{m}$. The atom separation at this error level can be pushed all the way to $R>40\ \mu\text{m}$ by exciting $n=200$ states. Although coherent excitation of $n=200$ Rydberg states has not been demonstrated, excitation of clusters of states has been reported up to $n=1100$ (Frey *et al.*, 1995) and state resolved excitation up to $n=390$ (Tannian *et al.*, 2000) and $n=500$ (Neukammer *et al.*, 1987) has been achieved. In contrast to collisional neutral atom gates (Brennen *et al.*, 1999; Jaksch *et al.*, 1999) which accumulate large errors if operated too fast, the Rydberg gate would fail if it were run too slowly. The necessity of achieving sufficiently fast excitation of high-lying levels puts demands on the laser system, but this is a technical not a fundamental challenge.

In addition to the intrinsic error due to the finite Rydberg lifetime, there are other errors due to technical imperfections. These include Doppler broadening of the excitation, spontaneous emission from intermediate levels when a two-photon excitation scheme is used, pulse area errors due to variations in atomic position, and errors due to imperfect polarization of the exciting laser pulses. All of these effects have been considered (Protzenko *et al.*, 2002; Saffman and Walker, 2005a) and will be discussed in Sec. IV. In principle, with proper experimental design, errors due to technical imperfections can be kept below 10^{-3} or less. It may be emphasized that the Rydberg blockade operation is not directly sensitive to the center of mass motion and it is therefore not necessary to work with atoms that are in the ground vibrational state of the confining potential. Using blockade to implement a CNOT gate requires additional single-qubit pulses. These can also be made insensitive to the motional state using two-photon copropagating Raman pulses (Yavuz *et al.*, 2006; Jones *et al.*, 2007). This implies an attractive robustness of the quantum gate with re-

spect to moderate vibrational heating of the atomic qubits.

There is also an adiabatic version of the blockade gate which does not require individual addressing of the atoms (Jaksch *et al.*, 2000). However, the adiabatic condition implies that the gate time is long compared to $1/\Omega$ which increases errors due to spontaneous emission. Thus, relaxing the requirement of individual addressing reduces the fidelity compared to the blockade gate described above.

C. Alternative gate protocols

1. Interaction gates

In the original Rydberg gate paper (Jaksch *et al.*, 2000) a second type of gate protocol was already proposed. The “interaction” gate assumes the excitation of both atoms from the qubit 1 state to the Rydberg state and makes use of the Rydberg interaction energy to accumulate a phase shift of π . Thus it works in the opposite regime of the blockade gate, and requires $\Delta_{\text{dd}}\ll\Omega$. The pulse sequence is (1) $R(\pi)_{1,r}^{c,t}$, (2) wait a time $T=\pi/\Delta_{\text{dd}}$, and (3) $R(\pi)_{1,r}^{c,t}$. Here $R(\theta)_{i,j}^{c,t}$ is an X rotation by θ between states i,j on the control and target atoms. The resulting gate is the same C_Z as given in Eq. (1) apart from an overall π phase shift. This protocol has the advantage that it does not require individual addressing of the atoms. We can perform an error analysis along the lines of that in the previous section assuming the orderings $\omega_{10}\gg\Omega\gg\Delta_{\text{dd}}$ and $\Delta_{\text{dd}}\tau\gg 1$. The interaction energy of two Rydberg excited atoms is Δ_{dd} which can be calculated from

$$\Delta_{\text{dd}}\approx\sum_{\varphi}\frac{|\kappa_{\varphi}|^2\Omega^2}{|\kappa_{\varphi}|^2\Omega^2+\Delta_{\varphi}^2}\Delta_{\varphi}. \quad (29)$$

We have dropped the atom labels on $\kappa_{\varphi},\Delta_{\varphi}$ since we are considering only a two-atom interaction. Note that when $\Omega^2\ll\min_{\varphi}|\Delta_{\varphi}/\kappa_{\varphi}|^2=|\Delta_{\varphi_{\text{min}}}/\kappa_{\varphi_{\text{min}}}|^2$ we get $\Delta_{\text{dd}}\approx|\kappa_{\varphi_{\text{min}}}|^2\Omega^2/\Delta_{\varphi_{\text{min}}}$ which verifies that the two-atom interaction tends to zero in the blockade limit where two atoms cannot simultaneously be excited. In the opposite limit of $\Omega^2\gg\max_{\varphi}|\Delta_{\varphi}/\kappa_{\varphi}|^2$ we find $\Delta_{\text{dd}}\approx\sum_{\varphi}\Delta_{\varphi}$ which is independent of Ω . Since the eigenvalues scale as R to a negative power, we infer that Δ_{dd} has a maximum at an intermediate value of R and tends to zero for R small or large. The implication of this is that at fixed n the interaction gate has an optimum fidelity at a finite value of R .

To see this in more detail consider the leading contributions to the input averaged gate error which are (Saffman and Walker, 2005a)

$$E\approx\frac{\pi}{\tau}\left(\frac{1}{\Delta_{\text{dd}}}+\frac{1}{\Omega}\right)+\left(\frac{2\Delta_{\text{dd}}^2}{\Omega^2}+\frac{\Omega^2}{\omega_{10}^2}\right). \quad (30)$$

For given values of ω_{10},τ the absolute minimum of the gate error can be shown to be

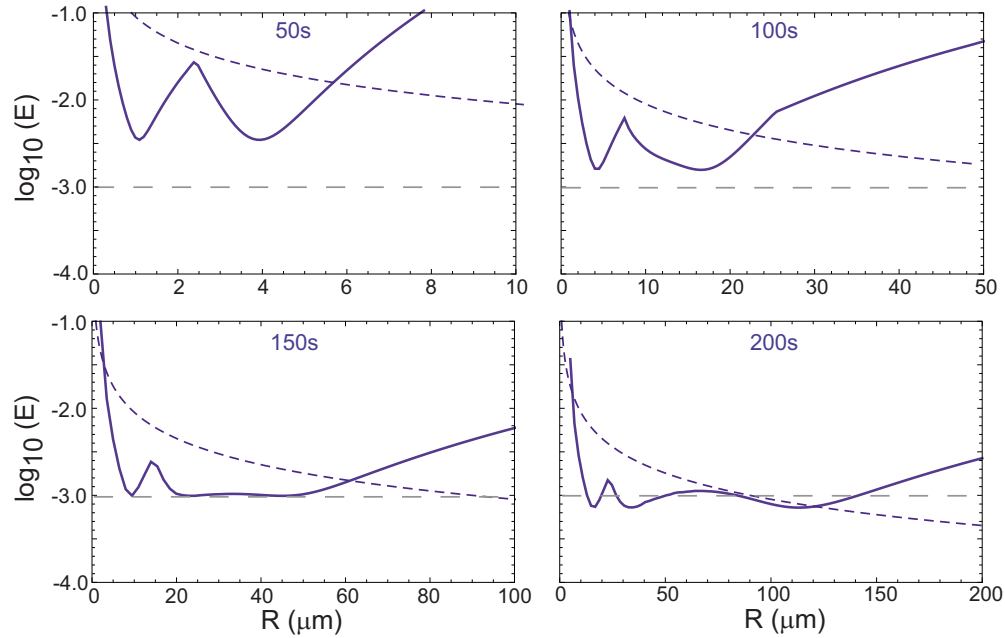


FIG. 15. (Color online) Intrinsic interaction gate error from Eq. (30) for ^{87}Rb ns states. The lifetimes for $n=(50,100,150,200)$ were calculated from Eq. (8) to be $\tau=(70,340,860,1600)$ μs . The long dashed line is $E=0.001$ and the short dashed curve gives the error limit at $\delta R=15$ nm.

$$E_{\min} = \left[\frac{2^{7/2} \pi}{\tau \omega_{10}} \right]^{1/2}. \quad (31)$$

The error for any particular choices of $\Delta_{\text{dd}}(n, R), \Omega$ will always exceed this lower bound. For ^{87}Rb we have $\omega_{10}/2\pi=6834$ MHz and $\tau=100$ μs gives $E_{\min} \approx 0.003$.

In order to evaluate the potential of the gate for different Rydberg levels n and separations R it is useful to find the optimum Ω for a given $\Delta_{\text{dd}}(n, R)$. We find

$$\Omega_{\text{opt}} \approx \frac{2^{1/2}}{3^{1/4}} (\Delta_{\text{dd}} \omega_{10})^{1/2}, \quad (32)$$

which leads to

$$E_{\text{opt}} \approx \frac{\pi}{\Delta_{\text{dd}} \tau} + \frac{5\Delta_{\text{dd}}}{3^{1/2} \omega_{10}}. \quad (33)$$

Equations (32) and (33) are only implicit relations for Ω_{opt} and E_{opt} since Eq. (29) also depends on Ω . We have therefore used a numerical search to find Ω_{opt} and E_{opt} at specific values of n and R with the results shown in Fig. 15 for Rb ns states. As discussed in connection with Eq. (29) the interaction strength has a maximum at intermediate values of R . However, the interaction can actually be too strong at intermediate R which violates the scaling $\Delta_{\text{dd}} \ll \Omega \ll \omega_{10}$ and results in a complex multi-peaked structure for the R dependence of the gate error. We see that low n states with small τ do not give particularly low gate errors, even at small separation R , due to the limit imposed by Eq. (31). For $n > 100$ we find errors of 10^{-3} or less over a wide range of R . If we are willing to consider very highly excited states with $n=200$, high fidelity gates are possible at $R > 100$ μm .

There is, however, a caveat to the above discussion since the interaction gate is sensitive to fluctuations in the atomic separation as emphasized by Protsenko *et al.* (2002). To estimate the sensitivity assume we are in the van der Waals limit so $\Delta_{\text{dd}}(R) = \Delta_{\text{dd},0}(R_0/R)^6$, with $\Delta_{\text{dd},0}, R_0$ constants. The two-atom phase depends on R as $\delta\phi(R) = \Delta_{\text{dd}}(R)T \approx \Delta_{\text{dd},0}T(1 - 6\delta R/R_0)$, with T the gate interaction time. The fractional phase error is thus $6\delta R/R_0$. The harmonic oscillator wave function of a ^{87}Rb atom in a trap with $\omega/2\pi=500$ kHz, which is a reasonable limit for what is experimentally feasible in an optical trap, has a characteristic length scale of about 15 nm. Taking $\delta R=15$ nm gives the short dashed curve in Fig. 15 which drops below 10^{-3} for $R > 100$ μm .

These error estimates treat the motion classically. If the atoms are in a pure quantum-mechanical motional state, then there is no position-dependent interaction. Nevertheless there are two-body forces when both atoms are excited to a Rydberg level. If these forces are strong enough, then excitation of the motional state will occur which leads to decoherence and gate errors. These errors have been estimated by Jaksch *et al.* (2000) and Saffman and Walker (2005a) and can again be made small provided that the atoms are well localized spatially. We conclude that the interaction mode of operation has potential for remarkably long-range gates, extending out to $R > 100$ μm with low errors, provided that the atoms are cooled close to the motional ground state or are otherwise trapped with a high degree of spatial localization.

A variation in the interaction gate described above was analyzed by Protsenko *et al.* (2002). There it was assumed that the excitation pulses are purposefully detuned from $|r\rangle$ and the presence of the two-atom inter-

action Δ_{dd} brings the excitation into resonance. This type of interaction-induced resonance was anticipated in an early paper (Varada and Agarwal, 1992) that predated the interest in quantum gates and was more recently proposed (Ates *et al.*, 2007a) and observed (Amthor *et al.*, 2010) in an ensemble of cold atoms. This “self-transparency” mode of operation has the same sensitivity as the interaction gate to fluctuations in atomic position.

A further variation on the interaction gate was described by Ryabtsev *et al.* (2005). There it was suggested to excite two atoms to weakly interacting states that are microwave coupled as in Sec. II.D. The microwaves are initially detuned from resonance between opposite parity Rydberg levels, and then the resonance condition is achieved for a controlled time using a Stark switching technique, which was demonstrated by Ryabtsev *et al.* (2003). This approach suffers again from sensitivity to fluctuations in the atomic separation although in the limit where the microwave coupling effectuates a $1/R^3$ resonant dipole-dipole interaction the sensitivity will only be half as large as in the van der Waals regime. In addition a somewhat different gate idea based on Stark switching together with nonholonomic control techniques can be found in Brion *et al.* (2006).

Adapting ideas developed in the context of trapped ion gates (García-Ripoll *et al.*, 2003) it was proposed by Cozzini *et al.* (2006) to implement a C_Z gate using controlled atomic motion due to two-body forces from the dipole-dipole interaction of simultaneously excited Rydberg atoms. This is reminiscent of the interaction gate although here the necessary conditional phase shift is due to a combination of a dynamic and geometrical phase. The fidelity of the gate can be 0.99 or better provided the atoms are again cooled close to the motional ground state.

2. Interference gates

A different type of gate which does not require strongly populating the Rydberg levels can be designed using the interference of different multiphoton transition paths. The dipole-dipole interaction suppresses the amplitude of one of the paths (Brion, Pedersen, and Mølmer, 2007) which creates a conditional phase shift. This general idea can be used to implement a universal set of gates in a decoherence free subspace of logical qubits, each encoded in two physical qubits (Brion, Pedersen, Mølmer, *et al.*, 2007). Unfortunately the gate is relatively slow due to the use of multiphoton transitions and consequently suffers from spontaneous emission errors despite the fact that the Rydberg states are never substantially populated. Attempts to design entangling gates that require only virtual excitation of Rydberg states and hence do not have any spontaneous emission errors turn out to be futile, since it can be shown that a minimum integrated Rydberg population of the control and the target atom during the gate execution, $\int (p_r^{(c)} + p_r^{(t)}) dt > 2/\Delta_{\text{dd}}$, is necessary for the creation of one bit of entanglement with arbitrary local operations and a

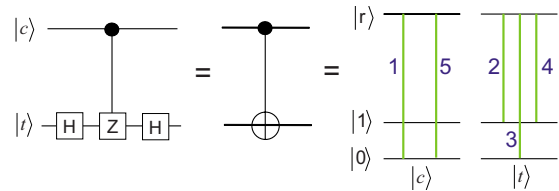


FIG. 16. (Color online) The CNOT gate (center) can be implemented with Hadamard gates and a C_Z (left) or directly with a controlled amplitude swap (right). All transitions are π pulses with the indicated ordering.

Rydberg-Rydberg interaction energy of $\hbar\Delta_{\text{dd}}$; cf. the Appendix in Wesenberg *et al.* (2007).

3. Amplitude swap gates

All of the approaches described above implement a C_Z gate which can be converted into a CNOT gate using the quantum circuit equivalence of Fig. 16. An alternative route to the CNOT dispenses with the Hadamard operations and directly swaps the states of the target qubit, conditioned on the state of the control qubit, as shown on the right in Fig. 16. When the control qubit is in state $|0\rangle$ it is Rydberg excited by pulse 1 which blocks the swap action of pulses 2–4, and when the control atom is in state $|1\rangle$ the swap is unhindered. The result is a CNOT gate with an overall minus sign. This method was first proposed in the context of quantum computing with rare earth doped crystals by Ohlsson *et al.* (2002) and was used for experimental demonstration of a two-atom CNOT gate (Isenhower *et al.*, 2010). It turns out that this approach is particularly well suited to blockade interactions which naturally enable or block the swap operation on the target qubit. As we will see in Sec. V.F.2 an adaptation of this approach is also efficient for creating multiparticle entangled states (Saffman and Mølmer, 2009).

A variation in the amplitude swap approach can be used to create three-terminal Toffoli gates which are important for efficient implementations of quantum algorithms. The Toffoli gate switches the value of the target qubit if both control qubits are 1 and otherwise leaves the target unchanged. This can be implemented in several ways using the population swap primitive. Consider the pulse sequence shown in Fig. 17 where we now allow for coupling to three Rydberg states $|r_1\rangle$, $|r_2\rangle$, and $|r_t\rangle$. It is possible to choose states $|r_1\rangle$, $|r_2\rangle$ that are weakly in-

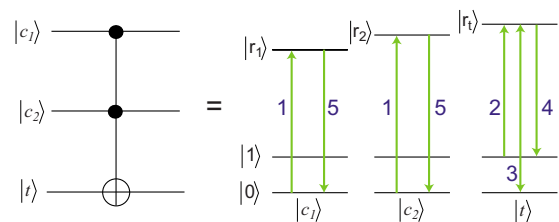


FIG. 17. (Color online) Implementation of the Toffoli gate as proposed by Brion, Mouritzen, and Mølmer (2007). All transitions are π pulses with the indicated ordering.

interacting, yet both interact strongly with $|r_i\rangle$. For example, we could set $|r_1\rangle, |r_2\rangle$ to be s and d parity Rydberg levels and $|r_i\rangle$ a p parity level. This case was analyzed for hydrogenic Rydberg levels by [Brion, Mouritzen, and Mølmer \(2007\)](#). Using these levels the pulse sequence shown in Fig. 17 implements the ideal Toffoli gate but with an overall minus sign which can be corrected by single-qubit operations. It may be noted that the requirement of weakly interacting control atoms can also be effectuated geometrically. If all three atoms are placed on a line with the target atom in the middle then in the van der Waals limit, the control-control Rydberg interaction will be a factor of 2^6 weaker than either control acting on the target. In this case the three Rydberg states can be replaced by one state, excited by the same laser frequency, as long as the laser can address the three atoms individually.

It has recently been shown ([Saffman and Isenhower, 2009](#)) that the Toffoli gate can be extended to a Toffoli gate with k control bits, or C^k -NOT gate. We note that the requirement of weakly interacting control qubits is actually not needed. If we assume individual addressing of the control and target qubits then the pulse sequence $R(\pi)_{0,r}^{c_1} R(\pi)_{0,r}^{c_2} R(\pi)_{1,r}^t R(\pi)_{0,r}^t R(\pi)_{1,r}^t R(\pi)_{0,r}^{c_2} R(\pi)_{0,r}^{c_1}$ implements the Toffoli gate with only one Rydberg level needed. If we consider k control atoms and a target atom, all within a blockade sphere of each other, then the $2k+3$ pulse sequence,

$$\left(\prod_{i=0}^{k-1} R(\pi)_{0,r}^{c_{k-i}} \right) R(\pi)_{1,r}^t R(\pi)_{0,r}^t R(\pi)_{1,r}^t \left(\prod_{i=1}^k R(\pi)_{0,r}^{c_i} \right),$$

immediately gives the C^k -NOT gate with an overall minus sign. The error scaling of this gate is approximately linear in k because of the less than k times larger spontaneous emission error than for the two-qubit blockade gate. This type of multi-qubit gate is of particular interest in design of efficient quantum circuits ([Beckman et al., 1996](#)).

4. Other approaches

For completeness we mention some alternative paradigms for quantum information processing with Rydberg atoms. In addition to the Rydberg CQED approach described in the Introduction which uses moving Rydberg atoms ([Raimond et al., 2001](#)) there are additional possibilities working with trapped atoms. Instead of only using Rydberg levels in a transient fashion for achieving a two-atom interaction, one might consider encoding many bits of information in the multiplicity of levels of a Rydberg atom. In this way Grover's search algorithm ([Grover, 1997](#)) was implemented in a Rydberg atom by [Ahn et al. \(2000\)](#) and other work has considered the implementation of logic gates between bits that are Rydberg encoded ([Remacle et al., 2001](#)). These ideas are constrained by the finite lifetime of Rydberg levels although some novel approaches to increasing the coherence time have been studied ([Brion et al., 2005](#); [Minns et al., 2006](#)). [Gillet et al. \(2010\)](#) showed using a density ma-

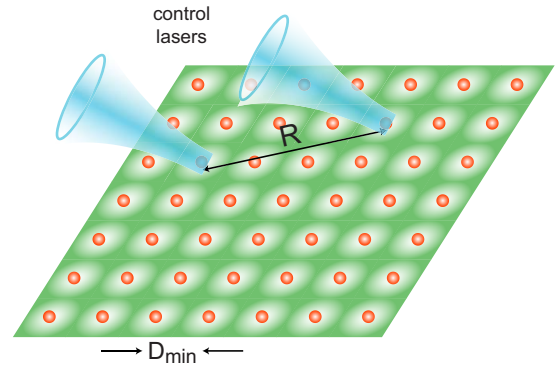


FIG. 18. (Color online) Neutral-atom qubit array in an optical lattice with period D_{\min} . A two-qubit gate between sites separated by R is implemented with focused laser beams.

trix analysis that continuous driving of a two-atom system leads to a stationary degree of entanglement despite radiative decay of the Rydberg levels.

On a more fundamental level it has been argued convincingly that even if the finite lifetime of excited states was not an issue, the spectrum of energy levels in atomic systems does not provide a scalable approach to quantum computing ([Blume-Kohout et al., 2002](#)). This is due to the fact that a single-atom encoding requires an exponential increase in the available physical resources to provide a linear increase in the dimension of Hilbert space available for computation.

D. Scalability of a Rydberg gate quantum computer

The various gate protocols described in the preceding sections rely on long-range interactions between Rydberg excited atoms. Since high fidelity gates are possible at tens of microns of separation (see Figs. 14 and 15) it is natural to ask how many qubits could be directly entangled, without mechanical motion, in an array of trapped atoms, such as that shown in Fig. 18. We envision an optical lattice of sites with one atom in each site. The largest possible separation R_{\max} depends on how high a value of n is feasible. The number of connected qubits then scales as $(R_{\max}/D_{\min})^d$, with d the space dimensionality of the array. The lattice spacing D_{\min} is constrained by technical considerations associated with creating the lattice sites but also by the requirement that a Rydberg excited electron with characteristic orbital radius $\sim a_0 n^2$ should not collide with a neighboring ground-state atom. An analysis of the scaling of gate errors with R and n in the van der Waals limit, taking these considerations into account, leads to the results ([Saffman and Mølmer, 2008](#))

$$N_{\max, \text{vdW}}^{(2D)} = C_{2D} E^{1/3} n^{2/3}, \quad (34a)$$

$$N_{\max, \text{vdW}}^{(3D)} = C_{3D} E^{1/2} n. \quad (34b)$$

Here C_{2D}, C_{3D} are constants that are expected to vary only slightly between different atomic species and E is the gate error discussed in Secs. III.B and III.C.

A realistic estimate assuming $n=100$ and $E=0.001$ results in (Saffman and Mølmer, 2008) $N_{\max, \text{vdW}}^{(2\text{D}, 3\text{D})} = 470, 7600$. Higher n would of course lead to even larger numbers. These estimates suggest that a moderately sized fully interconnected quantum computer with hundreds of qubits in two-dimensional (2D) and thousands of qubits in 3D is possible using Rydberg interactions. Actually building such a device will require solutions to several unresolved problems. A recent analysis of some of the issues related to scalability can be found in Beals *et al.* (2008). We do not intend to engage in a detailed discussion here. Nevertheless, a brief overview of what the challenges are seems appropriate.

A set of criteria for implementing a quantum computing device have been given by DiVincenzo (1998). In principle all requirements can be met by the type of neutral atom qubit array shown in Fig. 18. If we limit ourselves to a 2D geometry, site selective addressing of neutral atom qubits with focused laser beams or magnetic field gradients is relatively straightforward and has been demonstrated in several experiments (Schradler *et al.*, 2004; Lengwenus *et al.*, 2006; Yavuz *et al.*, 2006; Jones *et al.*, 2007; Urban, Johnson, *et al.* 2009). Taking advantage of the higher connectivity of a 3D array makes the problem of site selective addressing and measurement more challenging although possible solutions have been proposed (Weiss *et al.*, 2004; Vaishnav and Weiss, 2008).

The question of preparing single-atom occupancy in a large lattice is more challenging. Stochastic loading of atoms from a cold background vapor is governed by Poisson statistics giving a maximum success probability of $P_1=1/e \approx 0.37$ at each site. The probability of loading each of N sites with one atom thus scales as $P_N=P_1^N=e^{-N}$ which is not useful for large N . The situation can be improved slightly using collisional blockade (Schlosser *et al.*, 2001) or light assisted collisions (Nelson *et al.*, 2007) to raise the success probability to $P_1 \approx 0.5$. Of course it may be sufficient to simply register which sites are occupied and then use only those sites for performing calculations although this will imply a departure from the scaling relations of Eqs. (34).

It is therefore tempting to seek ways to approach deterministic single-atom loading in all sites of an array. An elegant solution involves exploiting the superfluid Mott insulator transition in a cloud of ultracold atoms, and then transferring the Mott insulator to a longer period lattice that is optically resolvable (Peil *et al.*, 2003). Other solutions involve imperfectly loading a lattice and then removing empty or doubly occupied sites, leading eventually to a zero entropy, perfect lattice (Rabl *et al.*, 2003; Weiss *et al.*, 2004; Vala *et al.*, 2005; Würtz *et al.*, 2009). There is also the possibility of using a movable optical tweezer to systematically transfer atoms between sites as needed (Beugnon *et al.*, 2007) or from a reservoir into lattice sites. A different type of approach, to be discussed in Sec. V.B, uses entanglement to enable deterministic single-atom loading (Saffman and Walker, 2002). Alternatively, collective encoding of qubits in many-atom ensembles (Brion, Mølmer, and Saffman, 2007) removes the requirement of single-atom loading

altogether. We discuss this approach in Sec. V.E.

Implementation of extended quantum algorithms requires error correction which depends on the ability to measure the state of a qubit and restore it to an initial state, without atom loss, and without disturbing qubits at neighboring sites. Implementation of multiple measurement cycles requires further either that the measurement does not heat the atom or that recoiling at a single site is possible. Measurement of the state and not just the presence of a neutral atom qubit in free space has until now relied on mechanical ejection of an atom in one of the qubit states, followed by a state insensitive atom number measurement (Kuhr *et al.*, 2003; Treutlein *et al.*, 2004; Jones *et al.*, 2007). Although a lost atom could be replaced from a reservoir the requirement of moving a replacement atom into the emptied site implies a slow measurement cycle. Recent developments in achieving stronger coupling between single atoms and light in free space with tightly focused optical beams (Tey *et al.*, 2008; Aljunid *et al.*, 2009), as well as resolution of individual sites in short period lattices (Bakr *et al.*, 2009), suggest that the capability of loss free state selective measurements is not far off.

A related issue in neutral atom systems is that optical traps have characteristic depths that are small compared to $k_B \times 300$ K so atom loss due to background collisions with room-temperature atoms cannot be completely eliminated. There will therefore be a requirement for monitoring and correcting qubit loss (Vala, Whaley, and Weiss, 2005), which could involve replacing lost atoms with fresh ones from a nearby reservoir. This appears feasible in 2D geometries but more difficult to implement in the interior of a 3D lattice. The number of sites that can be maintained for an arbitrary length of time is limited by $N < \tau_{\text{loss}}/t_{\text{replace}}$, where τ_{loss} is the time constant for atom loss and t_{replace} is the time needed to replace a lost atom. With excellent vacuum pressure of $P \sim 10^{-11}$ Pa a characteristic collision limited lifetime in an optical trap is $\tau_{\text{loss}} \sim 10^4$ s. Assuming a replacement time of $t_{\text{replace}} \sim 0.1$ s this implies an array size limit of $N \sim 10^5$. Note that actually reaching this limit is dependent on the ability to rapidly check all the sites for atom loss. This can be done without disturbing the qubit state at each site using an ancilla bit at a cost of four gates and one measurement (Preskill, 1998). The measurement time should satisfy $Nt_{\text{meas}} < t_{\text{replace}}$. Even a fast measurement time of, for example, $t_{\text{meas}} = 100 \mu\text{s}$ would limit the array to a much smaller $N=1000$. This highlights the necessity of performing parallel operations in order to build a scalable system.

Ultimately even a thousand qubit computer will not be sufficient to solve hard problems that are intractable on classical computers. Scaling to even larger numbers may require connecting multiple, smaller processors, using entanglement between stationary matter qubits and photonic qubits. This is also relevant for quantum networking and long-distance quantum communication (Kimble, 2008). Rydberg interactions present unique opportunities for quantum interfaces between light and

matter, and we defer a discussion of this topic to Sec. VI.B.

IV. EXPERIMENTS

Experimental demonstration of quantum logic with Rydberg atoms builds on several decades of development of techniques for cooling, trapping, and manipulating atoms with electromagnetic fields. A good overview of this field can be found in [Metcalf and van der Straten \(1999\)](#). In this section we discuss specific experimental capabilities needed for neutral atom logic gates. Much of the discussion in Sec. IV.A.1 is generic to schemes based on atomic qubits. We then turn to requirements specific to the use of Rydberg atoms and summarize experimental progress in realizing Rydberg-mediated quantum gates.

A. Experimental techniques

1. Traps for ground-state atoms

The starting point for neutral atom logic gate experiments is cooling, trapping, and detection of isolated atoms. Observation of a single cold neutral atom was first achieved by Hu and Kimble in a magneto-optical trap (MOT) ([Hu and Kimble, 1994](#)). Subsequently several research groups ([Frese et al., 2000](#); [Schlosser et al., 2001](#)) showed that a convenient setting for studying single atoms is provided by far-off-resonance optical traps (FORTs) ([Miller et al., 1993](#); [Grimm et al., 2000](#)).

FORTs can provide long atomic confinement times that are in practice limited only by collisions with untrapped room-temperature atoms. This is because the trap depth scales as $1/\Delta$ while the photon scattering rate, which leads to heating, scales as $1/\Delta^2$, with $\Delta = \omega - \omega_a$ the difference between the trapping laser frequency ω and the relevant atomic transition frequency ω_a . Trap lifetimes approaching 1 min ([Frese et al., 2000](#)) have been observed for Cs atoms in a 1064 nm Nd:YAG laser FORT. As long as the atoms can be cooled to $k_B T \ll E_{\text{trap}}$ there is no fundamental limit to the trap lifetime. However, as mentioned, optical traps have $E_{\text{trap}} \ll k_B \times 300$ K so trap lifetimes are limited by collisions with hot background atoms. Paul traps for ions can have $E_{\text{trap}} > k_B \times 300$ K and extremely long lifetimes up to several weeks have been observed.

With the availability of a single atom in an optical trap a qubit can be encoded in Zeeman or hyperfine ground states. Of particular importance for quantum information applications is the coherence time of an encoded quantum superposition state. In order to maximize the coherence time in the presence of background magnetic field fluctuations it is advantageous to use pairs of states that exhibit a field insensitive operating point, with a quadratic relative Zeeman shift for field deviations away from the optimum. In this way coherence times of many seconds have been observed with trapped ions in Paul traps ([Langer et al., 2005](#); [Benhelm et al., 2008a](#)).

In alkali atoms with a $^2S_{1/2}$ ground state and nuclear spin I the $f=I\pm 1/2$, $m_f=0$ hyperfine clock states have a quadratic relative shift at zero applied field. There are also pairs of states with $\Delta m_f=1$ that have a quadratic shift but only at bias fields greater than 10 mT, which is problematic in the context of excitation of magnetically sensitive Rydberg states. Alternatively one can find low field quadratic shifts for states that have $\Delta m_f \geq 2$. However, driving Raman transitions between these states requires multiphoton transitions that tend to be slow. The alkali clock states therefore appear best suited for qubit encoding at the present time.

In addition to decoherence due to external fields, the FORT traps themselves also limit qubit coherence ([Kuhr et al., 2005](#); [Saffman and Walker, 2005a](#); [Windpassinger et al., 2008](#)). At detunings large compared to the fine-structure splitting of the states that are excited by the FORT laser there is a cancellation of Raman amplitudes, so the rate of state changing photon scattering is very low, scaling as $1/\Delta^4$ ([Cline et al., 1994](#)). Hyperfine relaxation times of several seconds were originally observed ([Cline et al., 1994](#)) with Rb atoms. A subsequent demonstration with an extremely far detuned CO₂ laser operating at 10.6 μm pushed the relaxation time to greater than 10 s ([Takekoshi and Knize, 1996](#)). An additional source of decoherence arises from atomic motion in the optical trap which induces differential ac Stark shifts on the qubit states. This issue disappears for atoms in the motional ground state but is otherwise the limiting factor for qubit coherence in optical traps ([Saffman and Walker, 2005a](#)). The differential shift can be reduced using an additional weak laser beam that does not provide trapping, but cancels the trap-induced differential shift ([Kaplan et al., 2002](#)).

Photon scattering and motional decoherence effects can be significantly reduced by working with dark optical traps where the atoms are localized near a local minimum, instead of a local maximum of the trapping light intensity ([Chaloupka et al., 1997](#); [Arlt and Padgett, 2000](#)). Several research groups have demonstrated atom trapping in this type of setup ([Kuga et al., 1997](#); [Ozeri, Khaykovich, and Davidson, 1999](#); [Kulin et al., 2001](#); [Terraciano et al., 2008](#); [Isenhower et al., 2009](#); [Xu et al., 2010](#)). We anticipate that trapping and coherence times of at least several seconds will be achieved with single-atom qubits in optimized dark optical traps although a definitive experimental demonstration has not yet been presented. Although long coherence times are important in any quantum computing device, it is difficult to say whether or not errors in a quantum computer will be dominated by the memory coherence time or by gate errors. The scaling of memory to gate errors depends on many factors including the computation being performed, the size of the register, and other architectural considerations.

Scalability of optical trapping to many qubits relies on either multiplexing traps using diffractive optical elements ([Bergamini et al., 2004](#)) or lens arrays ([Dumke et al., 2002](#)) or taking a different route of optical trapping in lattices ([Jessen and Deutsch, 1996](#)). Lattices formed

from counterpropagating beams in the near infrared have submicron periods and are not readily compatible with site selective addressing, measurement, and control although possible solutions (Saffman, 2004; Zhang *et al.*, 2006; Cho, 2007; Yavuz and Proite, 2007; Gorshkov, Jiang, *et al.*, 2008; Vaishnav and Weiss, 2008) as well as experimental capabilities (Bakr *et al.*, 2009; Karski, Förster, Choi, Alt, *et al.*, 2009; Lundblad *et al.*, 2009) are being actively developed. Alternatives rely on lattices formed from a long wavelength CO₂ laser (Scheunemann *et al.*, 2000) or multibeam lattices that have adjustable longer scale periodicity (Peil *et al.*, 2003; Nelson *et al.*, 2007). A new idea recently demonstrated by Kübler *et al.* (2010) is to use micron-sized vapor cells, each small enough to enable an effective blockade interaction throughout the volume of the cell, as a means of defining an ensemble qubit.

Magnetic traps, which do not suffer from photon scattering, are an interesting alternative to optical approaches (Fortágh and Zimmermann, 2007). Lifetimes in the range of 10 min have been achieved with neutral atoms in a cryogenic magnetic trap (Emmert *et al.*, 2009) and hyperfine coherence times exceeding 1 s have been demonstrated (Treutlein *et al.*, 2004). Arrays of magnetic traps (Weinstein and Libbrecht, 1995; Hinds and Hughes, 1999; Grabowski and Pfau, 2003; Gerritsma *et al.*, 2007) are also a potential setting for encoding a qubit register.

Finally we note that a large scale atom based quantum computer will require accurate and fast spatial control of several laser beams. Different technologies are suitable for this task including electro-optic deflectors (Schmidt-Kaler *et al.*, 2003), acousto-optic deflectors (Nägerl *et al.*, 1999; Kim *et al.*, 2008), and micro-optoelectromechanical systems (Knoernschild *et al.*, 2009). Scaling to arrays with more than a few tens of qubits will likely require further development of specialized devices.

2. Traps for Rydberg atoms

Irrespective of the type of trap used to hold the qubits we must also consider the effect of the trapping potential on Rydberg states. Ideally we wish to have the same trapping potential for both ground and Rydberg states. If this is not the case, excitation to Rydberg levels will result in motional excitation of the atom and, more importantly, undesired entanglement between the center of mass and qubit degrees of freedom. This can be seen by the following simple argument. Suppose the qubit state $|\psi\rangle = a|0\rangle + b|1\rangle$ is stored in an atom in the ground state $|0\rangle_{\text{vib}}$ of the trapping potential. The total state of the qubit plus atom is $|\Psi\rangle = |\psi\rangle \otimes |0\rangle_{\text{vib}}$. Vibrational excitation during a Rydberg cycle will lead to the new state $|\Psi'\rangle = a|0\rangle \otimes |0\rangle_{\text{vib}} + b|1\rangle \otimes (c|0\rangle_{\text{vib}} + d|1\rangle_{\text{vib}})$ where, for simplicity, we have only considered excitation of the first vibrational state with amplitude d . Tracing over the vibrational degrees of freedom gives the reduced density matrix

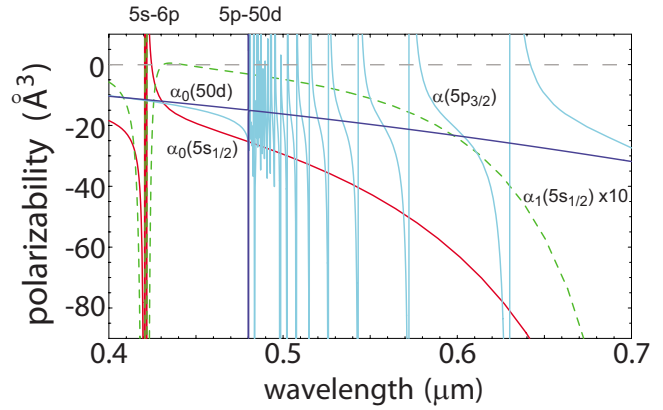


FIG. 19. (Color online) Polarizability of Rb ground ($5s_{1/2}$), first resonance level ($5p_{3/2}$), and Rydberg 50d states (solid line). The vector polarizability of the ground state (dashed line) is also shown.

$$\rho_{\text{qubit}} = \text{Tr}_{\text{vib}}[\rho] = \begin{pmatrix} |a|^2 & ab^*c^* \\ a^*bc & |b|^2 \end{pmatrix}. \quad (35)$$

Since $|c| < 1$, vibrational excitation results in reduced coherence of the qubit.

In order to have the same trapping potential for ground and Rydberg states in an optical trap the polarizability must be the same for both levels. The polarizability of a highly excited Rydberg state is negative being essentially that of a free electron, $\alpha = -e^2/m\omega^2$, where $-e$ is the electron charge and m is the electron mass. In a red detuned, bright ground-state trap the polarizability is positive. Nevertheless, matching can be achieved at specific wavelengths by working close to a ground-intermediate level resonance or a resonance between Rydberg and intermediate levels. Details of specific schemes are given by Safronova *et al.* (2003) and Saffman and Walker (2005a).

If we use a blue detuned dark optical trap or dark lattice then there is a broad region to the blue of the first resonance lines in the heavy alkalis where the ground-state polarizability is negative. As shown in Fig. 19 exact matching between the Rb $5s$ ground state and the $50d$ Rydberg state occurs at $\lambda = 430$ nm. It turns out that the polarizability of the first resonance level is also approximately equal to the ground-state polarizability at this wavelength, which is advantageous for Doppler cooling inside the optical trap. Furthermore the ground-state vector polarizability, which determines the rate of hyperfine changing Raman scattering events, is extremely small. This short wavelength matching point is thus attractive for neutral atom optical traps. The matching wavelength does not change significantly with choice of Rydberg level since the polarizability of the $50d$ state is already about 95% of the free electron polarizability. A similar coincidence point occurs at a longer wavelength for Cs atoms. The notion of an optical trap for Rydberg atoms can also be extended to an optical lattice setting as discussed by Dutta *et al.* (2000).

An important issue when using optical traps to confine Rydberg atoms is the problem of Rydberg photoionization due to the trapping light. Photoionization rates in mK trapping potentials substantially exceed the radiative decay rate (Saffman and Walker, 2005a; Potvliege and Adams, 2006) and represent the limiting factor for Rydberg trapping. Thus the experiments to date on coherent excitation in optical traps have relied on turning off the trapping potential during the Rydberg excitation pulse (see Sec. IV.B). This problem may be greatly reduced in a dark optical trap where the atom sits at a minimum of the trapping light intensity. However, if we consider excitation of very high-lying levels with $n > 100$ in order to achieve long-range gates, as in Sec. III.B, the wave function of the Rydberg electron will sample regions of non-negligible trapping light intensity, even in dark optical traps. As is well known, a free electron cannot absorb a photon, and therefore the photoionization cross section tends to be localized near the nucleus. A careful analysis of the photoionization rate in dark traps has not yet been performed.

An alternative to optical traps is to use low frequency electromagnetic traps which can be effective for both ground and Rydberg atoms, see Choi *et al.* (2007) for an extended discussion. Rydberg atoms in low field seeking Stark states were loaded into an electrostatic trap by Hogan and Merkt (2008). Magnetostatic trapping of high angular momentum Rydberg atoms was demonstrated in a strong field of several Tesla by Choi *et al.* (2005) and Choi, Guest, and Raithel (2006). Trapping in a high gradient quadrupole field and in combined magnetic and electric traps was studied (Lesanovsky and Schmelcher, 2005; Hezel *et al.*, 2007; Schmidt *et al.*, 2007). It was proposed (Hyafil *et al.*, 2004; Mozley *et al.*, 2005) to use the electrodynamic trap described by Peik (1999) together with conducting planes for inhibition of spontaneous emission to create a long coherence time trap for circular Rydberg states. A successful demonstration of this idea in two proximally located traps would open the door to long time scale high precision studies of the dipole-dipole interaction. We remark that the electromagnetic geometries, although capable of trapping Rydberg atoms, tend to rely on high m states which are not readily compatible with few photon laser excitation. This restriction has been relaxed in recent work (Mayle *et al.*, 2009a, 2009b) that has shown theoretically the feasibility of magnetic trapping of s, p , or d Rydberg states in Ioffe-Pritchard geometries, with good qubit coherence.

Approaches based on arrays of magnetic traps (Grabowski and Pfau, 2003; Gerritsma *et al.*, 2007), although promising for holding ground-state atoms, may be difficult to combine with Rydberg atoms. In order to achieve tightly confining magnetic traps the surface to trap distance is typically on the order of tens of microns, which can lead to undesired interactions between the surface and Rydberg atom. The question of Rydberg-surface interactions may also be problematic for the microcell approach demonstrated by Kübler *et al.* (2010). Indeed the coupling of Rydberg atoms to conductors

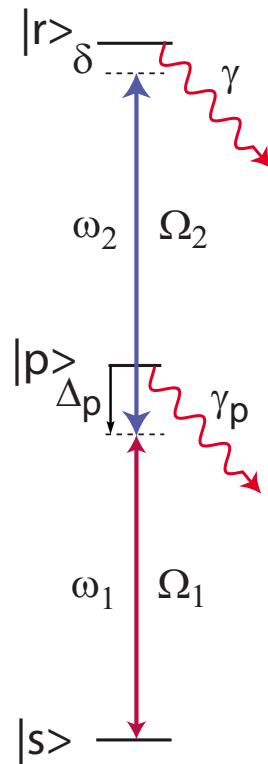


FIG. 20. (Color online) Two-photon excitation of Rydberg level $|r\rangle$. The radiative decay rates of $|p\rangle$ and $|r\rangle$ are $\gamma_p = 1/\tau_p$ and $\gamma = 1/\tau$, respectively.

forms the basis for hybrid entanglement schemes to be discussed in Sec. VI.D. A combination of magnetic trapping ideas and hybrid interfaces may eventually prove fruitful, but remains largely unexplored.

B. Coherent excitation of Rydberg states

Laser excitation and spectroscopy of Rydberg atoms has a long history dating back to the development of the tunable dye laser in the early 1970s. Early work is reviewed by Fabre and Haroche (1983). Starting from a ground state Rydberg states can be generated with 1, 2, 3, or more photon transitions. Using electric-dipole-allowed transitions ground s states can be coupled to p states with one photon, to s or d states with two photons, and p or f states with three photons. These selection rules can be modified by Stark or Zeeman mixing of the Rydberg states or by direct excitation via quadrupole transitions (Tong *et al.*, 2009). The gate protocols discussed in Sec. III require extremely precise, coherent excitation and deexcitation of Rydberg states. One photon excitation from the ground state requires a ~ 297 nm photon in Rb which is possible (Thoumany, Hänsch, *et al.*, 2009), but coherence has not yet been demonstrated.

A widely used approach, which does not require deep UV wavelengths, relies on two-photon excitation via the first resonance level as shown in Fig. 20. For example, in ^{87}Rb field 1 is at 780 nm for excitation via $5p_{3/2}$ and field 2 is near 480 nm. The first example of Rydberg spectroscopy with narrow linewidth lasers using this approach

was a study of Autler-Townes spectra in a cold ^{85}Rb sample (Teo *et al.*, 2003). Autler-Townes spectra in Rydberg excitation were also studied later by Grabowski *et al.* (2006). Three-photon excitation schemes with narrow linewidth lasers have also been used in experiments with Cs (Vogt *et al.*, 2006) and Rb (Thoumany, Germann, *et al.*, 2009).

When the intermediate level detuning $\Delta_p = \omega_1 - \omega_{ps}$ is large compared to the width of the hyperfine structure of the $|p\rangle$ level the two-photon Rabi frequency is given by $\Omega = \Omega_1 \Omega_2 / 2\Delta_p$. The one-photon Rabi frequencies are $\Omega_1 = -e\mathcal{E}_1 \langle p | \mathbf{r} \cdot \boldsymbol{\varepsilon}_1 | s \rangle / \hbar$, $\Omega_2 = -e\mathcal{E}_2 \langle r | \mathbf{r} \cdot \boldsymbol{\varepsilon}_2 | p \rangle / \hbar$, with $\mathcal{E}_j, \boldsymbol{\varepsilon}_j$ the field amplitudes and polarizations. The transition matrix elements can be reduced via the Wigner-Eckart theorem to an angular factor plus the radial integral of Eq. (7). For the s - p transition the radial integral is known (for ^{87}Rb $\langle r \rangle_{5s}^{5p} = 5.1a_0$) and for the p - r transition it can be readily calculated numerically. The following expressions are accurate to better than 10% for ^{87}Rb :

$$\langle r \rangle_{5p}^{ns} = 0.014 \times (50/n)^{3/2} a_0$$

and

$$\langle r \rangle_{5p}^{nd} = -0.024 \times (50/n)^{3/2} a_0.$$

There are several potential sources of errors when using two-photon excitation with well-defined pulse areas for coherent population transfer between ground and Rydberg states. Partial population of the intermediate $|p\rangle$ level results in spontaneous emission and loss of coherence. The probability of this occurring during a π excitation pulse of duration $t = \pi/|\Omega|$ is $P_{\text{se}} = (\pi\gamma_p/4|\Delta_p|)(q+1/q)$, where $q = |\Omega_2/\Omega_1|$. The spontaneous emission is minimized for $q=1$ which allows us to write the Rabi frequency as

$$\Omega = \frac{P_{\text{se}} |\Omega_2|^2}{\pi \gamma_p}.$$

We see that fast excitation with low spontaneous emission is possible provided Ω_2 is sufficiently large. This is increasingly difficult as n is raised since $\langle r \rangle_{5p}^{nl} \sim 1/n^{3/2}$. Put another way, at constant Ω and P_{se} the required optical power scales as n^3 .

Another issue is detuning errors due to Doppler broadening. These can be reduced from $\delta_{\text{max}} = (k_1 + k_2)v$ to $\delta_{\text{max}} = (k_1 - k_2)v$ for atomic velocity v using counter-propagating excitation beams. Excitation can be made Doppler free if $|\mathbf{k}_1| = |\mathbf{k}_2|$ (Lee *et al.*, 1978) or by tuning close to the intermediate level (Reynaud *et al.*, 1982). However, neither approach is well suited for coherent experiments due to the slow rate of the first approach, which has no intermediate level resonance, and the large spontaneous emission probability incurred in the second.

Another source of detuning errors arises from the ac Stark shifts caused by the excitation lasers. The dominant contributions come from the near resonant interactions of ω_1 with $|s\rangle$ and ω_2 with $|r\rangle$. The ground state $|s\rangle$ is Stark shifted by $\delta_s = |\Omega_1|^2/4\Delta_p$, while the Rydberg state

$|r\rangle$ is shifted by $\delta_r = -|\Omega_2|^2/4\Delta_p$. We see that the transition shift $\delta_s + \delta_p$ vanishes when $|\Omega_1| = |\Omega_2|$ or $q=1$, which is another reason to work with equal Rabi frequencies, in addition to the minimization of spontaneous emission. The cancellation is not perfect since there are additional off-resonant contributions from ω_1 acting on $|r\rangle$ (which tends to be small) and ω_2 acting on $|s\rangle$, which tends to be larger due to the high intensity of the field driving p - r . The intensity-dependent Stark shift of the transition frequency has been observed in experiments with trapped ^{87}Rb atoms (Urban, Henage, *et al.*, 2009).

When working with trapped atoms it is also necessary to take account of the differential trap shift between ground and Rydberg levels. Besides the loss of coherence described by Eq. (35) the trap shifts, which depend on the position of the atom in the trap, can easily exceed $|\Omega|$ in a few mK deep trap, which would be disastrous for coherent excitation. For this reason and also because the trapping light in all experiments performed to date rapidly photoionizes the Rydberg atoms, the trap is turned off during the Rydberg excitation pulse. This is problematic in the context of many-qubit systems and therefore the development of trap architectures that are insensitive to the internal state, as discussed in Sec. IV.A.2, will be an important topic for future work.

Transition shifts due to magnetic fields and Rydberg level shifts due to small electric fields are also of concern. The magnetic sensitivity is manageable in optical traps but could be problematic for atoms in thermal motion in a magnetic trap. Ground-state polarizabilities of alkali atoms are small enough that typical stray laboratory fields have a negligible effect. However, as discussed in Sec. II.A, the dc Stark shift of a Rydberg state scales as n^7 . This puts severe limits on the field stability needed for excitation of very high-lying levels.

A convenient way of measuring and controlling the small field strengths involved is to use the shift of the Rydberg level itself as a diagnostic (Frey *et al.*, 1993; Osterwalder and Merkt, 1999). Recent work has used electromagnetically induced transparency (EIT) (Fleischhauer *et al.*, 2005) for precise Rydberg spectroscopy. EIT is a destructive interference effect with a very narrow linewidth, and it can hence be used to measure precisely the Rydberg series of energy levels. Mohapatra *et al.* (2007) measured the fine-structure splitting of the Rb nd series with n up to 96. In the same work, it was pointed out that due to the large dipole moment of Rydberg excited states they are very sensitive electric field probes. The narrow EIT linewidth thus makes it possible to detect a small electric field or, conversely, to control the transmission properties of an atomic ensemble with very weak switching fields (Mohapatra *et al.*, 2007, 2008; Bason *et al.*, 2008). Rydberg spectroscopy using EIT signals in Cs cells has also been demonstrated (Zhao *et al.*, 2009). In addition EIT has been shown to be useful for the determination of atom-wall-induced light shifts and broadenings in thermal vapor microcells (Kübler *et al.*, 2010).

In order to get a sense of the errors involved consider the following example of excitation of the ^{87}Rb $100d_{5/2}$ level via $5p_{3/2}$. Assume π polarized beams with powers of $1\ \mu\text{W}$ at $780\ \text{nm}$ and $300\ \text{mW}$ at $480\ \text{nm}$ focused to spots with Gaussian waist $w=3\ \mu\text{m}$. This gives single-photon Rabi frequencies of 225 and $210\ \text{MHz}$. The light is detuned from $5p_{3/2}$ by $\Delta_p/2\pi=20\ \text{GHz}$. These parameters couple $m=0$ ground states to $m=\pm 1/2$ Rydberg states with a Rabi frequency $\Omega/2\pi=1.2\ \text{MHz}$. The probability of spontaneous emission from the p level during a π pulse is $P_{\text{se}}=5\times 10^{-4}$. The fractional excitation error after a π pulse due to Doppler broadening is $P_{\text{Doppler}}=|\delta/\Omega|^2$. For ^{87}Rb atoms at $T=10\ \mu\text{K}$ and counterpropagating excitation beams we find $P_{\text{Doppler}}=4\times 10^{-4}$. Thus, coherent excitation of a very high-lying Rydberg level with combined spontaneous emission and Doppler errors below 10^{-3} is within reach of current experimental capabilities.

It is also necessary that the two-photon excitation be performed with well-stabilized lasers so that the detuning $\delta=\omega_1+\omega_2-\omega_{rs}$ is small compared to Ω . This can be achieved by locking the lasers to stabilized optical reference cavities (Bohlouli-Zanjani *et al.*, 2006; Johnson *et al.*, 2008). It is also possible to use the Rydberg atoms themselves as a frequency reference (Abel *et al.*, 2009). The relative phase of ω_1, ω_2 should also be well defined for the duration of a Rabi pulse. Locking the lasers to stable, high finesse resonators readily gives linewidths at the $\sim 100\ \text{Hz}$ level which is more than adequate for μs time scale pulses. Modern frequency comb techniques (Cundiff and Ye, 2003) could also be used for both frequency and phase stabilization of the Rydberg lasers.

Even with the above imperfections under control there is one more significant issue that must be confronted before coherent Rabi oscillations can be observed. We are coupling hyperfine ground states characterized by quantum numbers $n, l, j, l', s, f, m_l, m_f$ to highly excited Rydberg fine-structure states that have negligible hyperfine structure and are therefore described by the quantum numbers $n', l, j', l', s, m_l', m_f'$. In most cases there are two Rydberg Zeeman states with different values of m_f' that have nonzero electric dipole matrix elements with the ground state. Only one Rydberg Zeeman state is coupled to if we start from a stretched ground state $m_f=\pm f$ or use ω_1 with σ_{\pm} polarization coupling via a $np_{1/2}$ level. Apart from these special cases any difference in energy between the excited states due to m_f' dependent Stark or Zeeman shifts will lead to a complex nonsinusoidal excitation dynamics since Ω is also dependent on m_f' . To avoid this problem it is necessary to optically pump the ground-state atoms into a specific m_f state and apply a bias field to separate the m_f' states by an amount that is large compared to Ω .

Taking the above considerations into account the first demonstrations of Rabi oscillations between ground and Rydberg levels were reported in 2008 (Johnson *et al.*, 2008; Reetz-Lamour, Amthor, *et al.*, 2008). Figure 21(a) shows oscillations of single ^{87}Rb atoms confined to an

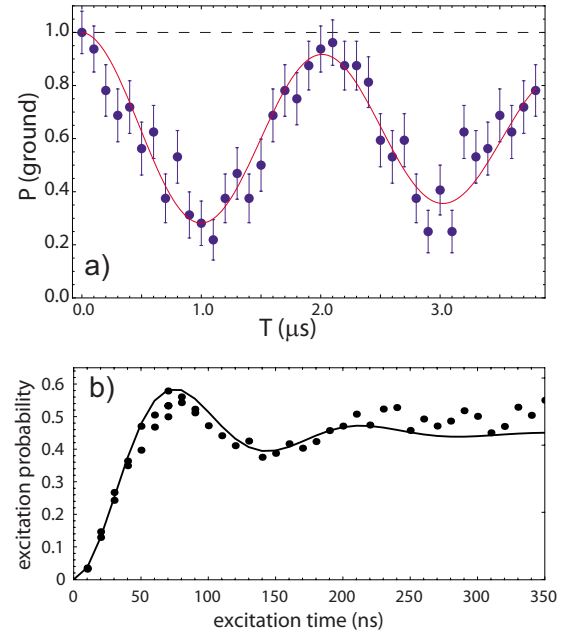


FIG. 21. (Color online) Rabi oscillations between ground and Rydberg levels: (a) using single atoms from Johnson *et al.* (2008) and (b) in a sample with ~ 100 atoms from Reetz-Lamour, Amthor, *et al.* (2008).

optical trap with radius of about $3\ \mu\text{m}$ and optically pumped into $f=2, m_f=2$. Rydberg excitation to $43d_{5/2}, m_f=1/2$ used π polarized lasers at 780 and $480\ \text{nm}$. The excitation laser beams had waists that were a few times larger than the width of the optical trap so the effects of spatial variation in the Rabi frequency were minimized. The confining to an optical trap was turned off before the excitation lasers were applied. After a variable length excitation pulse the trap was turned on again which photoionized the Rydberg atoms before they could radiatively decay. Loss of a Rydberg atom from the trap therefore provided a signature of successful Rydberg excitation. The less than 100% probability of exciting a Rydberg atom was attributed mainly to Doppler broadening at $T=200\ \mu\text{K}$ and the finite Rydberg detection efficiency since the ratio of the photoionization to radiative decay rates was $\gamma_{\text{pi}}/\gamma\sim 20$.

Subsequent experiments extended these single-atom results to even higher levels: $58d_{3/2}$ (Gaëtan *et al.*, 2009), $79d_{5/2}$, $90d_{5/2}$ (Urban, Johnson, *et al.*, 2009), $97d_{5/2}$ (Isenhower *et al.*, 2010), and $43d_{5/2}$ (Zuo *et al.*, 2009). With sufficient optical power, and careful minimization of stray electric fields, there is no reason why coherent excitation cannot be pushed to even higher n . This is attractive as a way of directly entangling many qubits, with the number scaling as $n^{2/3}$ in a 2D array [see Eq. (34)]. A new constraint arises when the energy separation between states n, l, j and $n\pm 1, l, j$ becomes comparable to Ω . Since the blockade gate spontaneous emission error from Eq. (26) has a $1/\Omega\tau\sim 1/\Omega n^3$ contribution, and the error due to excitation of multiple n levels goes as $[\Omega/(E_{n,l,j}-E_{n\pm 1,l,j})]^2\sim \Omega^2 n^6$ minimization of the sum of these errors is independent of n for large n . However,

undesired excitation of the noncoupled ground state which normally scales as Ω^2/ω_{10}^2 will become significant when $\delta_{n,n\pm 1} = |E_{n,l,j} - E_{n\pm 1,l,j}| \ll \omega_{10}$. A conservative estimate of the limit can be deduced by putting $\Omega/2\pi \sim 1$ MHz so that a 10^{-4} gate error requires $\delta_{n,n\pm 1}/2\pi > 200$ MHz which corresponds to $n \sim 325$. We conclude that coherent two-photon oscillations with high fidelity are in principle feasible up to $n \sim 300$ given the requisite high power narrow linewidth laser system. A practical limit may arise at lower n due to the need to control external electric fields to limit Stark shifts which grow $\sim n^7$.

Much work has been done pursuing the observation of coherent oscillations in a many-atom regime which is an essential capability for the ensemble qubit protocols mentioned in the Introduction, and discussed in Sec. V. If the atomic sample is smaller than the range of the Rydberg interaction, a \sqrt{N} collective enhancement of the Rabi frequency is expected. However, even when a full blockade is not achieved, Rydberg interactions serve to dephase the coherent oscillations. Dephasing without blockade was observed by Johnson *et al.* (2008) by loading a small number of atoms into the optical trap. The visibility of the Rabi oscillations quickly decayed as the number of atoms was increased from one to close to ten. As shown in Fig. 21(b) relatively weak oscillations have also been observed in excitation to $47d_{5/2}$ with much larger samples containing about 100 atoms (Reetz-Lamour, Amthor, *et al.*, 2008; Reetz-Lamour, Deiglmayr, *et al.*, 2008). In that work the size of the cold atom sample was larger than the counterpropagating excitation beams. In order to reduce the broadening effects associated with a spatially dependent Rabi frequency the much smaller 480 nm beam was given a close to “top hat” spatial profile. Inspection of Fig. 21(b) shows that the excitation is only partially returned to the ground state due to the presence of dephasing mechanisms, as well as “excitation trapping” resulting from population transfer to additional Rydberg levels not coupled to the light field (Reetz-Lamour, Deiglmayr, *et al.*, 2008). These dephasing effects are qualitatively well reproduced by model calculations describing mesoscopic samples (Stanojevic and Côté, 2009).

Other excitation schemes going beyond simple square pulses have also been used in attempts to observe collective oscillations. Stimulated Raman adiabatic passage using a counterintuitive pulse sequence where the 480 nm laser is applied before the 780 nm was used to demonstrate excitation probabilities as high as $\sim 70\%$ in mesoscopic samples of cold atoms (Cubel *et al.*, 2005; Deiglmayr *et al.*, 2006). Excitation of mesoscopic blockaded samples has been studied using ultracold Rb atoms close to the Bose-Einstein condensate (BEC) transition temperature (Heidemann *et al.*, 2007, 2008). The \sqrt{N} scaling was observed, and will be discussed in connection with collective effects in Rydberg ensembles in Sec. V.A. The dephasing effects of atomic motion and Rydberg interactions can be compensated for using rotary echo techniques, which have been explored in recent

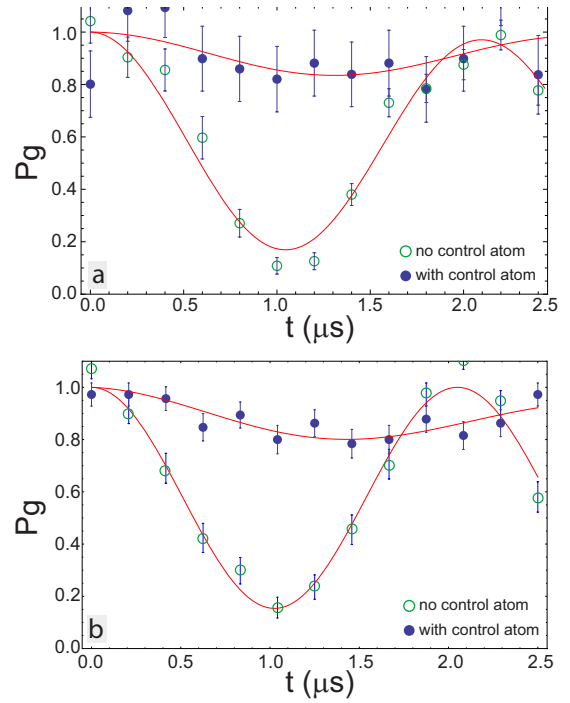


FIG. 22. (Color online) Two-atom Rydberg blockade. (a) The experimental data for Rydberg excitation of the target atom with and without a control atom present. (b) A Monte Carlo simulation accounting for experimental imperfections. The amplitude of the curve fit to the blockaded oscillations is $a = 0.09$ (experiment) and $a = 0.11$ (simulation). From Urban, Johnson, *et al.*, 2009.

calculations (Hernández and Robicheaux, 2008b) and experiments (Raitzsch *et al.*, 2008; Younge and Raithel, 2009). Although coherent excitation in many-atom samples has been studied in several experiments, and signatures of collective effects are clearly seen, a high visibility time domain record of many-body Rabi oscillations has not been achieved. This remains a challenge for quantum information applications of Rydberg ensembles.

C. Two-atom blockade, two-qubit gates, and entanglement

Recently it has been shown by experimental groups at Wisconsin and at Institute of Optics, Palaiseau that the experimental methods described above can be combined to demonstrate Rydberg blockade (Gaëtan *et al.*, 2009; Urban, Johnson, *et al.*, 2009), two-qubit quantum gates (Isenhower *et al.*, 2010), and entanglement generation between two atoms (Isenhower *et al.*, 2010; Wilk *et al.*, 2010).

The blockade experiment in Wisconsin (Urban, Johnson, *et al.*, 2009) showed that excitation of a Rb atom to $90d_{5/2}$ blocked the subsequent excitation of an atom at $R \geq 10 \mu\text{m}$ with a fidelity of about 90%. Experimental data together with a Monte Carlo simulation taking into account the finite blockade strength and experimental imperfections are shown in Fig. 22.

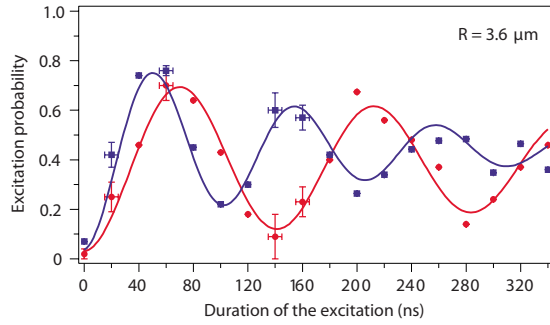


FIG. 23. (Color online) Collective excitation in the blockade regime. Excitation of one atom vs collective excitation of two atoms separated by $3.6 \mu\text{m}$. The circles represent the probability to excite atom a when atom b is absent. A fit to the data yields a frequency of this Rabi oscillation $\Omega/2\pi = 7.0 \pm 0.2$ MHz. The squares represent the probability to excite only one atom when the two atoms are trapped and are exposed to the same excitation pulse. The fit gives an oscillation frequency $\Omega/2\pi = 9.7 \pm 0.2$ MHz. The ratio of the oscillation frequencies is 1.38 ± 0.03 close to the value $\sqrt{2}$ expected for the collective oscillation of two atoms. From Gaëtan *et al.*, 2009.

A closely related experiment in Palaiseau (Gaëtan *et al.*, 2009) used simultaneous excitation of two Rb atoms in traps separated by $R \sim 3.6 \mu\text{m}$. A strong blockade shift was obtained using the $58d_{3/2}$ Förster resonance, which was first identified by Reinhard *et al.* (2007). The first stage of the excitation used 794 nm light coupling via the $5p_{1/2}$ level. This is preferable since the radial matrix elements for excitation of $nd_{3/2}$ states are about $8\times$ larger when exciting via the $5p_{1/2}$ level rather than the $5p_{3/2}$ level. As shown in Fig. 23 excitation of two atoms with $B \gg \Omega$ couples the two-atom state $|ss\rangle$ to the symmetric singly excited state $(1/\sqrt{2})(|gr\rangle + e^{i\phi}|rg\rangle)$ at the collectively enhanced Rabi frequency $\Omega_c = \sqrt{2}\Omega$. The $\sqrt{2}$ speedup is clearly seen in the data which are strong evidence for the creation of a two-atom entangled state.

The entanglement resides in the Rydberg levels and is therefore very short lived. In a subsequent experiment (Wilk *et al.*, 2010) the Palaiseau group mapped the state $|r\rangle$ to a different hyperfine ground state to create long-lived entanglement of the form $|\psi\rangle = (1/\sqrt{2})(|01\rangle + |10\rangle)$. Note that the phase ϕ present in the Rydberg entangled state has been canceled by the mapping pulse, provided it is applied fast enough to neglect atomic motion, which is the case in the experiment. To verify the presence of entanglement the coherence of the two-atom density matrix was extracted from parity oscillation measurements on the output states (Turchette *et al.*, 1998) shown in Fig. 24. The experimental results gave an entanglement fidelity of $F = 0.46$ which is just under the threshold of $F = 0.5$ for entanglement, whereas a perfectly entangled state would have $F = 1$. In the experiments there was only a 61% probability of both atoms remaining in the trap at the end of the entanglement sequence. Correcting for the atom loss (Gaëtan *et al.*, 2010) it was inferred that the remaining atom pairs were entangled with a fidelity $F = 0.75(7)$.

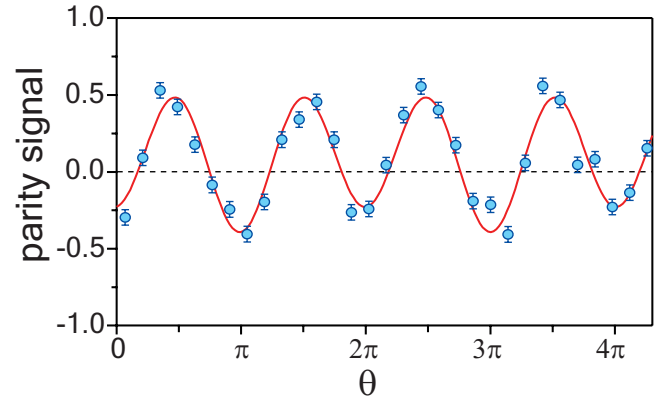


FIG. 24. (Color online) Measured parity signal. For different durations $\theta = \Omega t$ of the analyzing Raman pulse. The data are fitted by a function of the form $y_0 + A \cos(\Omega t) + B \cos(2\Omega t)$. The error bars on the data are statistical. From Wilk *et al.*, 2010.

In work completed at the same time the Wisconsin group extended their observation of blockade to demonstration of a CNOT gate. Taking advantage of their larger $10 \mu\text{m}$ atom separation and the ability to apply different pulses to the two atoms they used a version of the amplitude swap gate (see Fig. 16), as well as the standard Hadamard C_Z sequence of Fig. 16 to acquire the data shown in Fig. 25. They also showed that by putting the control atom in a superposition state $(1/\sqrt{2})(|0\rangle + |1\rangle)$ before running the CNOT gate they could create approximations to the entangled states $|B_1\rangle = (1/\sqrt{2})(|00\rangle + |11\rangle)$ or $|B_2\rangle = (1/\sqrt{2})(|01\rangle + |10\rangle)$ depending on the input state of the target atom. Using parity oscillations the entanglement fidelity of $|B_1\rangle$ was measured to be $F = 0.48 \pm 0.06$. The probability of losing at least one of the atoms during the gate was measured to be 0.17, and correcting for the atom loss an *a posteriori* entanglement fidelity of $F = 0.58$ was inferred.

These recent experiments represent the first demonstration of quantum gates and entanglement between a single pair of trapped neutral atoms. The quality of the results is comparable to that obtained much earlier in Rydberg atom CQED experiments (Hagley *et al.*, 1997; Rauschenbeutel *et al.*, 1999). In both recent experiments the entanglement fidelity obtained deterministically, without correction for atom loss, was close to, but just under the threshold of $F = 0.5$. Correcting for atom loss reveals a significant level of entanglement in the remaining atom pairs. This nondeterministic entanglement is not generally useful for quantum computing but is relevant for other tasks such as Bell inequality experiments (van Enk *et al.*, 2007). Although promising, the initial results should only be considered as first steps as they lag far behind the high fidelity results obtained with trapped ions (Benhelm *et al.*, 2008b). Both the Palaiseau and Wisconsin experiments suffer from excess atom loss during the gate operation. This is in part due to the fact that pulse or blockade errors, which leave the atoms with a nonzero amplitude to be in a Rydberg state at the end of the gate, lead to a corresponding probability for

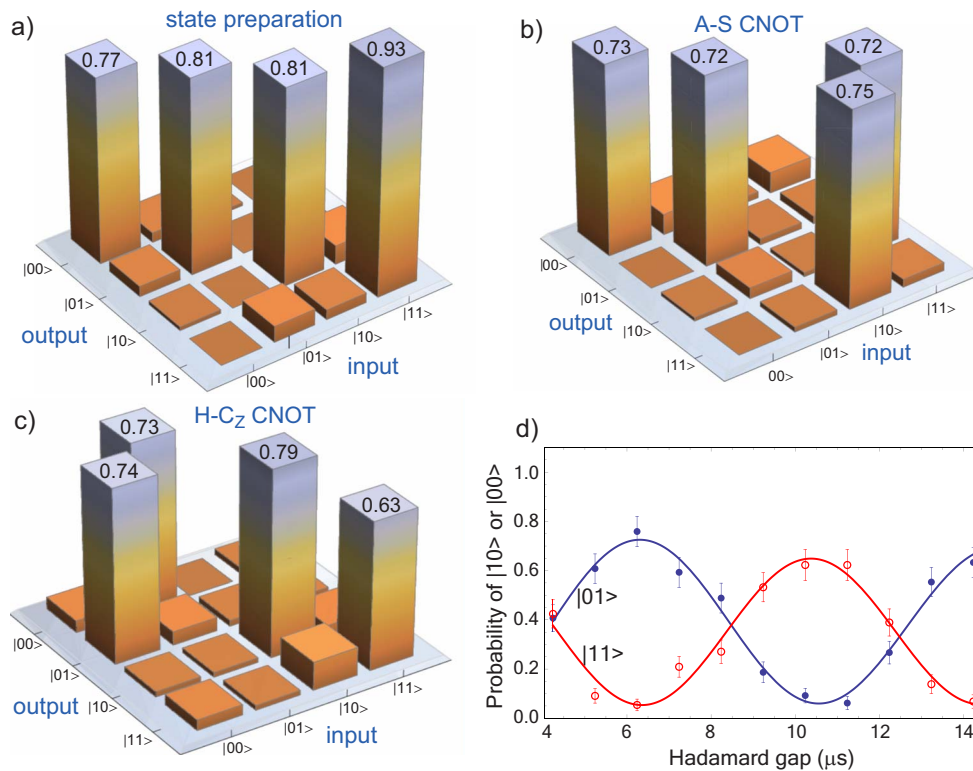


FIG. 25. (Color online) Rydberg blockade CNOT gate. Measured probabilities for (a) state preparation, (b) amplitude swap (A-S) CNOT, (c) Hadamard controlled-Z (H-C_Z) CNOT, and (d) output states of the H-C_Z CNOT under variation in the relative phase of the $\pi/2$ pulses. The reported matrices are based on an average of at least 100 data points for each matrix element and the error bars are ± 1 standard deviation. From [Isenhower *et al.*, 2010](#).

photoionization when the optical traps are turned back on after the gate operation. Thus, the measured probability to observe two atoms after completion of the gate was 0.61 in the Palaiseau experiments and 0.74–0.83, depending on the input state, in the Wisconsin experiments.

There is clearly a large gap between the theoretical fidelity estimates presented in Sec. III.B and the experimental results which show errors in the range of 30–50%. These errors can be largely attributed to technical issues (atom loss due to finite vacuum, laser stability) as well as motional effects since the atoms were relatively hot in both sets of experiments [60 μK in [Wilk *et al.* \(2010\)](#) and $>200 \mu\text{K}$ in [Isenhower *et al.* \(2010\)](#)]. The ability to obtain quite good results with such hot atoms is a testament to the robustness of the blockade interaction. The Rydberg gate intrinsic errors are potentially 100–1000 times smaller than has been demonstrated. It is likely that significant progress will be achieved in the coming years, which will pave the way for quantitative comparisons with the theoretical fidelity predictions, as well as demonstrations of more complex operations with several qubits. Continued development of the requisite optical and laser systems, combined with improved control of the spatial and momentum distributions of the atoms, will be important ingredients in ongoing work aimed at approaching the theoretical limits.

V. COLLECTIVE EFFECTS IN RYDBERG COUPLED ENSEMBLES

A. Blockade scaling laws in extended samples

The original concept of quantum information processing in atomic ensembles using dipole blockade ([Lukin *et al.*, 2001](#)) applies to localized samples small enough for the blockade to act across the whole ensemble. To date, no experiments have been done that satisfy this criterion. However, a number of experiments, on much larger samples, nevertheless show signs of the blockade effect; these will be discussed below. These larger samples are generally not useful for quantum information processing but are of interest in giving insights into the blockade effect. We refer to these samples as “extended,” reserving the term “ensemble” for situations where blockade will allow only one Rydberg excitation at a time.

The study of the behavior of cold Rydberg atoms in MOTs began with the studies of [Anderson *et al.* \(1998\)](#) and [Mourachko *et al.* \(1998\)](#) that showed clear effects of Rydberg-Rydberg interactions. Subsequent work is reviewed by [Gallagher and Pillet \(2008\)](#). Many interesting collisional phenomena have been observed in the transition of a Rydberg gas into a plasma and vice versa ([Killian *et al.*, 2001](#); [Gallagher *et al.*, 2003](#); [Choi *et al.*, 2007](#)). Collective radiative phenomena, such as Rydberg superradiance, have also been seen ([Wang *et al.*, 2007](#);

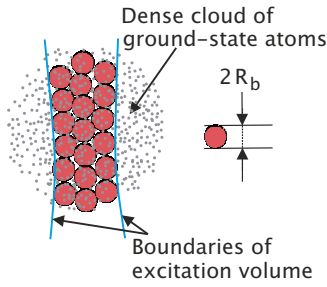


FIG. 26. (Color online) In an extended sample under conditions of blockade, only one Rydberg excitation is allowed per blockade sphere, which also contains many ground-state atoms. These blocked superatoms fill the excitation volume, saturating the maximum number of excited Rydberg atoms to a small value, and leading to sub-Poissonian Rydberg counting statistics. From [Cubel Liebisch et al., 2005](#).

[Day et al., 2008](#)). A distinguishing characteristic of blockade is a dramatic suppression of excitation, leading to low Rydberg densities. Even so, in extended samples Rydberg transport is efficient enough for these effects to still occur, making distinguishing blockade effects from plasma dynamics difficult in many cases ([Li et al., 2006](#); [Westermann et al., 2006](#)). Other examples of fast resonant excitation transfer at 100 ns–1 μ s time scales are given by [Mudrich et al. \(2005\)](#), [Nascimento et al. \(2009\)](#), and [Younge et al. \(2009\)](#). In cases where a MOT-sized volume is excited, superradiance may compete with excitation transfer effects ([Day et al., 2008](#)). These effects will not be present for a single blocked ensemble where the probability of more than one Rydberg excitation at a time is greatly suppressed. Thus in this section we restrict our discussion to those extended sample studies that directly bear on blockade phenomena.

In extended samples subject to strong local Rydberg interactions, it is convenient to introduce the concept of the “blockade sphere” ([Tong et al., 2004](#)), shown in Fig. 26. The excitation of a single Rydberg atom prohibits, via the blockade mechanism, subsequent excitations of other ground-state atoms within the radius R_b of the blockade sphere. Since the N_b atoms within the blockade sphere are indistinguishable, they comprise an effective “superatom” ([Vuletic, 2006](#); [Heidemann et al., 2008](#)) that interacts with the excitation light via a collective $\sqrt{N_b}$ enhancement of the Rabi frequency. These basic ideas explain much of the phenomena that have been observed in extended samples.

1. Suppression of optical Rydberg excitation

We consider first the optical excitation of Rydberg atoms by a single-frequency laser. The blockade radius is determined, within a geometrical factor, by the condition that the collective Rabi frequency be comparable to the dipole-dipole shift ([Lów et al., 2009](#)):

$$\sqrt{\eta R_b^3} \Omega \approx V(R_b), \quad (36)$$

where η is the atom density. For a van der Waals interaction, the density of Rydberg atoms therefore saturates at the value

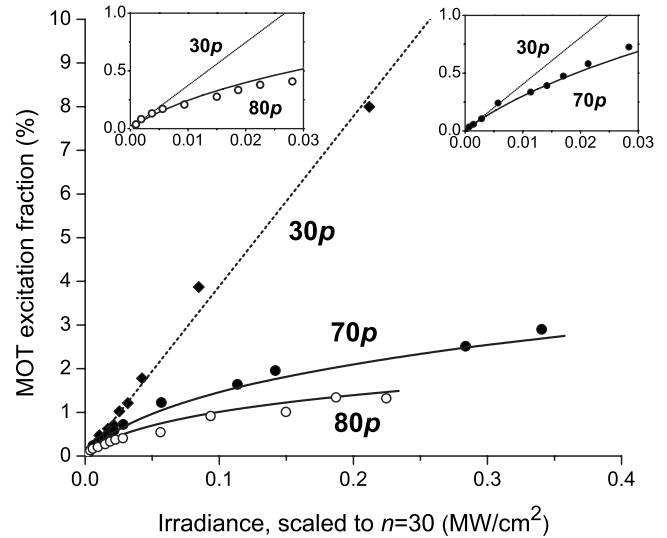


FIG. 27. Dependence of excitation fraction on principle quantum number. From [Tong et al., 2004](#).

$$\eta_R \sim \frac{1}{R_b^3} \propto \frac{\eta^{1/5} \Omega^{2/5}}{C_6^{2/5}} \quad (37)$$

or, equivalently, the excitation fraction is

$$\frac{\eta_R}{\eta} \propto \left(\frac{\Omega}{\eta^2 C_6} \right)^{2/5}. \quad (38)$$

The striking density, intensity, and principal quantum number dependences implied by this relation are key signatures of the blockade effect.

Equation (36) assumes that the collective Rabi frequency is much larger than other line broadening mechanisms such as laser linewidth or inhomogeneous broadening by external fields. When the opposite limit holds, the density of Rydberg atoms is limited to

$$\eta_R \propto \sqrt{\frac{\Gamma}{C_6}} \quad \text{or} \quad \frac{\eta_R}{\eta} \propto \sqrt{\frac{\Gamma}{\eta^2 C_6}}, \quad (39)$$

where Γ is the linewidth of the Rydberg excitation. In addition to the Rydberg density being independent of the atomic density, the n^{11} dependence of C_6 on principal quantum number is another strong sign of the blockade effect.

The dependence of the excitation fraction on C_6 is shown in Fig. 27. Using a nearly transform-limited 8.6 ns laser pulse [Tong et al. \(2004\)](#) measured the excitation fraction as a function of pulse intensity. The roughly factor of 2 ratio of the excitation fraction for the 70p and 80p data is consistent with the blockade density scalings, and the comparison of either with the 30p case dramatically shows the overall blockade effect. [Singer et al. \(2004\)](#) and [Singer, Reetz-Lamour, et al. \(2005\)](#) used continuous-wave two-photon excitation to s states with similar results, which in addition showed clear line-shape modifications due to interactions.

These suppression effects should be considerably enhanced if the atom-atom interactions are made to be

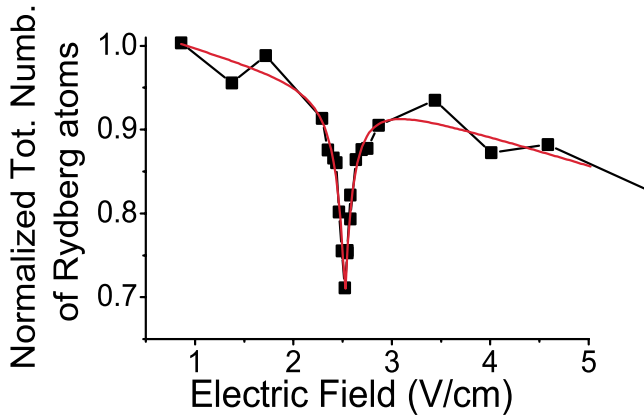


FIG. 28. (Color online) Enhanced excitation suppression by tuning a Förster resonance in Cs. From [Vogt et al., 2006](#).

$1/R^3$. [Vogt et al. \(2006\)](#) showed a greatly enhanced suppression by tuning a Förster resonance with an electric field, as shown in Fig. 28, and [Vogt et al. \(2007\)](#) directly compared van der Waals and Förster-enhanced blockade. The Stark tuned Förster resonance between just two Rydberg atoms has also been observed ([Ryabtsev et al., 2010](#)).

The most comprehensive study of the density and intensity dependence of the scaling relation (38) is shown in Fig. 29, which shows data from [Heidemann et al. \(2007\)](#) represented according to the universal scaling theory of [Lów et al. \(2009\)](#). The experiment was done with an evaporatively cooled Rb cloud just above the BEC transition. The densities, approaching 10^{14} cm^{-3} , put the experiment well into the fully blocked regime where the collective Rabi frequencies were much greater than the single-atom linewidth. By varying densities and Rabi frequencies, the dimensionless parameter ([Weimer et al., 2008](#))

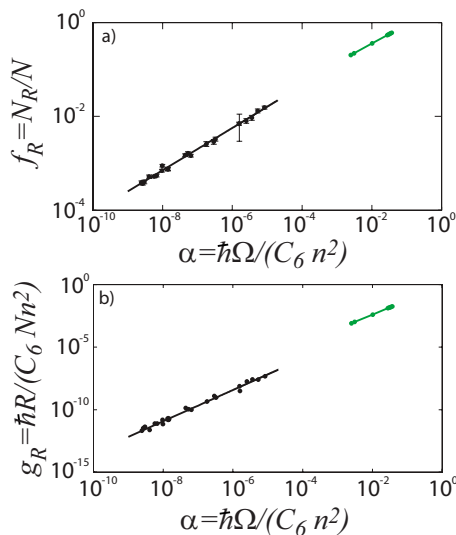


FIG. 29. (Color online) Scaling of (a) Rydberg excitation probability and (b) excitation rate with density-scaled Rabi frequency. Adapted from [Lów et al., 2009](#).

$$\alpha = \frac{\Omega}{C_6 n^2} \quad (40)$$

was varied by two orders of magnitude. The cloud geometry, an elongated cylinder, was nearly fully blocked along the short cloud dimension, so the effective dimensionality was likely somewhat less than 3. [Lów et al. \(2009\)](#) showed that the data are consistent with the scaling relations assuming either 1D or 3D.

2. Blockade effects on excitation dynamics

The excitation dynamics are also affected by blockade. In extended samples, there will be substantial inhomogeneous broadening that causes strong dephasing of the collective Rabi oscillations. This inhomogeneous broadening can be due to variation in the excitation laser Rabi frequencies across the sample, as well as Poissonian fluctuations in the number of atoms within each blockade sphere. Thus the strongly dephased Rabi oscillations average out to a mean excitation rate \mathcal{R} for each superatom that is proportional to the ratio of the square of the collective Rabi frequency to the linewidth. The transition between individual and collective excitation is evident at very low intensities in [Tong et al. \(2004\)](#).

For monochromatic excitation, the superatom linewidth is determined by power broadening and is therefore proportional to the collective Rabi frequency. Thus the superatom excitation rate will be approximately the collective Rabi frequency. The measured quantity is

$$\frac{dN_R}{dt} \approx \frac{\mathcal{R}V}{R_b^3} \approx \frac{\Omega \sqrt{\eta/R_b^3}}{R_b^3} \approx \frac{N\Omega^{6/5}}{\eta^{2/5} C_6^{1/5}}, \quad (41)$$

where N is the total number of atoms in the sample of volume V . Again, this constitutes a highly nontrivial scaling with accessible experimental parameters. [Lów et al. \(2009\)](#) derived a universal scaling of the dimensionless combination

$$g_R = \frac{dN_R/dt}{C_6 N \eta^2} \propto \alpha^{6/5}. \quad (42)$$

The measurements of [Heidemann et al. \(2007\)](#) are shown in this way in Fig. 29 and obey this scaling law quite closely.

[Heidemann et al. \(2008\)](#) studied Rydberg excitation in Bose-Einstein condensates with variable thermal and condensate components. The dramatic density variations between the condensate and the thermal cloud give rise to multiple time scales for the blockade dynamics. The superatom model was again successful in explaining the main features of the experiment.

[Raitzsch et al. \(2008\)](#) presented results of a rotary echo experiment, done in a highly blocked sample. This involves exciting the atoms for a time τ , phase shifting the Rabi frequency by π , followed by deexcitation for time τ . The echo should, in the absence of dephasing processes, allow reversal of coherent excitation even in the presence of the very large collective Rabi frequency fluctuations due to the fluctuations in atom number for different blockade spheres. The dephasing rate, mea-

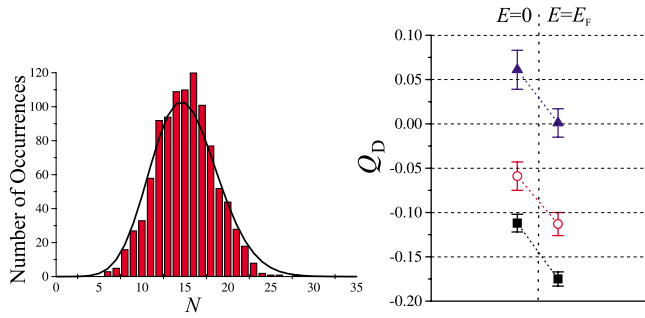


FIG. 30. (Color online) Sub-Poissonian atom statistics. Left: Experimental Rydberg counting statistics, compared to a Poisson distribution of the same mean. Right: Mandel Q parameter for atom densities in the range $(1-5) \times 10^{11} \text{ cm}^{-3}$ (top to bottom) and for zero electric field and a Förster-resonant field E_F . Adapted from Reinhard, Younge, and Raithel, 2008.

sured by the decay of the visibility with pulse time, was found to increase with increasing density. An EIT experiment, done with larger atom numbers, was also used to deduce the dephasing rate by Raitzsch *et al.* (2009). The roughly N_R^2 observed dependence of the dephasing on Rydberg atom number is in reasonable agreement with numerical simulations.

3. Sub-Poissonian atom excitation

The excitation of Rydberg atoms in a dense extended sample will tend to fill the volume V to a maximum number of Rydberg atoms V/R_b^3 . As pointed out by Cubel Liebisch *et al.* (2005), the fluctuations in the number of Rydberg atoms should therefore be sub-Poissonian. Figure 30 shows results from Reinhard, Younge, and Raithel (2008) that demonstrate this effect. The narrowing effect is clearly seen there and quantified by the Mandel Q parameter

$$Q = \frac{\langle N_R^2 \rangle - \langle N_R \rangle^2}{\langle N_R \rangle^2} - 1 \quad (43)$$

that is zero for a Poisson distribution and negative for a sub-Poissonian distribution. Note that the experimental Q values are diluted by finite detection efficiency (Ryabtsev *et al.*, 2007; Reinhard, Younge, and Raithel, 2008) so that the actual distributions are more sub-Poissonian than would be indicated from Fig. 30.

4. Modeling of ensemble blockade

It is desirable to go beyond the scaling type arguments used above and improve understanding via detailed and quantitative models of how blockade physics plays out in large volume samples. A variety of approaches have been taken as described here. In general, the various methods are quite successful in accounting for a range of experimental results.

For resonant excitation of Rydberg states, the basic Hamiltonian to be simulated is

$$H = \sum_i \left(\frac{\Omega_i}{2} |r_i\rangle\langle g| + \text{H.c.} \right) + \sum_{j<i} V_{ij} |r_i r_j\rangle\langle r_i r_j|. \quad (44)$$

The first term is the Rabi coupling of the ground-state atoms to the light, while the second is the interaction between atom pairs. Three-body interactions are usually ignored, though they may come in surprising ways as recently pointed out by Pohl and Berman (2009); see also the discussion in Sec. II.E.

The first approach from Tong *et al.* (2004) was a mean-field description where the effective Rydberg-Rydberg van der Waals interaction was averaged to obtain a nonlinear Bloch equation for the Rydberg amplitudes. The blockade volume was adjusted to have exactly one atom in it at all times. Agreement with experiment was obtained when the density or C_6 coefficient was scaled by a moderate value of 2.5.

Robicheaux and Hernández (2005) performed a simulation of a limited volume cube containing 30–160 atoms. Inside the cube the atoms were randomly placed and they treated the effects of atoms outside the cube with a mean-field model. The still untractable Hilbert space was reduced in dimension by recursively introducing pseudoatoms of the closest atom pairs, with new collectively enhanced Rabi frequencies. By further limiting the Hilbert space to amplitudes with fewer than six excitations, they were able to make the simulation tractable. They got results similar to those of Tong *et al.* (2004) and also presented calculations of the two-atom correlation function, which as expected was nearly zero inside the blockade radius, went through an intermediate peak above 1, and settled to 1 within a couple of microns of the blockade radius. They pointed out that the pair correlation function is quite sensitive to the detuning of the laser as compared to the sign of the van der Waals shift. This approach was further extended by Hernández and Robicheaux (2006), who also pointed out the effects of anisotropic interactions on the pair correlation functions and studied sub-Poissonian Rydberg excitation statistics. A further fully quantum study of 1D blockade (Sun and Robicheaux, 2008) looked particularly at the pair correlation functions and whether they are reflective of entanglement or classical correlation. Hernández and Robicheaux (2008a) compared this general class of methods to simplified Monte Carlo approaches in the context of the experiment of Heidemann *et al.* (2007) and found them to underestimate the number of excited atoms, for reasons not clear.

Direct simulations using a truncated Hilbert space have been done for up to 100 atoms (Weimer *et al.*, 2008; Löw *et al.*, 2009; Wüster *et al.*, 2010). By removing states from the full Hilbert space with Rydberg-Rydberg energies greater than some cutoff E_c , the size of the space can be made tractable. A mean-field theory was also found to compare quite closely, and both results agree with the scaling laws.

Ates *et al.* (2006) approximated the coherent Rabi interactions by rate equations, thereby reducing the computational difficulties and allowing up to a few thousand atoms to be treated in a Monte Carlo approach. The

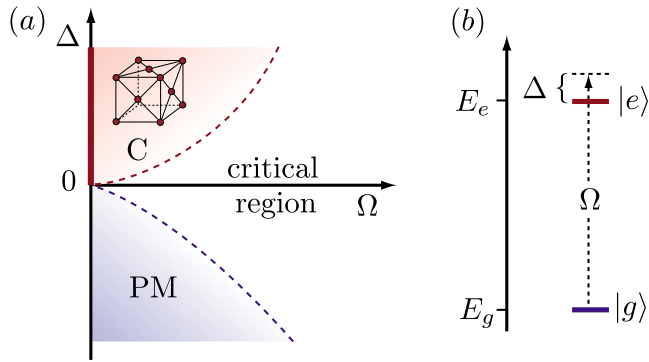


FIG. 31. (Color online) Phase diagram of blocked Rydberg excitation. A crystalline phase C is predicted to form for positive detunings when the van der Waals interactions are repulsive. For negative detunings, the excitation is off-resonance for all atoms and the paramagnetic phase simply constitutes the atom population predominantly in the ground state. From Weimer *et al.*, 2008.

justifications for these approximations were described by Ates *et al.* (2007b), where master and rate equation solutions were found to be similar in tractable cases. This approach was used to analyze excitation suppression and sub-Poissonian atom statistics. The results were found to be insensitive to the shape of the potential for distances inside the blockade radius, consistent with the blockade shift concept of Eq. (36). The effects of adiabatic elimination of the intermediate p state for two-photon excitation were discussed, and in particular Ates *et al.* (2007a) pointed out that when the s - p coupling is sufficiently strong to produce an Autler-Townes splitting of the Rydberg spectrum, there can be an antiblockade effect where the Rydberg-Rydberg interaction increases the excitation probability by tuning the Autler-Townes peaks into resonance. Such effects are clearly sensitive to atom-atom spacings and would be most prominent on an ordered lattice.

Chotia *et al.* (2008) presented a related kinetic Monte Carlo simulation of blockade physics, along with a mean-field Hartree-Fock density matrix analysis. A few thousand atoms are simulated, including effects of field-induced blockade interactions. These methods reproduced the experimental data of the same group.

Weimer *et al.* (2008) reasoned that there is a strong analogy between Rydberg blockade and second-order phase transitions for the case of repulsive isotropic Rydberg-Rydberg interactions. Thus they approached the problem of blockade from the perspective of statistical mechanics. They transformed the problem into an effective pseudospin representation. As shown in Fig. 31, when the light is tuned below resonance there is no excitation in steady state. For positive detuning, Rydberg excitation is possible and the atoms are predicted to form a crystalline lattice. This appears related to the prediction of Robicheaux and Hernández (2005) of peaks in the two-atom correlation function under similar excitation conditions, as well as a recent calculation of the formation of a 2D lattice structure in a Rydberg ex-

cited ensemble (Pupillo *et al.*, 2009). At zero detuning, the Hamiltonian of the system depends only on the single dimensionless parameter $\alpha = \Omega / C_6 \eta^2$ defined in Eq. (40). In this regime the system is argued to exhibit universal behavior; the fraction of Rydberg atoms $f_R = \eta_R / \eta$ is a universal function of α . A mean-field analysis leads to $f_R \sim \alpha^{2/5}$ for small α , in agreement with the scaling laws above.

Extending these ideas, Löw *et al.* (2009) argued that the system should exhibit a quantum critical point. Drawing an analogy with ferromagnetism, they predicted that for positive detunings (and repulsive van der Waals interactions) the system should condense into a ferromagnetic phase with the Rydberg fraction being a definite universal function of the parameter α and a similar dimensionless detuning $\Delta = \delta_L / C_6 \eta^2$, where δ_L is the laser detuning. It is an important experimental challenge to see if the predicted ferromagnetic phase can be observed for positive detuning.

A statistical mechanics approach to blockade was analyzed from another perspective by Olmos, González-Férez, and Lesanovsky (2009a) and Olmos, Müller, and Lesanovsky (2010), who compared direct integration of the Schrödinger equation of a ring of atoms with perfect nearest-neighbor blockade to a microcanonical ensemble. The steady state of both approaches agreed well.

Most of the theoretical approaches to ensemble blockade described above have used a simplified treatment of the Rydberg-Rydberg interactions. We note that in the context of fully blocked ensembles (sample size smaller than the blockade radius), effects such as Zeeman degeneracies and the angular distribution of excitation, discussed in Sec. II.C, play essential roles in determining the probability of double excitation. The general success of the theoretical approaches in describing suppression and other blockadelike effects for samples containing many blockade regions is an interesting probe of blockade physics, but the direct implications for the success of quantum information applications of fully blocked clouds are not evident. For experiments and simulations with s states, where the blockade shifts are nearly isotropic and Zeeman degeneracy is not an issue, these complications may be of less importance and extrapolation to fully blocked situations should be more reliable.

B. Preparation of single-atom states

An outstanding challenge for neutral atom quantum computing is controlled loading of single atoms into an optical lattice that is compatible with site specific addressing and control. A number of different approaches to this problem have been discussed in Sec. III.D. Saffman and Walker (2002) proposed to use many-atom entangled states created by Rydberg blockade as a means of achieving deterministic single-atom loading. Entanglement is here a resource that is used, not just for computation but for preparation of atomic number states.

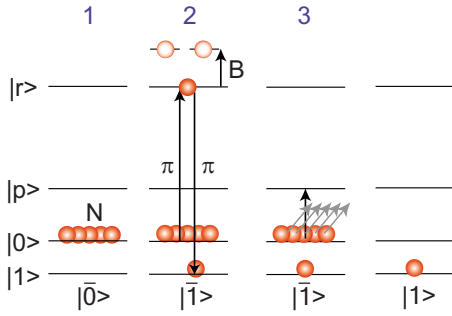


FIG. 32. (Color online) Three-step protocol proceeding from left to right for deterministic preparation of single-atom occupancy following Saffman and Walker (2002). The initial number of atoms N is a stochastic variable.

The loading protocol is shown in Fig. 32. We start by loading N atoms into an optical trap and preparing them in state $|\bar{0}\rangle$. Under conditions of Rydberg blockade a π pulse to Rydberg level $|r\rangle$ followed by a π pulse to $|1\rangle$ creates the singly excited symmetric state $|\bar{1}\rangle$. The remaining $N-1$ atoms left in $|0\rangle$ can then be ejected by applying unbalanced radiation pressure from light that is resonant with an auxiliary level $|p\rangle$. The trap can also be lowered during this “blow-away” phase to facilitate ejection after only a small number of photon scattering events. After the blow-away phase we are left with a single atom in state $|1\rangle$ despite the fact that the initial number N was random.

The essential question is the probability of success of this protocol. Clearly if the initial atom number is $N=0$, the protocol fails. With Poissonian loading statistics we can restrict the probability of this happening to 10^{-3} by choosing $\langle N \rangle \geq 7$. It is not difficult to confine such a small number of atoms to a volume of size much less than a blockade sphere. A more serious difficulty is that the Rabi frequency in step 2 is given by $\Omega_N = \sqrt{N}\Omega$. Since N is unknown, it is not possible with a simple uniform pulse to have a pulse area that is independent of N .

One solution is to make $\langle N \rangle \gg 1$. It is then easy to show that the error in exciting a single Rydberg atom in the first half of step 2 is $E = \pi^2/16\langle N \rangle$ which requires $\langle N \rangle \sim 600$ for a 10^{-3} error. A more fruitful approach is likely to take advantage of a composite pulse sequence to reduce the dependence of the pulse area on N . If we take a moderate $\langle N \rangle = 10$ then the spread of pulse areas due to variations in N is only about 30%. This spread can be corrected for with high accuracy using composite pulse schemes. Even without composite pulses success probability of roughly 80% is possible at $\langle N \rangle = 10$ by optimizing with respect to the single-atom pulse area.

It is also possible to remove the dependence on N entirely by relying on ejection of atoms from the Rydberg state instead of from the ground state (Mølmer, 2009). Applying a 2π pulse to a single atom returns it to the ground state, whereas an ensemble of N atoms experiences a pulse area of $\sqrt{N}2\pi$. As long as N is not a perfect square there is a nonzero amplitude for an atom

to be left in the Rydberg state after the pulse. This atom can then be photoionized before it returns to the ground state, and the sequence repeated until only one atom remains. Cases where N is a perfect square can be handled by adjusting the detuning of the Rydberg excitation pulse.

C. Collective qubit encoding

At the current stage of development of quantum information processing demonstration experiments have been limited to less than ten qubits. The development of new approaches to encoding and interconnecting many qubits is therefore a central challenge of current research. The long-range nature of Rydberg interactions together with the availability of a strong and controllable blockade interaction enable a “collective” approach to encoding of a multiqubit register (Brion, Mølmer, and Saffman, 2007). As described in this section collective encoding takes advantage of a multiplicity of stable atomic ground states to encode a multiqubit register in a many-atom ensemble, without requiring separate addressing of the atoms. Quantum information is thereby encoded in a distributed fashion that is an alternative to the usual serial encoding of one qubit for each two-level quantum system. Using blockade interactions one- and two-bit gates can be performed between any pair of qubits using only globally applied control pulses. This feature of the collective encoding approach has the potential of simplifying the wiring of a quantum computer.

In order to take full advantage of this approach we store information in all of the atomic Zeeman states, not just clock states with optimum coherence properties. Effective utilization of collective encoding therefore presupposes control of the magnetic field environment of the atoms. While this is a technical challenge, it appears fruitful to nevertheless explore the collective approach due to the potential for a substantial reduction in complexity of a functioning quantum register.

Figure 3 shows the proposal in Lukin *et al.* (2001) to encode a single qubit in symmetric, collective states of an ensemble of atoms, either having all atoms in the same internal state $|0\rangle$ or having precisely one atom transferred to the other internal state $|1\rangle$. If an external perturbation couples these states with exactly the same strength g for all atoms,

$$V_N = \sum_{j=1}^N g(|0_j\rangle\langle 1_j| + |1_j\rangle\langle 0_j|), \quad (45)$$

the collective states $|0^N\rangle \equiv |0_1 \cdots 0_N\rangle$ and $|1^1 0^{N-1}\rangle \equiv (1/\sqrt{N})\sum_j |0 \cdots 1_j \cdots 0\rangle$ experience an enhanced coupling strength $g_N = \langle 1^1 0^{N-1} | V_N | 0^N \rangle = \sqrt{N}g$. In Eq. (45), spatially dependent phases of the exciting laser fields have been absorbed in the atomic internal states $|0_j\rangle$, $|1_j\rangle$. This is a convenient approach for atoms at rest, while time-dependent phases for moving atoms translate into Doppler shifts. In the following we assume cold, trapped atoms in an optical lattice potential. The interaction (45)

also drives further excitation of symmetric states $|1^2 0^{N-2}\rangle$, $|1^3 0^{N-3}\rangle \dots$, with two, three, and more state $|1\rangle$ atoms, and for sufficiently large N , these states form the ladder of states of an effective harmonic oscillator. Together with the enhanced coupling strength this constitutes the basis for using atomic ensembles as quantum memories for quantum states of a light pulse (Julsgaard *et al.*, 2004).

Lukin *et al.* (2001) suggested if the Rydberg blockade applies to the whole collection of atoms, it is possible to restrict the collective states of the ensemble to the pair of states ($|0^N\rangle$ and $|1^1 0^{N-1}\rangle$) with zero and one atom in state $|1\rangle$, only, and thus to implement a logical qubit in the atomic ensemble. To carry out an arbitrary qubit operation on this qubit without accessing states with more than a single atom in state $|1\rangle$, one applies the following sequence of three pulses: (i) a resonant π pulse on the $|1\rangle - |r\rangle$ internal state transition transfers the collective state $|1^1 0^{N-1}\rangle$ component to the symmetric state with one Rydberg excited atom,

$$|r^1 0^{N-1}\rangle \equiv \frac{1}{\sqrt{N}} \sum_j |0 \dots r_j \dots 0\rangle; \quad (46)$$

(ii) the desired qubit operation is implemented as a coherent, resonant transition in the closed two-level system of states $|0^N\rangle$ and $|r^1 0^{N-1}\rangle$; and (iii) a resonant π pulse on the $|r\rangle - |1\rangle$ transition finally transfers the resulting $|r^1 0^{N-1}\rangle$ component back to the qubit level $|1^1 0^{N-1}\rangle$.

Note that these operations act as if resonant lasers are only applied to single atoms (except that the $|0\rangle - |r\rangle$ transitions are collectively enhanced) and during pulse (ii), the Rydberg blockade interaction takes care of the restriction of the dynamics to the desired collective states of the system. Lukin *et al.* (2001) also proposed to implement conditional quantum gates on several qubits stored in separate ensembles, either by direct interaction if the ensembles are within the long-range Rydberg interaction of each other or by transferring the states of the ensembles into a single intermediate ensemble and carrying out the operation here, before transferring the (now entangled) qubits back to their original ensembles.

Making use of more states in the internal level structure of the atoms, it is possible (Brion, Mølmer, and Saffman, 2007; Brion *et al.*, 2008) to encode several quantum bits in the collective states of a single atomic ensemble. Figure 33 shows the conventional encoding of K quantum bits in K separate two-level systems [part (a)] and collective schemes making use of a large ensemble of $(K+1)$ -level systems [part (b)], and $(2K+1)$ -level systems [part (c)], respectively. Figure 33(a) shows the lower and upper states $|0\rangle$ and $|1\rangle$ of K separate particles encoding a full register of K qubits, while Figs. 33(b) and 33(c) show the multilevel structure of a single atom and the collective population of the individual levels in a collection of atoms. It is assumed that the collective states in Figs. 33(b) and 33(c) are symmetric under permutation of the individual atoms and that the filled circles merely indicate the number of atoms populating the different internal states. With the

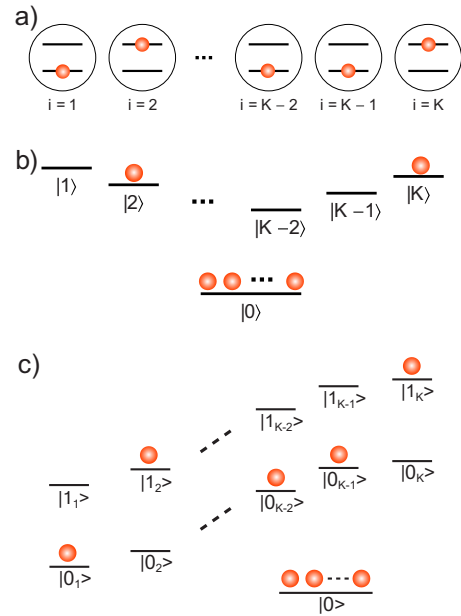


FIG. 33. (Color online) Three different ways of encoding the K -bit state $|01 \dots 001\rangle$. (a) Conventional encoding in K two-level systems. (b) Collective encoding in an ensemble of $(K+1)$ -level systems. Filled circles represent the number of atoms populating the given single-particle state $|i\rangle$. (c) Collective encoding in an ensemble of $(2K+1)$ -level systems. Each qubit value is determined by the population, represented by the filled circles, within the pair of states $\{|i_0\rangle, |i_1\rangle\}$, and each pair of states has a definite total population of unity.

definition that a unit population of the i th level implies a bit value of 1, while a vanishing population implies a bit value of 0 in Fig. 33(b), we can encode a register with K qubits in an ensemble of $(K+1)$ -state atoms provided that the ensemble size $N \geq K$ so that all K qubit states can be populated by a single atom. Figure 33(c) shows a slightly more involved level scheme where K pairs of levels are identified and where qubit values zero and unity are identified with symmetric atomic states populating one or the other of the states in each pair by a single atom. Observe that Figs. 33(a)–33(c) show the different encoding schemes for the same K -qubit register state $|01 \dots 001\rangle$. In Figs. 33(b) and 33(c), the population in the internal state denoted $|0\rangle$ plays the role of an atomic “reservoir,” being crucial for the exchange of population in one- and two-bit gates and for initialization and implementation of error correction (Brion, Mølmer, and Saffman, 2007; Brion *et al.*, 2008).

We now discuss the collective encoding scheme shown in Fig. 33(b). We formally associate the binary register state $|n_1, n_2, \dots, n_K\rangle$ ($n_i=0, 1$) with the symmetric state of the ensemble with n_i atoms populating the internal states $|i\rangle$. In this way the binary representation becomes a number state representation of the symmetric states of the ensemble specifying the number of atoms $n_i=0, 1$ populating each register level $|i\rangle$.

Using a notation as in Fig. 3, for a single ensemble qubit, with bars over numbers 0 and 1 indicating logical

qubit values, we can write the following examples of 3-bit register states:

$$|\bar{0}, \bar{0}, \bar{0}\rangle = |0_1 0_2 \cdots 0_N\rangle,$$

$$|\bar{0}, \bar{1}, \bar{0}\rangle = \frac{1}{\sqrt{N}} \sum_j |0_1 0_2 \cdots 2_j \cdots 0_N\rangle, \quad (47)$$

$$|\bar{1}, \bar{0}, \bar{1}\rangle = \frac{1}{\sqrt{N(N-1)}} \sum_{j,k} |0_1 \cdots 1_j \cdots 3_k \cdots 0_N\rangle.$$

Including the superposition states, the basis $\{|n_1, n_2, \dots, n_K\rangle, n_i=0,1\}$ fully explores the 2^K dimensionality, of the register Hilbert space of a K qubit quantum computer. The full Hilbert-space dimension of our ensemble of $N \geq K$ atoms is, indeed, much larger, but the restriction to symmetric states with no register state population exceeding unity, yields precisely the qubit register dimension. Physically, these restrictions are imposed by the interactions: by addressing the system collectively we preserve the symmetry of states with respect to permutations among the atoms and by application of the Rydberg blockade, we restrict the population of all information carrying states to zero and unity. In practice, ensemble sizes an order of magnitude larger than the register size, $N \approx 10K$, or even more, may improve a number of properties of our proposal and do not impose major experimental problems: atomic ensembles of thousands of atoms are routinely produced and manipulated in quantum optics laboratories.

The states $|0\rangle$ and $|i\rangle$ can be chosen as the Zeeman sublevels of atomic hyperfine ground states or metastable excited atomic states. One must ensure that the interaction with the atoms does not entangle their internal state with their motion, i.e., they must be trapped by potentials which act identically on all internal states. Far-off-resonance optical traps, or small (micron-sized) glass cells (Kübler *et al.*, 2010) may meet this demand. One must also ensure that ground-state collisions among the atoms do not perturb their internal states. This can be ensured by trapping the atoms in an optical lattice. Note that the distance between the trapping sites in typical optical lattices is of the order of a few hundred nanometers, and hence the Rydberg blockade may be efficient over a volume containing thousands of such sites. A more detailed estimate of the maximum size of a blockaded ensemble can be found in Sec. III.D.

A specific implementation for Cs atoms is shown in Fig. 34. We initially prepare the register state $|\bar{0}, \bar{0}, \dots, \bar{0}\rangle = |0_1 0_2 \cdots 0_N\rangle$, where all atoms are optically pumped into the internal “reservoir” state $|0\rangle = |f=4, m_f=0\rangle$. An applied magnetic field Zeeman shifts all hyperfine states, such that state selectivity is obtained through the resonance condition on the optical transitions. For effective Rydberg blockade the atoms are transferred by a two-photon excitation from the hyperfine ground state to high-lying interacting s states with $n \geq 50$. The hyperfine interaction is very weak for Rydberg excited atoms, and the hyperfine structure of the Rydberg level is un-

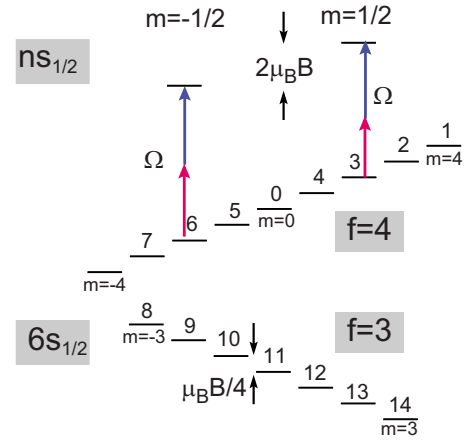


FIG. 34. (Color online) Cesium level scheme and identification of qubit register. Encoding of reservoir state 0 and 14 register states in the Zeeman ground states of Cs. Coupling of $|3\rangle = |f=4, m=2\rangle$ and $|6\rangle = |f=4, m=-2\rangle$ to Rydberg states is shown.

resolved. The hyperfine ground states are thus coupled to excited fine-structure states with good electron spin magnetic quantum numbers, $|ns_{1/2}, m = \pm 1/2\rangle$. In Cs, different ground- to Rydberg excited-state transitions are separated by at least $\mu_B B / 4\hbar$, with μ_B the Bohr magneton, and as long as this quantity is large compared to the two-photon excitation Rabi frequency Ω the ground states can be selectively excited. Taking into account the finite lifetime of the Rydberg level, optimum parameters are $\Omega/2\pi \sim 1$ MHz, and a modest field of $B \sim 15$ G will provide a sufficient splitting of levels to suppress undesired excitation to the 1% level. Due to the value of the Landé factor, however, two transitions, $|6s_{1/2}, f=4, m=-4\rangle \leftrightarrow |ns_{1/2}, m=-1/2\rangle$ and $|6s_{1/2}, f=4, m=4\rangle \leftrightarrow |ns_{1/2}, m=1/2\rangle$, are degenerate. This implies that the ground states of these transitions are not as easily distinguished, and we suggest to exclude one of them from the encoding, leaving 15 readily distinguishable ground states for the register encoding. This implies that with a small cloud of Cs atoms, we can encode a 14-qubit quantum register using only collective addressing. In addition to the use of external fields to lift degeneracies as shown in Fig. 34, techniques from optimal control theory may serve to identify shaped pulses that may even distinguish degenerate register states.

Since the individual bits refer to the population amplitudes of different internal states, one- and two-bit operations are carried out as if they are effectively operations on single atoms, as detailed in the following section, but we emphasize that due to the collective nature of the encoding and the blockade, there is no need for addressing of individual atoms.

An effective readout mechanism can be achieved by coupling the register levels in a controlled manner to excited states from which ionization can be observed, or by repeatedly transferring the qubit content by a C-NOT operation to another readout collective qubit, which may be probed by fluorescence on an optical transition decaying back to the reservoir state [cf. the similar ap-

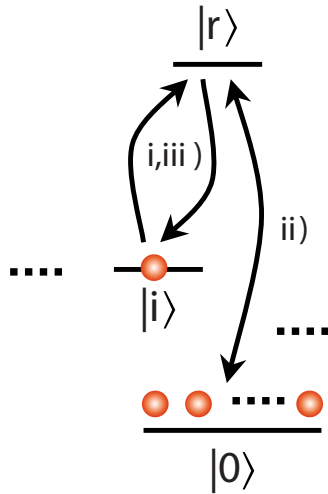


FIG. 35. (Color online) qubit in the collective encoding scheme. A π pulse transfers (i) the population in $|i\rangle$ to $|r\rangle$, (ii) a coherent coupling is applied on the two-state system with zero and one atom in $|r\rangle$, and (iii) a π pulse transfers level population in $|r\rangle$ to $|i\rangle$.

proach applied in ion traps (Rosenband *et al.*, 2008)]. The directed, collective photon emission of extended atomic samples and the Rydberg blockade may also be utilized for effective readout, as proposed by Saffman and Walker (2002, 2005b).

D. Ensemble gates and error correction

We now show how to implement one- and two-bit gates on collectively encoded qubits in atomic ensembles, assuming that the atomic ground states are spectroscopically distinguishable and making use of state selective resonant optical transitions and the Rydberg blockade mechanism.

1. Single qubit gates

In the encoding suggested in Fig. 33(b), a phase gate on the i th qubit can be implemented straightforwardly by selectively perturbing the i th energy level, leading to a phase shift of precisely the components of the states with a single atom populating that state. In Fig. 35 we show how to use the Rydberg blockade to perform a selective rotation on the i th qubit, i.e., between the collective states of the ensemble with zero and one atom populating the atomic level $|i\rangle$. As in our explanation of how single-qubit gates are performed on the ensemble qubit, shown in Fig. 3, this rotation requires three steps: (i) a swap of the population between the state $|i\rangle$ and the Rydberg state $|r\rangle$, (ii) a coherent coupling on the $|0\rangle$ – $|r\rangle$ atomic transition, and (iii) return of the $|r\rangle$ component to the atomic state $|i\rangle$. None of these processes require individual addressing of the atoms, but while the first and last processes are driven as single-atom state selective π pulses, the middle process is collectively enhanced due to the population of the reservoir state $|0\rangle$. Since the occupation of all register states are quantum

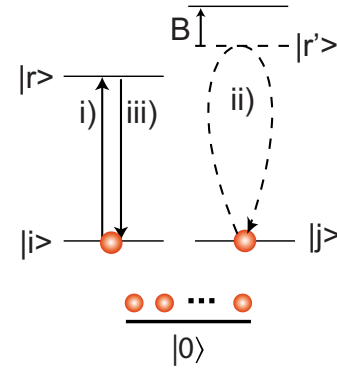


FIG. 36. (Color online) Two-qubit operation in the collective encoding of qubits: (i) transfer of the population in $|i\rangle$ to $|r\rangle$, (ii) an attempted transfer of the population in $|j\rangle$ to another Rydberg state $|r'\rangle$ and back, blocked in the presence of an atom in state $|r\rangle$, and (iii) return of the population in $|r\rangle$ to $|i\rangle$. This sequence of operations is equivalent to the sequence shown in Fig. 2 for individually encoded qubits and causes a Z gate on the j th collectively encoded qubit, conditioned on the state of the i th qubit.

degrees of freedom, the reservoir population $n_0 = N - \sum_i n_i$ may attain a wide range of values, and it is an advantage to assume $N \gg K$, so that the collectively enhanced Rabi frequencies are almost identical, or sufficiently close that composite pulses (Cummins *et al.*, 2003) may compensate for their differences.

In the collective encoding using a pair of states for each qubit, shown in Fig. 33(c), single-qubit gates are simpler, as they are obtained by coupling directly the relevant pair of atomic states $|i_0\rangle$ and $|i_1\rangle$, e.g., via an optically excited state. There is no collective enhancement of the transition, which thus proceeds as if we were interacting with only a single atom, and Rydberg blockade is not needed to restrict the total population of the states involved.

2. Two-qubit gates

The implementation of two-bit gates in our ensemble scheme is different from the Rydberg blockade gate in the individual atom proposal shown in Fig. 2, where the excitation of one atom prevents the excitation and accumulation of a phase shift by another atom in the qubit 1 state. In the collective scheme, shown in Fig. 36, we use that the excitation of the Rydberg state from a logical 1 of the i th bit, i.e., from a single atom populating the “control” state $|i\rangle$, prevents the resonant driving toward another Rydberg state $|r'\rangle$ of an atom populating the “target” state $|j\rangle$, if atoms in these two Rydberg states experience the blockade interaction. Unlike the individual atom proposal (Jaksch *et al.*, 2000), we make use here of two different Rydberg states $|r\rangle$ and $|r'\rangle$, because an atom excited from $|i\rangle$ into $|r\rangle$ may be subsequently driven into $|j\rangle$ if these states are coupled sequentially to

the same Rydberg state.⁴ In the encoding via state pairs, shown in Fig. 33(c), two-bit gates are carried out in essentially the same way, namely, by transfer of one of the qubit i states to a Rydberg state $|r\rangle$, followed by a conditional dynamics on the j th qubit via another Rydberg state. The possibility to couple simultaneously (bright) linear superpositions of the $|i_{0(1)}\rangle$ states and of the $|j_{0(1)}\rangle$ states to the respective Rydberg states makes a wider variety of two-bit gates available in single shot operations (Roos and Mølmer, 2004).

3. Error correction

We now turn to the issue of errors occurring in the collective encoding scheme for quantum computing. The conventional paradigm for quantum computing is that individual bits are stored in individual physical systems and correction of errors that occur to individual bits is possible by a suitable redundant encoding of logical qubits in special code words using several physical qubits. These error correction techniques, which can check and restore the code words without destroying the quantum content of the states, however, do not apply if errors happening to a single atom do not just affect a single qubit and if we can only collectively and symmetrically address all atoms in the ensemble. In the case of collective qubit encoding via pairs of states, cf. Fig. 33(c), it is, however, possible to check for errors and repair them by simple encoding schemes. We give here a review of the main ideas and refer the interested reader to Brion *et al.* (2008) for further details.

Since the ensemble is supposed to consist of a number of particles much larger than the number of qubits ($N \gg K$), each atom most likely occupies the reservoir state $|0\rangle$, and the loss of a particle therefore most likely leaves the unit population in the qubit state pairs $|i_0\rangle, |i_1\rangle$ intact. We therefore propose to monitor the total population in each qubit pair of states and as long as this population is unity, we assume that no error has occurred. If, however, one finds zero occupancy of a qubit state pair, one reverts to a unit occupancy by transferring a single atom from the reservoir state, via the Rydberg state, to the state $|i_0\rangle$. This is very unlikely to be the correct state of the qubit, but we know which qubit position in the register has been thus compromised, and if we use a simple redundant code of two physical qubits per logical qubit, we can reestablish the correct state by a C-NOT gate operation, where the compromised qubit is the target and the uncompromised partner qubit is the control qubit. A more worrisome situation occurs if an atom decays into a qubit state, which is already collectively occupied by other atoms in the sample. This is a problem both because it leads to a logically meaningless double occupancy of a collective qubit level and because the erroneous single atom is capable of controlling the other atoms

⁴The requirement of two Rydberg states can in principle be dropped if we use composite Rydberg pulses to discriminate between the $\sqrt{2}$ difference in Rabi frequency of singly and doubly occupied states.

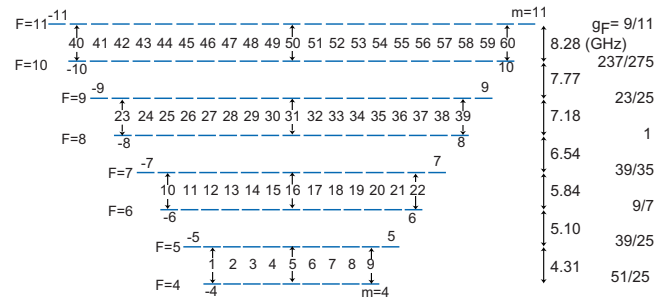


FIG. 37. (Color online) Hyperfine structure of the Ho $4f^{11}6s^2$ ($^4I_{15/2}$) ground state. Assignment of 60 qubits with two atomic states per bit is indicated together with values of the hyperfine splittings and g factors.

by the Rydberg blockade. We have only the same access to all the atoms, but we recall that the collectively occupied states experience a \sqrt{N} enhanced coupling strength, whenever the internal atomic state is coupled to the macroscopically populated reservoir state. Precisely this enhancement distinguishes a single atom populating a given state from a symmetric collective population and by driving suitable transitions in the system, it is possible to either dispose of the single atom with the erroneous population or return it to the reservoir state (Brion *et al.*, 2008).

E. A 1000-bit collectively encoded computer

Using cesium atoms, we achieve 14 collectively encoded qubits or alternatively seven qubits with the encoding of qubits in pairs of states. We are not, however, restricted to alkali atoms, and in Fig. 37 we show the hyperfine structure of the ground state in holmium atoms. Holmium has one stable isotope ^{165}Ho which has a ground electron configuration $4f^{11}6s^2$ with $J=15/2$ and a nuclear spin of $I=7/2$ giving hyperfine levels with $4 \leq F \leq 11$, i.e., a total of 128 hyperfine states. In Fig. 37 we show all these states with a proposed qubit assignment to each pair of states, cf. Fig. 33(c), and we indicate the energy splittings and the Landé factors for the different levels, of relevance to the selective addressing of different transitions, when the atoms reside in a uniform magnetic field. Holmium is a rare-earth atom, and like other rare-earth atoms, we expect laser cooling and trapping of holmium to be possible based on success with other rare-earth elements (McClelland and Hanssen, 2006; Lu *et al.*, 2010), and hence implementation of 60 qubits in a small trapped ensemble of holmium atoms may be possible with our proposal.

Saffman and Mølmer (2008) further analyzed the possibility to trap several ensembles, each providing 60 bits of information, and thus approached a 1000-bit quantum computer with only 16 ensembles in a 2D architecture. With a few micron separation between the ensembles it is possible to use the Rydberg interaction gate as in Sec. III.C to accommodate interensemble gate operations. Hence neither optical communication nor transport of

atoms is necessary to reach a moderately large scale quantum computer.

There are undeniably many challenges associated with implementing a large scale collectively encoded register. Since the interaction gate depends sensitively on the separation between atoms (see Fig. 15), it appears difficult to reach a gate error of 0.001, especially considering the finite size of each ensemble, relative to the interensemble spacing. The interensemble gate errors will therefore tend to be higher than for gates between qubits in one ensemble. There are possible solutions to this difficulty, including implementing gates via a two-step process that uses an intermediary single ensemble (or single atom) located far enough away to minimize sensitivity to the interensemble spacing. Rare-earth atoms that are relatively poorly studied and have not been widely used for laser cooling present an additional set of challenges. A large number of lasers of different wavelengths and frequencies are required for the various internal state manipulations. In addition, as mentioned above, excellent magnetic field stability is needed to achieve long coherence times between states with a linear differential Zeeman shift. Again, there are possible approaches to mitigating this sensitivity. One possibility is to encode information in logical bits, each containing four internal states with quantum numbers $|f, \pm m\rangle$, $|f', \pm m\rangle$. Such a combination has zero linear Zeeman shift, at the expense of reducing the register size by a factor of 2.

In some sense we have transferred the complexity of moving quantum information spatially, by implementing gates between qubits in an array, to the problem of implementing gates between a multiplicity of nondegenerate internal states. Although the overall complexity required to build a large quantum processor will remain high, we believe it is worthwhile to explore a range of approaches. Indeed, there is no known simple approach to building a 100- or 1000-qubit scale quantum logic device.

F. Many-particle entanglement

We note that our collective coding of qubits makes explicit use of many-particle entangled states, and a single collective qubit attaining the classical logical value 1 is equivalent to an entangled, so-called W state. Entangled logical qubits, e.g., a Bell state in a two-bit register $|\bar{0}\bar{1}\rangle + |\bar{1}\bar{0}\rangle$, are physical states of our ensemble which are not particularly more entangled than the “classical” logical qubit states $|\bar{0}\bar{1}\rangle$ and $|\bar{1}\bar{0}\rangle$ in our collective encoding of the same quantum register. In this section, we consider how the Rydberg blockade may be used to engineer a variety of entangled states, but our focus here is not on quantum states for quantum computing, but on the few- and many-particle states that find other applications, e.g., in high precision measurements. Internal state energy differences provide the definition of time in atomic clocks and they are sensitive to external perturbations, such as magnetic fields, which can hence be

probed more precisely with squeezed states or other kinds of entangled states. With state dependent forces, entangled states may be used in interferometers and yield enhanced sensitivity to external motion and inertial effects. This also implies that we explore symmetric states of the atomic ensembles, where the collective population of the internal states is the interesting quantum degree of freedom, and is not restricted to the values of zero or unity.

1. Spin squeezing

Bouchoule and Mølmer (2002) proposed to use Rydberg blockade to squeeze the collective spin variable associated with the effective spin-1/2 description of stable pairs of atomic states. Spin-squeezed states show less quantum mechanical spreading of one of the collective spin components at the expense of increased fluctuations in another component. The possibility to squeeze the spin has led to suggestions for the use of spin-squeezed states in precision metrology and is described by Wineland *et al.* (1994), while the connection between measured values for the mean and variance of different collective spin components and the degree of multiparticle entanglement among the individual particles is quantified by Sørensen and Mølmer (2001) and Tóth *et al.* (2007). By analogy with the quantum optical squeezing of light, which is achieved by a Hamiltonian, quadratic in photon creation and annihilation operators,

$$H_{\text{sq}} = \xi \hat{c}^2 + \xi^* (\hat{c}^\dagger)^2, \quad (48)$$

we obtain spin squeezing by processes that simultaneously transfer pairs of atoms between the internal levels, while processes that transfer the atoms independently of each other only cause a rotation of the collective spin vector. The spin-squeezed state is a superposition of states with different even numbers of atoms transferred to the initially unpopulated state.

Bouchoule and Mølmer (2002) observed that two-photon transitions between a pair of ground states and the Rydberg state constitute an effective four-photon Raman transition between the ground atomic states. If lasers are used which accommodate two oppositely detuned transition paths for these Raman transitions, single-atom transitions are energetically suppressed, while the eight-photon process where two atoms are simultaneously transferred from one to the other ground state becomes resonant, provided the atoms follow transition paths with opposite four-photon Raman detunings. The high order collective pairwise transition of two atoms with no intermediate single-atom resonances is of course very weak, see for example, Brion, Mouritzen, and Mølmer (2007), but as suggested by Bouchoule and Mølmer (2002) the collective enhancement applies to speed up the transitions. Furthermore, the degree of squeezing, measured by the reduced variance of the squeezed spin component relative to the value in the spin coherent state, is given by the total number of atoms transferred, and in large samples of atoms substan-

tial spin squeezing thus requires only a small transfer of ground-state population per atom.

2. GHZ states

Stronger and also more fragile entanglement is shown by the Greenberger-Horne-Zeilinger (GHZ) states, which are superposition states of the form $|0\rangle^N + |1\rangle^N$, where all atoms occupy one or the other internal state $|0\rangle$ or $|1\rangle$. Several schemes have been suggested for the production of GHZ states by Rydberg blockade, and we here distinguish between the situation where one has access to a single atom, which is capable of controlling the evolution of an ensemble of N other atoms, and the situation in which we have only access to the collective degrees of freedom of a single ensemble consisting of N atoms.

If a single individually addressable atom in the vicinity of N atoms in the ground state $|0\rangle$ can be excited into a superposition of a ground and Rydberg excited state, the joint system will occupy the state

$$|\Psi_{r,\text{ind}}\rangle = \frac{1}{\sqrt{2}}(|0\rangle + |r\rangle) \otimes |0^N\rangle. \quad (49)$$

Following the ideas presented by Lukin *et al.* (2001) and assuming that all atoms are within the Rydberg blockade distance of each other, a sequence of resonant pulses on the $|0\rangle - |r\rangle$ and the $|r\rangle - |1\rangle$ transition directed onto the sample of N atoms can then lead to the GHZ state by producing first the state

$$|\Psi_{r,\text{col}}\rangle = \frac{1}{\sqrt{2}}(|0\rangle \otimes |r^1 0^{N-1}\rangle + |r\rangle \otimes |0^N\rangle), \quad (50)$$

where we observe the Rydberg blockade of simultaneous excitation of the control atom and the N -atom ensemble (for simplicity, we disregard phase factors associated with Rabi oscillations in the following arguments). The symbol $|r^1 0^{N-1}\rangle$ denotes the permutation symmetric state of the N indistinguishable atoms with one Rydberg atom and $N-1$ state $|0\rangle$ atoms. A subsequent pulse of light on the N -atom sample on the $|r\rangle - |1\rangle$ transition leads to the state

$$|\Psi_{\text{ent}}\rangle = \frac{1}{\sqrt{2}}(|0\rangle \otimes |1^1 0^{N-1}\rangle + |r\rangle \otimes |0^N\rangle), \quad (51)$$

and repeating the pair of pulses on the N -atom sample on the two transitions with durations matched to the collective transfer Rabi frequencies, the sample state, correlated with the ground state $|0\rangle$ of the control atom is gradually transferred to the state $|1^N\rangle$. The joint state of all atoms is then equivalent to the GHZ form.

Recently Müller *et al.* (2009) demonstrated that by a careful choice of field parameters the control atom is capable of blocking a Raman transition via the Rydberg state between $|0\rangle$ and $|1\rangle$ of all N atoms at once and hence produce the same entangled state in one single step. This process relies on a delicate destructive interference effect like the dark state phenomenon used in electromagnetically induced transparency. Via measure-

ments on the control atom, the interaction with the ensemble offers means to characterize the entanglement in the N -atom system (Müller *et al.*, 2009).

It is also possible to produce the GHZ and other many-atom entangled states without separate access to a single atom, which can control the sample. We now review two methods relying on adiabatic processes, where the fields are turned gradually on and off on different internal atomic transitions, and another method making use of the possibilities to excite different Rydberg states with different interaction characteristics.

Two adiabatic schemes have been proposed, where the ground states and the Rydberg states are coupled in a lambda transition and a ladder transition, respectively. In the lambda configuration scheme (Unanyan and Fleischhauer, 2002), where both ground states couple to the Rydberg state, one uses the blockade to prepare first a superposition state of the form

$$|\Psi_{r,\text{sup}}\rangle = \frac{1}{\sqrt{2}}(|r^1 0^{N-1}\rangle + |0^N\rangle). \quad (52)$$

A subsequent Raman adiabatic process from $|0\rangle$ to $|1\rangle$ via the Rydberg state is blocked in the first component of the state, but happens unhindered in the second part without ever populating the Rydberg state, and finally the $|r\rangle$ component can be driven back to $|0\rangle$ to yield the desired state.

The ladder configuration, studied by Møller *et al.* (2008), couples the lower ground state $|0\rangle$ directly to $|1\rangle$, which in turn is coupled to $|r\rangle$. Here the rapid adiabatic passage is used with the “counterintuitive” pulse sequence (Bergmann *et al.*, 1998), where the coupling on the $|1\rangle - |r\rangle$ transition is gradually switched off while the coupling on the lower $|0\rangle - |1\rangle$ transition is turned on, having the effect on a single atom to reliably transfer it to the Rydberg state from the lower ground state. When applied to two atoms, the Rydberg blockade prevents the atoms to be both transferred to the Rydberg state, and, in fact, the final state contains no Rydberg population at all but instead leaves the atoms in an entangled superposition state $(1/\sqrt{2})(-|0^2\rangle + |1^2\rangle)$. For higher numbers of atoms N , one realizes that for even values of N that no Rydberg population exists in the final state, which instead becomes a Dicke collective spin eigenstate with zero eigenvalue of the collective spin operator

$$\hat{J}_x \equiv (\hat{a}_0^\dagger \hat{a}_1 + \hat{a}_0 \hat{a}_1^\dagger) \hbar/2, \quad (53)$$

where the oscillator raising ($\hat{a}_{0,1}^\dagger$) and lowering ($\hat{a}_{0,1}$) operators add and remove a single atom in the two atomic ground states $|0\rangle$ and $|1\rangle$. For N odd, the final state is a permutation symmetric state with a single Rydberg excited atom, and the remaining atoms populating a collective $\hat{J}_x=0$ Dicke eigenstate. The Dicke states are themselves interesting entangled states with possible applications in metrology, and Møller *et al.* (2008) demonstrated how to use the Rydberg excitation conditioned on the odd-even atom number parity to accumulate non-trivial phase factors and produce a GHZ state.

Both proposals (Unanyan and Fleischhauer, 2002; Møller *et al.*, 2008) recognize the presence of an effective Jaynes-Cummings Hamiltonian in the coupling of the N ground-state atoms due to the saturation of the two-level transition between states with zero and one Rydberg excited states. It is thus possible to perform “cavity QED” experiments with the atomic sample, and the nonlinearity of the Jaynes-Cummings model suggests that, with the adiabatic switching between two different Hamiltonian terms, the system may also be used as a quantum simulator to explore phase transition dynamics, as done with trapped ions (Friedenauer *et al.*, 2008).

As described in Sec. II.B, the Förster resonance provides strong interactions for particular “coincidental” degeneracies of pairs of Rydberg excited states while, in the absence of Förster resonances, the interaction between Rydberg excited states is much weaker and has shorter range. We assume the existence of two Rydberg states $|s\rangle$ and $|p\rangle$ with strong mutual interactions between pairs of atoms in the $|s\rangle$ state and between a pair of atoms in the $|s\rangle$ and $|p\rangle$ states, while two atoms in the $|p\rangle$ state feel only a weak interaction. Examples of such states in ^{87}Rb are $|s\rangle = |41s_{1/2}, m=1/2\rangle$ and $|p\rangle = |40p_{3/2}, m=1/2\rangle$, for which the p - p interaction is more than two orders of magnitude weaker than the s - p interaction for all relevant parameters (Saffman and Mølmer, 2009), as shown in Fig. 11. Instead of a definite single atom controlling an ensemble, we can use the Rydberg blockade to introduce a single excitation in an ensemble which can subsequently control the collective population in other states. Beginning with all atoms in the state $|0^N\rangle$, a pulse on the 0 - s transition creates the superposition state,

$$|\Psi_{s,\text{sup}}\rangle = \frac{1}{\sqrt{2}}(|s^1 0^{N-1}\rangle + |0^N\rangle). \quad (54)$$

Driving subsequently the transition 0 - p , the absence of a strong p - p interaction allows transfer of all atoms into the $|p\rangle$ state, provided $|s\rangle$ is not populated,

$$|\Psi_{s,p}\rangle = \frac{1}{\sqrt{2}}(|s^1 0^{N-1}\rangle + |p^N\rangle). \quad (55)$$

Following this process by driving the p - 1 transition toward the other atomic ground state and inverting the initial pulse on the 0 - s transition finally produces the desired state,

$$|\Psi_{\text{GHZ}}\rangle = \frac{1}{\sqrt{2}}(|0^N\rangle + |1^N\rangle). \quad (56)$$

In all of the above proposals, the fidelity with which the entangled states can be prepared is an important issue. The fidelity is reduced by atomic decay out of the excited states and by fluctuations in the value of the Rydberg interactions among different pairs of atoms. For the proposals relying on adiabatic transfer, nonadiabatic transitions should be avoided as much as possible, and for the latter proposal the not completely vanishing

interaction between atoms in the $|p\rangle$ Rydberg state should be taken into account. For larger atom numbers these errors imply that GHZ states become more and more difficult to produce with high fidelity. In comparison, the entanglement in spin-squeezed states is less critical to losses and noise (Bouchoule and Mølmer, 2002), and in samples with many atoms, already a small population transfer and entanglement per atom is associated with considerable squeezing making this a much easier task.

VI. RYDBERG-EXCITED ENSEMBLES AND QUANTUM OPTICAL EFFECTS

Quantum optics is widely defined as the field of physics dealing with the preparation, application, and detection of quantum states of the radiation field. The research involves demonstration of quantum mechanical effects and it finds application in precision probing at the limits sets by quantum uncertainty relations and in optical strategies for quantum computing and communication. Single atoms and materials with optical nonlinearities have been used to produce a wide variety of field states (squeezed states, Fock states, “Schrödinger cat” states, etc.), and in this section we present a few examples of the possibilities offered by the strong Rydberg interaction energy in atomic ensembles to manipulate quantum states of light.

A. Nonlinear and quantum optics in atomic ensembles

1. Optical and electric control of transmission properties of an atomic ensemble

Friedler *et al.* (2005) suggested to use the Rydberg interaction to effectively provide a phase gate between two single-photon pulses propagating from opposite sides through the atomic medium. The proposal is an application of several aspects of EIT (Fleischhauer *et al.*, 2005). The pulses are assumed to excite the macroscopically populated ground state toward two different optically excited states $|e_1\rangle$ and $|e_2\rangle$, which are already coupled in a ladder configuration by classical control fields toward two different, mutually interacting Rydberg states $|r_1\rangle$ and $|r_2\rangle$ (see Fig. 38). The atomic three-level transition transforms each photon wave packet into a polariton (Fleischhauer and Lukin, 2000), i.e., a coherent superposition of a field and an excited atomic component, which travels through the medium with a reduced speed, controlled by the intensity of the classical control field.

At weak control fields, the propagation is very slow, and the polariton has an atomic character in the form of a collectively shared single excitation of the Rydberg state within a spatial volume which is compressed relative to the initial pulse length by the reduction in propagation speed. Since only single photons are present in the incident quantum fields, there is no effect of the Rydberg interaction on the properties of the individual polaritons. When the two counterpropagating polaritons

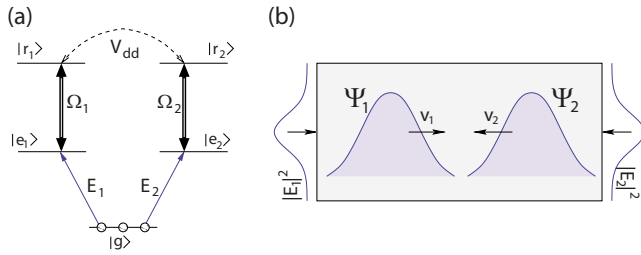


FIG. 38. (Color online) Rydberg mediated interaction between optical fields. (a) Level scheme of atoms interacting with weak (quantum) fields $E_{1,2}$ on the transitions $|g\rangle \rightarrow |e_{1,2}\rangle$ and strong driving fields of Rabi frequencies $\Omega_{1,2}$ on the transitions $|e_{1,2}\rangle \rightarrow |r_{1,2}\rangle$, respectively. V_{dd} denotes the dipole-dipole interaction between pairs of atoms in Rydberg states $|r\rangle$. (b) Upon entering the medium, each field having Gaussian transverse intensity profile is converted into the corresponding polariton $\Psi_{1,2}$ representing a coupled excitation of the field and atomic coherence. These polaritons propagate in opposite directions with slow group velocities $v_{1,2}$ and interact via the dipole-dipole interaction. From [Friedler *et al.*, 2005](#).

meet in the middle of the ensemble, however, state components with nearby pairs of atoms excited to Rydberg states $|r_1\rangle$ and $r_2\rangle$ are populated in a time-dependent manner, and these components will hence accumulate a phase factor due to the interaction energy. [Friedler *et al.* \(2005\)](#) showed, perhaps surprisingly, that rather than a complicated distortion and correlation of the phase fronts of the two polariton modes, the interaction when the two polaritons pass each other, leads to a single uniform phase shift ϕ of the state, determined by the polariton transverse width and velocity and the Rydberg interaction strength. As calculated by [Friedler *et al.* \(2005\)](#) for parameters corresponding to a $100\ \mu\text{m}$ long sample of cold atoms this phase may attain the value π and hence paves the way to use atomic samples as an environment for deterministic entanglement of optical fields and photonic quantum gates.

Experimental progress in this direction using a sample of cold Rb atoms is evident in [Pritchard *et al.* \(2009\)](#) where, with reference to Fig. 38, a control field on the $|e\rangle$ - $|r\rangle$ transition is used to strongly modify the transmission of a probe field on the $|g\rangle$ - $|e\rangle$ transition via the EIT mechanism. The presence of Rydberg interactions modifies the EIT dark state [in a manner similar to that invoked by [Møller *et al.* \(2008\)](#) for creation of GHZ states] such that the optical transmission becomes a function of the atomic density and the strength of the probe field. Although the parameters were not yet in the π phase shift regime needed for a single-photon phase gate, the experiments do demonstrate mapping of the dipolar Rydberg interaction onto an optical nonlinearity.

B. Light-atom quantum interfaces with Rydberg blockade

A large working register for quantum computing may for practical reasons have to be split into separate physical units each holding part of the register qubits, and flying photonic qubits may be applied for quantum gates

between these physical units. Long-distance quantum communication suffers from propagation and coupling losses, and it has been proposed to transmit information only over shorter distances and store it in so-called repeaters, while the errors are still small and may be corrected via quantum error correction applied to subsequently transmitted and retrieved flying qubits. By further exchange of entangled qubit pairs with similar distant repeaters, it is thus possible, by error correction and rejection of erroneous qubits, to establish entangled qubit pairs at long distances or between several components of a large quantum computer.

For these reasons, interfacing of stationary and flying qubits constitutes an active field of research ([Hammerer *et al.*, 2010](#)). In this section we discuss how a sample with a few hundred atoms within a few micron-sized region of space is large enough to provide efficient cooperative absorption and emission of light and still small enough to ensure strong dipole-dipole interactions when atoms are excited into high-lying Rydberg states. Based on our collective qubit encoding scheme, we propose to build few-qubit quantum registers in such samples which can receive and emit quantum information in the form of single photons. Using the internal atomic level structure to implement logical operations on just a few bits, the samples can then employ entanglement pumping protocols ([Dür and Briegel, 2003](#); [Jiang *et al.*, 2007](#)) to perform ideally in networks for scalable quantum computing and long-distance quantum communication. It is furthermore possible to exploit the availability of multiple excitation paths to prepare superposition states that emit more complex multiphoton entangled states. Protocols for generation of complex photonic states have been developed ([Porras and Cirac, 2007, 2008](#); [Nielsen and Mølmer, 2010](#)).

The atomic sample may also receive and store subsequent single-photon wave packets in separate collective internal states. With the availability of collective encoding two-qubit gates, it can then be used as a processing unit for gates between photonic qubits.

1. Cooperative emission of single photons

Spontaneous emission of light from an ensemble of atoms is related to the process of superradiance and has been extensively studied in the literature. Within quantum information theory, the collectively enhanced coupling strength of atomic ensembles has been proposed as a means to implement effective single-photon absorbers ([Imamoglu, 2002](#); [James and Kwiat, 2002](#)) and to construct quantum repeaters for long-distance quantum communication with atomic ensembles ([Duan *et al.*, 2001](#)), and following [Lukin *et al.* \(2001\)](#) it was shown by [Saffman and Walker \(2002\)](#) that even a fairly small cloud of Rydberg blocked atoms constitutes a directional source of single photons. The Rydberg blockade ensures that only a single atomic excitation is created in the system, and the directional emission follows from the coherent addition of scattering amplitudes for the individual atoms and the phase matching over the sample.

Assuming an atomic distribution with a width w_a , Saffman and Walker (2005b) estimated that a Gaussian radiation mode with a $1/e^2$ intensity waist of $w_0 = \sqrt{2}w_a$ which radiates into a solid angle of $\Omega_c = 2\pi/(kw_0)^2$ will be populated with a probability related to the cooperativity parameter C by Lugiato (1984)

$$P = \frac{C}{1+C} = \frac{N/2k^2w_0^2}{1+N/2k^2w_0^2}. \quad (57)$$

If we want the photon to function properly as a qubit, not only the directional distribution but also the temporal dependence of the emitted photon field is important. Interestingly the full time-dependent problem of collective emission has recently received considerable interest (Mazets and Kurizki, 2007; Das *et al.*, 2008; Porras and Cirac, 2008; Mandilara *et al.*, 2009), and Pedersen and Mølmer (2009) provided a solution for the light emission from an atomic sample, containing initially a single distributed atomic excitation.

We assume the initial collective atomic state

$$|\Psi_0\rangle = \frac{1}{\sqrt{N}} \sum_{j=1}^N e^{i\mathbf{k}_0 \cdot \mathbf{r}_j} |e_j\rangle \otimes |0\rangle, \quad (58)$$

where $|e_j\rangle$ is shorthand for the state with atom j excited and the other atoms in their ground state $|g\rangle$. This state, containing a single excitation collectively shared among the atoms, with a position-dependent complex phase is prepared with three laser fields as shown in Fig. 4. The first two fields with wave vectors $\mathbf{k}_1, \mathbf{k}_2$ drive a resonant excitation into a Rydberg state, where the blockade interaction prevents transfer of more than a single atom. A resonant π pulse with wave vector \mathbf{k}_3 hereafter drives the atomic excitation into the excited state $|e\rangle$, producing the state (58) with $\mathbf{k}_0 = \mathbf{k}_1 + \mathbf{k}_2 - \mathbf{k}_3$.

Since the system is restricted to states with only a single excitation, we can expand the time-dependent state of the atoms and the quantized field

$$|\Psi(t)\rangle = \sum_{j=1}^N \alpha_j e^{-i\omega_0 t} |e_j\rangle \otimes |0\rangle + \sum_{\mathbf{k}} \kappa_{\mathbf{k}} e^{-i\mathbf{k}t} |g\rangle \otimes |\mathbf{k}\rangle, \quad (59)$$

where $|\mathbf{k}\rangle$ denotes the single-photon state in the plane wave mode with wave number \mathbf{k} , $|g\rangle$ is shorthand for the collective state with all atoms in the ground state, and α_j and $\kappa_{\mathbf{k}}$ are time-dependent expansion coefficients in the interaction picture. For simplicity, polarization of the light and the atomic Zeeman sublevel structures are omitted from this analysis, and we assume that the interaction between the atoms and the quantized radiation field is described by $V_I = \sum_{j=1}^N \sum_{\mathbf{k}} \hbar g_{\mathbf{k}} a_{\mathbf{k}}^\dagger |g\rangle \langle e| e^{-i\mathbf{k} \cdot \mathbf{r}_j} e^{i(\mathbf{k} - \omega_0)t}$.

The Schrödinger equation for the photon state amplitudes $\kappa_{\mathbf{k}}$ can be formally solved in terms of the atomic amplitudes and substituted back into the Schrödinger equation for the atomic amplitudes,

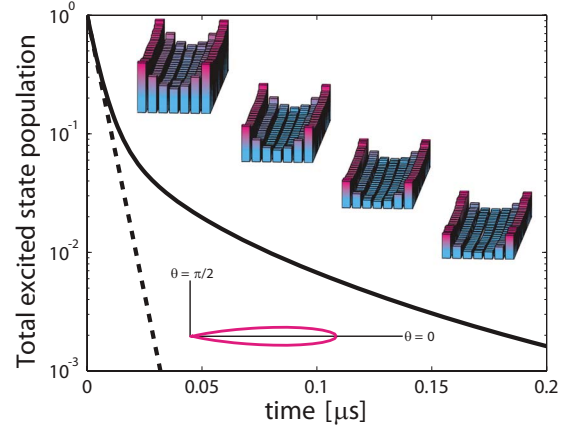


FIG. 39. (Color online) Excited-state population in an ^{87}Rb sample with $7 \times 7 \times 20$ atoms (solid curve). The population follows an exponential collective decay law (dashed line) until $t = 10^{-8}$ s, where the excitation is no longer uniform in the sample as shown by the excited-state population in the four top layers of the sample, shown in the upper part of the graph. The bottom inset shows the directional photon density at $t = 10^{-7}$ s.

$$\dot{\alpha}_j = - \sum_{j'=1}^N \sum_{\mathbf{k}} |g_{\mathbf{k}}|^2 e^{i\mathbf{k} \cdot (\mathbf{r}_j - \mathbf{r}_{j'})} \int_0^t e^{i(\mathbf{k} - \omega_0)(t' - t)} \alpha_{j'}(t') dt'.$$

This expression is the starting point for the Weisskopf-Wigner approximation, which argues that the atomic amplitudes $\alpha_j(t')$ can be taken outside the integral over t' and be simply evaluated at the time t , in which case we only need to solve a simple set of first-order differential equations. The number of equations is the same as the number of atoms, and hence the decay problem can be readily solved on a computer for up to several thousand atoms. Singular value decomposition (SVD) provides numerical eigenvalues and eigenvectors which parametrize a formal solution of the equations in terms of exponentially decaying and oscillating terms. The Schrödinger equations for the field amplitudes $\kappa_{\mathbf{k}}(t)$ contain the atomic amplitudes as source terms, and by formally integrating the exponentially evolving atomic amplitudes we thus obtain the asymptotic values $\kappa_{\mathbf{k}}(t)$ for t much larger than the atomic excited-state lifetime, as simple expressions parametrized by the SVD eigenvectors and eigenvalues.

In the case that the single collective atomic population resides in ground or metastable states coupled by a classical control field to the optically excited state, the atomic emission occurs by a spontaneous Raman transition and $2N$ coupled equations for the atomic amplitudes must be solved (Poulsen and Mølmer, 2010), and one subsequently gets the spatiotemporal field distribution in the same way as above.

In the numerical simulations presented in Fig. 39, we have studied a cubic lattice with an elongated sample of $7 \times 7 \times 20 = 980$ atoms. With a lattice spacing of $0.37 \mu\text{m}$, the maximum distance between any two atoms is $8.3 \mu\text{m}$, short enough to achieve the Rydberg blockade

for the preparation of the initial state and for later qubit manipulation. We use numbers characteristic for ^{87}Rb and the $5P_{1/2}$ excited state with a spontaneous emission rate of $\gamma_1 = 37 \mu\text{s}^{-1}$.

As shown in Fig. 39, the excited-state population initially decays as $\exp(-\gamma_{\text{col}}t)$ (dashed line), where $\gamma_{\text{col}} = 5.7\gamma_1$. The upper insets show the excited-state population on individual atoms in the four upper layers of the ensemble at $t = 10^{-8}$ s (the sample is mirror symmetric in the central plane of atoms shown as the lowest layer in the figure). As shown by the inset, at this time the symmetry of the atomic excited-state population in the sample is broken, and this explains the slower decay of the remaining few percent of excitation in the system.

In the superradiant stage, light emission occurs predominantly within a narrow emission cone. This is illustrated in the lower inset of Fig. 39, showing the total photon emission probability as function of direction. With more than 95% probability the photon is emitted in a direction within 0.3 rad off the axis of the sample, which is in qualitative agreement with the estimate (57).

One might worry that the loss or misplacement of a few atoms from the sample would cause a significant change in the field mode, and hence unrealistic demands on the ability to trap atoms would have to be met to reliably produce high fidelity photonic qubits. We have tested this concern by removing tens of atoms from random locations in the system studied in Fig. 39. We have then solved the coupled atomic equations and computed the field mode emitted by the modified structure as described in the text and in each case determined the overlap of the resulting field with the one emitted by the original sample. These overlaps are robust and in excess of 99% in all our simulations.

C. Quantum communication protocols

In the previous section we have reviewed how a cloud of atoms, small enough to enable an efficient Rydberg blockade of the collective excitation, may serve as a directional single-photon emitter. For quantum communication it is equally important to be able to receive information as it is to send it, and, indeed, a time-reversal argument ensures that a field with a spatial dependence which is the complex conjugate of the fields emitted by our sample found above will travel in the opposite direction and converge upon the sample. Moreover, this time or motion reversal also applies to the solution of the coupled atom-light system, and the conjugate field hence becomes extinct by collectively exciting the atomic system. The small atomic cloud is an atomic storage medium for a single photon if it is incident on the sample in a particular mode. With controllable classical fields engaged in the Raman processes of light emission from one sample and absorption in another one, we get more degrees of freedom to tailor the single-photon mode function so that it may be absorbed with high efficiency. The atomic excited state has finite lifetime, and the

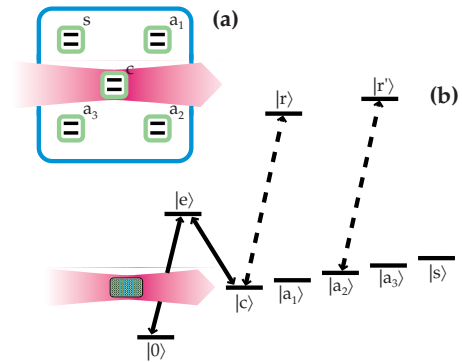


FIG. 40. (Color online) Quantum communication with a small quantum register. (a) A five-qubit register consisting of a communication qubit (c), a storage qubit (s), and three auxiliary qubits ($a_{1,2,3}$) (Jiang *et al.*, 2007; Gorshkov, Calarco, *et al.*, 2008). (b) The collective encoding implementation, with a collective internal state transition interacting with the field mode, and long-lived and Rydberg internal states used for encoding and coupling of the five qubits.

population should hence quickly be transferred coherently to a stable atomic state.

The use of much larger atomic ensembles for light storage, e.g., by electromagnetically induced transparency (Fleischhauer and Lukin, 2000; Liu *et al.*, 2001), has capacity to store a much larger number of modes (Nunn *et al.*, 2008), and the precise shape and arrival time of the weak probe field does not need to be specified for storage of a single incident pulse to work. Note, however, that this apparent robustness to imprecision and noise in the storage and retrieval of light pulses in large samples does not remove the necessity to address precisely the spatiotemporal photon wave packet if the coherent qubit space of the photon is to be fully explored.

A storage fidelity of 95% may be enough to demonstrate simple operations, but it is not enough to provide scalability in quantum computing or in long-distance quantum communication. Here, however, we make use of the fact that this fidelity is obtained for a few hundred atoms within a $10 \mu\text{m}$ wide volume. An incident field state with a single photon may thus be transferred to a state of this ensemble, which is an even superposition of states where each atom is in a stable state $|c\rangle$ while all other atoms are in another specific ground state. This is precisely a state of the form of the collectively encoded qubits described in Sec. V.C. Using the ensemble Rydberg blockade gates developed in Sec. V.D, it is possible to perform entanglement pumping (Dür and Briegel, 2003) via two-bit gates from the information receiving qubit toward other bits in the register; cf. Fig. 40.

Jiang *et al.* (2007) showed that under the assumption of gates being possible between 4 and 5 auxiliary qubits, measurements and multiple rounds of communication can raise a 90% transmission fidelity to arbitrarily high degrees of entanglement between two samples. We refer the interested reader to Jiang *et al.* (2007) for the algorithmic details and simply note that using our collective encoding scheme with five internal levels as shown in

Fig. 40 we have access to the needed auxiliary qubits and the gates between them. Figure 40 shows the five-qubit register designs, proposed by Jiang *et al.* (2007) (a), and the ensemble qubit proposal of Pedersen and Mølmer (2009) (b). In Fig. 40(a) five separate physical systems take the role of a communication qubit, c , three auxiliary qubits for temporary storage and entanglement pumping, $a_i, i=1,2,3$, and a storage qubit for the perfected state, s . A chain of trapped ions with a single ion residing in an optical cavity for communication or ^{13}C atoms in the proximity of an optically addressable NV center in diamond are proposed by Jiang *et al.* (2007) as candidates for these five physical qubits. In Fig. 40(b) a generic single-atom level scheme is shown for our collective encoding with a reservoir state, and five different long-lived states playing the same roles as the five physical qubits in Fig. 40(a), and an optically excited state and two Rydberg excited states, needed for optical interfacing and one- and two-bit operations, respectively. 1000 atoms should suffice to allow near-perfect one- and two-qubit gate operations even when the population of the spectator qubits is not definitely zero or unity. We emphasize that the collective encoding both yields the efficient coupling to single photons and alleviates the need for addressing of individual atoms.

D. Hybrid qubit interfaces with Rydberg atoms

The strong interactions between Rydberg excited atoms makes the Rydberg blockade mechanism an attractive mediator in hybrid proposals for quantum information processing.

In Sec. V.F, we presented several examples where a single Rydberg excitation was able to control collective states of an entire ensemble, and one can easily imagine how this mechanism can be used to interface effectively between the standard encoding scheme of qubits stored in individually addressable atoms, as in Sec. III.D, and the collective encoding in Sec. V.C. Similarly, an interface between continuous variables associated with the oscillator ladder of multiply excited ensemble states and the discrete qubit scenario may take its starting point in the Rydberg blockade interaction.

In this section we comment on the possibility to use hybrid physical systems to extend the advantages of the Rydberg mechanism to larger systems of particles. It may be desirable to extend the Rydberg interactions to longer distances, as many atoms can then be more easily addressed in experiments, and with more atoms a photon-atom interface may become more efficient due to the larger optical depth. Also, the dipole moment of a Rydberg atom is sufficiently large that a single-atom or a Rydberg blocked ensemble may provide an adequate strongly coupled nonlinear component in various cavity QED setups. Sørensen *et al.* (2004) proposed to locate two Rydberg atoms in suitable vicinity of antenna surfaces and use a superconducting transmission line to mediate the interaction between the atoms over centimeter distances. Stripline cavities have been produced and extensively studied in interaction with Cooper-pair boxes

(Blais *et al.*, 2004), and it seems realistic to trap atoms in the vicinity of such striplines and approach the strong coupling cavity QED regime, both with a single atom and with the collectively enhanced coupling of an ensemble of atoms to the cavity field.

The stripline cavities have their resonance frequencies in the GHz range (Blais *et al.*, 2004), and they may be tuned to couple efficiently to transitions among different Rydberg states. Petrosyan and Fleischhauer (2008) proposed to use the cavity field to mediate long-range interactions between individual atoms, and to obtain an effective blockade effect over samples large enough to provide effective single-photon emitters and media for single-photon quantum gates. Alternatively a single Rydberg atom may be entangled with the cavity field as described by Saffman *et al.* (2009), and the single atom then entangled with an ensemble atomic qubit to mediate an interface with photonic qubits. The stripline cavities interact efficiently with the so-called transmon, Cooper-pair box qubits (Blais *et al.*, 2004), which however offer lifetimes of only a few microseconds. Equivalent to similar proposals using samples of polar molecular (Rabl and Zoller, 2007), it has thus been proposed to transfer the qubit between the transmon and the atomic ensemble via the cavity field (Petrosyan *et al.*, 2009) in a truly hybrid proposal making optimum use of the fast gate processing of one and the long storage times of the other component.

Making further use of external laser fields or static fields to address collective spin waves with different wave numbers

$$|1_k\rangle \equiv \frac{1}{\sqrt{K}} \sum_j e^{ikz_j} |0 \cdots 1_j \cdots 0\rangle, \quad (60)$$

a single atomic ensemble is capable of hosting a large number of collective modes as previously proposed in molecular ensembles (Tordrup *et al.*, 2008) and in solid-state spin ensembles (Wesenberg *et al.*, 2009). In the collective encoding scheme for qubits each spatial spin-wave mode encodes a qubit and the number of modes thus provides the size of the quantum registers. Note that the spin-wave modes are only independent for a sufficiently large ensemble, and hence the cavity mediated long-range blockade interaction is necessary for this encoding to be effective.

The trapping of cold neutral atoms in the vicinity of a superconducting cavity surely constitutes a major experimental challenge that will have to be solved (Petrosyan *et al.*, 2009; Saffman *et al.*, 2009), but if a successful solution is found, the hybrid system with Rydberg atoms and resonant cavities holds potential for scalable quantum computing.

E. Rydberg atoms and alternative quantum computing paradigms

We have in this review mainly focused on the possibilities to perform quantum computing with Rydberg excited atoms as described in the circuit model of quantum

computation, i.e., quantum computation based on sequences of one- and two-bit operations applied to a register of memory qubits. The collective encoding scheme partly evades the common conception of separate logical qubits being stored in separate physical systems in the circuit model, but the collective modes are, indeed, well-characterized degrees of freedom. As emphasized by our explicit presentation of the implementation of one- and two-bit gates, quantum computation with collectively encoded qubits evolves according to the usual circuit model apart from special means needed to counter errors.

Since the emergence of the first proposals for quantum computing other ideas for the implementation and use of quantum computers have appeared. It would take us too far afield to present a detailed account of these ideas, but we mention a few examples where the properties of the Rydberg excited atoms have been shown to be particularly interesting. Cluster state or one-way quantum computers (RausENDORF and Briegel, 2001; RausENDORF *et al.*, 2003) apply physical interactions to establish a multiparticle entangled state, which serves as the initial state for a sequence of one-bit measurements which suffices to produce a final state of the remaining bits of the same universal generality as the output register obtained by a quantum computation in the circuit model. Making use of the Rydberg blockade interaction within atomic ensembles and the ability for atomic ensembles to effectively absorb single photons, it has been proposed that the production of ensemble cluster states has a much higher probability of success than conventional schemes using light and atoms (Mei *et al.*, 2009; ZWIER and Kok, 2009). Using the few bit per ensemble and distillation ideas (Pedersen and Mølmer, 2009) described above, one may achieve an effectively deterministic protocol for cluster state preparation along the same lines, and one may consider tests with cluster states encoded collectively in a single atomic ensemble.

The one-way computer is based on measurements and thus on a dissipative element. By engineering dissipative channels acting jointly on nearest neighbor qubits in a physical architecture, one can also provide the entanglement capabilities needed for universal quantum computing (Diehl *et al.*, 2008; Verstraete *et al.*, 2009). One may think of the state prepared by this dissipation as a stationary, dark state of the dynamics, and for this state to be an entangled state, the dissipation must be engineered to act in a correlated manner on pairs or larger collections of qubits. In a recent proposal (Weimer *et al.*, 2010), it is suggested to use the Rydberg interaction to engineer these correlated multibit dissipative terms by effectively transforming the desired quantum jump operators into the natural jumps, associated with decay of optically excited states of individual atoms in regular lattice structures.

An important process that has gained recent interest is the quantum random walk, where a physical parameter walks in opposite directions according to coin tosses, and where a quantum coin in a superposition state causes a ballistic rather than diffusive spreading of

the walker caused by a classical random coin. The more rapid exploration of a wide range of parameter values may have implications for search problems, and quantum random walks have been proposed and even studied experimentally in several physical systems (Perets *et al.*, 2008; Karski, Förster, Choi, Steffen, *et al.*, 2009; Schmitz *et al.*, 2009) which may also be used for the usual circuit model of quantum computing. Côté *et al.* (2006) suggested to implement quantum random walks of a specific collective Rydberg state excitation between an array of atomic ensembles. Using the Rydberg blockade, the ensembles in a number of traps are first excited to have a single ns excited Rydberg atom, except in one trap, which is initially excited to have a single np Rydberg atom. The interaction permits a fast exchange of the excitation degree of freedom between nearest-neighbor ensembles, and thus the np excitation becomes the quantum walker, which may diffuse over the entire ensemble and eventually be detected, e.g., by field ionization. For a related study of excitation transport in an irregular trap array of atomic ensembles, see Mülken *et al.* (2007).

Last but not least quantum simulators present a topic of current interest, with the goal to use engineered quantum systems to simulate complicated many-body physics and readout information, which may not be addressed in the real systems simulated. Quantum magnetism, black hole physics, lattice gauge theories, topological quantum field theories, superconductivity, and a host of phase transition phenomena are among the topics that are currently being addressed. The Rydberg interaction is particularly useful here because it is strong and hence allows simulation of steady-state dynamics within realistic time scales and because it is switchable in a way that allows decomposition of a wide range of effective bipartite and multipartite interaction operators (Weimer *et al.*, 2010). Quantum gases of dipole-dipole interacting particles present a major challenge for many-body theory and experiment (Lahaye *et al.*, 2009), and since polar molecules and Rydberg excited atoms experience this interaction and are experimentally available and may be detected with well-established atomic physics tools, they have been proposed as a test bench for the study of cluster and supersolid formation and nonclassical crystal structures (Olmos, González-Férez, and Lesanovsky, 2010; Pohl *et al.*, 2010; Pupillo *et al.*, 2010), stabilized by quantum fluctuations (Olmos, González-Férez, and Lesanovsky, 2009b; Pupillo *et al.*, 2009).

VII. SUMMARY AND OUTLOOK

As emphasized throughout this review there is currently a high level of activity devoted to exploring the use of strong atomic interactions mediated by transient excitation of Rydberg states for a variety of quantum information processing tasks. Approximately one decade after the initial proposal of a Rydberg quantum gate (Jaksch *et al.*, 2000), the achievement of precise control of well-localized single atoms has resulted in demonstration of a two-qubit quantum gate (Isenhowser

et al., 2010; Wilk *et al.*, 2010). At the other extreme collective effects in blockaded ensembles hold promise for multiqubit registers, for robust light-atom quantum interfaces, and as a tool for simulating quantum many-body physics. The degree of control that has been achieved experimentally still lags behind theoretical expectations which suggest that high fidelity quantum gates with errors well below 0.001 are feasible. Continued development of the requisite optical and laser systems combined with improved control of the spatial and momentum distribution of single atoms will be important ingredients in ongoing work aimed at approaching theoretical limits.

Current experimental work is concentrated on alkali atoms. The alkali atoms are convenient as regards the experimental requirements needed for cooling and trapping as well as Rydberg excitation. Single electron alkali atoms are also amenable to a detailed treatment of Rydberg state properties and interactions using relatively straightforward theoretical tools. Looking to the future other parts of the periodic table may take on increased importance. Two-electron alkaline earth atoms have been widely used in quantum optics experiments in recent years with applications including high precision optical clocks and quantum gases. The possibility of incorporating Rydberg-mediated effects into alkaline earth systems is a promising, yet unexplored direction. The rare-earth atoms with their complex spectra, and large numbers of hyperfine ground states are another interesting direction which has so far only been touched on theoretically (Saffman and Mølmer, 2008). Rydberg interactions have also turned out to be important for creation of long-range molecular dimers (Farooqi *et al.*, 2003; Stanojevic *et al.*, 2006; Bendkowsky *et al.*, 2009; Overstreet *et al.*, 2009) which may prove useful as part of the current interest in applications of molecules to quantum information processing (Rabl and Zoller, 2007).

A significant aspect of Rydberg-mediated interactions is that they bridge the gap between single-atom qubits, with excellent coherence properties, and many-atom ensembles, with poorer coherence, yet the potential for establishing a deterministic quantum interface between light and atoms (Hammerer *et al.*, 2010). Many signatures of Rydberg interactions have been studied in atomic ensembles, yet a demonstration of controlled excitation of a single quantum in a many-body setting with $N > 2$ atoms has not yet been achieved. For many (but not all) potential ensemble applications, the number of atoms needs to be known with sub-Poissonian precision. Thus nondestructive number measurements are important, and these may be challenging due to light-assisted collisions. Furthermore, atomic collisions act to reduce the coherence time of ensemble based qubits.

It is likely that progress with ensemble-based qubits will be made by moving toward lattice-based experiments where there is a natural minimum barrier to the two-atom separations. The concept of collective encoding has many attractive features but to date has not been pursued experimentally. Successful implementation of this approach again seems to favor structuring the atom

distribution with a subwavelength lattice, as suggested by Saffman and Mølmer (2008).

The predictions of universal scaling behavior, quantum critical points, and mesoscopic phases of dipolar ensembles (Weimer *et al.*, 2008; Löw *et al.*, 2009; Pupillo *et al.*, 2009) are examples of direct realization of nontrivial many-body physics with Rydberg ensembles. Recent proposals (Weimer *et al.*, 2010) to use Rydberg atoms for implementing multipartite interaction operators point to broad possibilities for simulating quantum many-body physics. The potential for demonstrating controlled quantum dynamics has been well established, which will promote continued interest in this rich field for the foreseeable future.

ACKNOWLEDGMENTS

M.S. and T.G.W. thank the talented group of experimentalists at UW Madison who have contributed to the demonstration of Rydberg quantum effects over the past many years. This work was supported by NSF Grant No. PHY-0653408, ARO/IARPA under Contract No. W911NF-05-1-0492, and the European Union Integrated Project SCALA.

REFERENCES

- Abel, R. P., A. K. Mohapatra, M. G. Bason, J. D. Pritchard, K. J. Weatherill, U. Raitzsch, and C. S. Adams, 2009, "Laser frequency stabilization to excited state transitions using electromagnetically induced transparency in a cascade system," *Appl. Phys. Lett.* **94**, 071107.
- Afrousheh, K., P. Bohlouli-Zanjani, J. D. Carter, A. Mugford, and J. D. D. Martin, 2006, "Resonant electric dipole-dipole interactions between cold Rydberg atoms in a magnetic field," *Phys. Rev. A* **73**, 063403.
- Afrousheh, K., P. Bohlouli-Zanjani, D. Vagale, A. Mugford, M. Fedorov, and J. D. D. Martin, 2004, "Spectroscopic observation of resonant electric dipole-dipole interactions between cold Rydberg atoms," *Phys. Rev. Lett.* **93**, 233001.
- Ahn, J., T. C. Weinacht, and P. H. Bucksbaum, 2000, "Information storage and retrieval through quantum phase," *Science* **287**, 463.
- Aliferis, P., and J. Preskill, 2009, "Fibonacci scheme for fault-tolerant quantum computation," *Phys. Rev. A* **79**, 012332.
- Aljunid, S. A., M. K. Tey, B. Chng, T. Liew, G. Maslennikov, V. Scarani, and C. Kurtsiefer, 2009, "Phase shift of a weak coherent beam induced by a single atom," *Phys. Rev. Lett.* **103**, 153601.
- Amthor, T., C. Giese, C. S. Hofmann, and M. Weidemüller, "Evidence of antiblockade in an ultracold Rydberg gas," 2010, *Phys. Rev. Lett.* **104**, 013001.
- Anderlini, M., P. J. Lee, B. L. Brown, J. Sebby-Strabley, W. D. Phillips, and J. V. Porto, 2007, "Controlled exchange interaction between pairs of neutral atoms in an optical lattice," *Nature (London)* **448**, 452.
- Anderson, W. R., J. R. Veale, and T. F. Gallagher, "Resonant dipole-dipole energy transfer in a nearly frozen Rydberg gas," 1998, *Phys. Rev. Lett.* **80**, 249.
- Arlt, J., and M. J. Padgett, 2000, "Generation of a beam with a dark focus surrounded by regions of higher intensity: The

- optical bottle beam,” *Opt. Lett.* **25**, 191.
- Ates, C., T. Pohl, T. Pattard, and J. M. Rost, 2006, “Strong interaction effects on the atom counting statistics of ultracold Rydberg gases,” *J. Phys. B* **39**, L233.
- Ates, C., T. Pohl, T. Pattard, and J. M. Rost, 2007a, “Anti-blockade in Rydberg excitation of an ultracold lattice gas,” *Phys. Rev. Lett.* **98**, 023002.
- Ates, C., T. Pohl, T. Pattard, and J. M. Rost, 2007b, “Many-body theory of excitation dynamics in an ultracold Rydberg gas,” *Phys. Rev. A* **76**, 013413.
- Bakr, W. S., J. I. Gillen, A. Peng, S. Fölling, and M. Greiner, 2009, “A quantum gas microscope for detecting single atoms in a Hubbard-regime optical lattice,” *Nature (London)* **462**, 74.
- Barthel, C., D. J. Reilly, C. M. Marcus, M. P. Hanson, and A. C. Gossard, 2009, “Rapid single-shot measurement of a singlet-triplet qubit,” *Phys. Rev. Lett.* **103**, 160503.
- Bason, M. G., A. K. Mohapatra, K. J. Weatherill, and C. S. Adams, 2008, “Electro-optic control of atom-light interactions using Rydberg dark-state polaritons,” *Phys. Rev. A* **77**, 032305.
- Beals, T. R., J. Vala, and K. B. Whaley, 2008, “Scalability of quantum computation with addressable optical lattices,” *Phys. Rev. A* **77**, 052309.
- Beckman, D., A. N. Chari, S. Devabhaktuni, and J. Preskill, “Efficient networks for quantum factoring,” 1996, *Phys. Rev. A* **54**, 1034.
- Bendkowsky, V., B. Butscher, J. Nipper, J. P. Shaffer, R. Löw, and T. Pfau, 2009, “Observation of ultra-long-range Rydberg molecules,” *Nature (London)* **458**, 1005.
- Benhelm, J., G. Kirchmair, C. F. Roos, and R. Blatt, 2008a, “Experimental quantum-information processing with $^{43}\text{Ca}^+$ ions,” *Phys. Rev. A* **77**, 062306.
- Benhelm, J., G. Kirchmair, C. F. Roos, and R. Blatt, 2008b, “Towards fault-tolerant quantum computing with trapped ions,” *Nat. Phys.* **4**, 463.
- Bergamini, S., B. Darquié, M. Jones, L. Jacubowicz, A. Browaeys, and P. Grangier, 2004, “Holographic generation of microtrap arrays for single atoms by use of a programmable phase modulator,” *J. Opt. Soc. Am. B* **21**, 1889.
- Bergmann, K., H. Theuer, and B. W. Shore, 1998, “Coherent population transfer among quantum states of atoms and molecules,” *Rev. Mod. Phys.* **70**, 1003.
- Bernu, J., S. Deléglise, C. Sayrin, S. Kuhr, I. Dotsenko, M. Brune, J. M. Raimond, and S. Haroche, 2008, “Freezing coherent field growth in a cavity by the quantum Zeno effect,” *Phys. Rev. Lett.* **101**, 180402.
- Beterov, I. I., I. I. Ryabtsev, D. B. Tretyakov, and V. M. Entin, 2009, “Quasiclassical calculations of blackbody-radiation-induced depopulation rates and effective lifetimes of Rydberg nS , nP , and nD alkali-metal atoms with $n \leq 80$,” *Phys. Rev. A* **79**, 052504; **80**, 059902(E) (2009).
- Beterov, I. I., D. B. Tretyakov, I. I. Ryabtsev, A. Ekers, and N. N. Bezuglov, 2007, “Ionization of sodium and rubidium nS , nP , and nD Rydberg atoms by blackbody radiation,” *Phys. Rev. A* **75**, 052720.
- Beugnon, J., C. Tuchendler, H. Marion, A. Gaëtan, Y. Miroshnychenko, Y. R. P. Sortais, A. M. Lance, M. P. A. Jones, G. M. A. Browaeys, and P. Grangier, 2007, “Two-dimensional transport and transfer of a single atomic qubit in optical tweezers,” *Nat. Phys.* **3**, 696.
- Blais, A., R.-S. Huang, A. Wallraff, S. M. Girvin, and R. J. Schoelkopf, 2004, “Cavity quantum electrodynamics for superconducting electrical circuits: An architecture for quantum computation,” *Phys. Rev. A* **69**, 062320.
- Blatt, R., and D. Wineland, 2008, “Entangled states of trapped atomic ions,” *Nature (London)* **453**, 1008.
- Bloch, I., 2008, “Quantum coherence and entanglement with ultracold atoms in optical lattices,” *Nature (London)* **453**, 1016.
- Blume-Kohout, R., C. M. Caves, and I. H. Deutsch, 2002, “Climbing mount scalable: Physical resource requirements for a scalable quantum computer,” *Found. Phys.* **32**, 1641.
- Bohlouli-Zanjani, P., K. Afrousheh, and J. D. D. Martin, 2006, “Optical transfer cavity stabilization using current-modulated injection-locked diode lasers,” *Rev. Sci. Instrum.* **77**, 093105.
- Bohlouli-Zanjani, P., J. A. Petrus, and J. D. D. Martin, 2007, “Enhancement of Rydberg atom interactions using ac Stark shifts,” *Phys. Rev. Lett.* **98**, 203005.
- Boisseau, C., I. Simbotin, and R. Côté, 2002, “Macrodimers: Ultralong range Rydberg molecules,” *Phys. Rev. Lett.* **88**, 133004.
- Bouchoule, I., and K. Mølmer, 2002, “Spin squeezing of atoms by the dipole interaction in virtually excited Rydberg states,” *Phys. Rev. A* **65**, 041803R.
- Brekke, E., J. O. Day, and T. G. Walker, 2008, “Four-wave mixing in ultracold atoms using intermediate Rydberg states,” *Phys. Rev. A* **78**, 063830.
- Brennen, G. K., C. M. Caves, P. S. Jessen, and I. H. Deutsch, 1999, “Quantum logic gates in optical lattices,” *Phys. Rev. Lett.* **82**, 1060.
- Brion, E., V. M. Akulin, D. Comparat, I. Dumer, G. Harel, N. Kébaili, G. Kurizki, I. Mazets, and P. Pillet, 2005, “Coherence protection by the quantum Zeno effect and nonholonomic control in a Rydberg rubidium isotope,” *Phys. Rev. A* **71**, 052311.
- Brion, E., D. Comparat, and G. Harel, 2006, “Implementation of a CNOT gate in two cold Rydberg atoms by the nonholonomic control technique,” *Eur. Phys. J. D* **38**, 381.
- Brion, E., K. Mølmer, and M. Saffman, 2007, “Quantum computing with collective ensembles of multilevel systems,” *Phys. Rev. Lett.* **99**, 260501.
- Brion, E., A. S. Mouritzen, and K. Mølmer, “Conditional dynamics induced by new configurations for Rydberg dipole-dipole interactions,” 2007, *Phys. Rev. A* **76**, 022334.
- Brion, E., L. H. Pedersen, and K. Mølmer, 2007, “Implementing a neutral atom Rydberg gate without populating the Rydberg state,” *J. Phys. B* **40**, S159.
- Brion, E., L. H. Pedersen, K. Mølmer, S. Chutia, and M. Saffman, 2007, “Universal quantum computation in a neutral-atom decoherence-free subspace,” *Phys. Rev. A* **75**, 032328.
- Brion, E., L. H. Pedersen, M. Saffman, and K. Mølmer, 2008, “Error correction in ensemble registers for quantum repeaters and quantum computers,” *Phys. Rev. Lett.* **100**, 110506.
- Carroll, T. J., K. Claringbould, A. Goodsell, M. J. Lim, and M. W. Noel, 2004, “Angular dependence of the dipole-dipole interaction in a nearly one-dimensional sample of Rydberg atoms,” *Phys. Rev. Lett.* **93**, 153001.
- Carroll, T. J., C. Daniel, L. Hoover, T. Sidie, and M. W. Noel, 2009, “Simulations of the dipole-dipole interaction between two spatially separated groups of Rydberg atoms,” *Phys. Rev. A* **80**, 052712.
- Carroll, T. J., S. Sunder, and M. W. Noel, 2006, “Many-body interactions in a sample of ultracold Rydberg atoms with varying dimensions and densities,” *Phys. Rev. A* **73**, 032725.
- Chaloupka, J. L., Y. Fisher, T. J. Kessler, and D. D. Meyer-

- hofer, 1997, “Single-beam ponderomotive-optical trap for free electrons and neutral atoms,” *Opt. Lett.* **22**, 1021.
- Cho, J., 2007, “Addressing individual atoms in optical lattices with standing-wave driving fields,” *Phys. Rev. Lett.* **99**, 020502.
- Choi, J.-H., J. Guest, and G. Raithel, 2006, “Magnetic trapping of strongly magnetized Rydberg atoms,” *Eur. Phys. J. D* **40**, 19.
- Choi, J.-H., J. R. Guest, A. P. Povilus, E. Hansis, and G. Raithel, 2005, “Magnetic trapping of long-lived cold Rydberg atoms,” *Phys. Rev. Lett.* **95**, 243001.
- Choi, J. H., B. Knuffman, T. C. Leibisch, A. Reinhard, and G. Raithel, 2007, “Cold Rydberg atoms,” *Adv. At., Mol., Opt. Phys.* **54**, 131.
- Chotia, A., M. Viteau, T. Vogt, D. Comparat, and P. Pillet, 2008, “Kinetic Monte Carlo modeling of dipole blockade in Rydberg excitation experiment,” *New J. Phys.* **10**, 045031.
- Clarke, J., and F. K. Wilhelm, 2008, “Superconducting quantum bits,” *Nature (London)* **453**, 1031.
- Cline, R. A., J. D. Miller, M. R. Matthews, and D. J. Heinzen, 1994, “Spin relaxation of optically trapped atoms by light scattering,” *Opt. Lett.* **19**, 207.
- Côté, R., A. Russell, E. E. Eyler, and P. L. Gould, 2006, “Quantum random walk with Rydberg atoms in an optical lattice,” *New J. Phys.* **8**, 156.
- Cozzini, M., T. Calarco, A. Recati, and P. Zoller, 2006, “Fast Rydberg gates without dipole blockade via quantum control,” *Opt. Commun.* **264**, 375.
- Cubel, T., B. K. Teo, V. S. Malinovsky, J. R. Guest, A. Reinhard, B. Knuffman, P. R. Berman, and G. Raithel, 2005, “Coherent population transfer of ground-state atoms into Rydberg states,” *Phys. Rev. A* **72**, 023405.
- Cubel Liebisch, T., A. Reinhard, P. R. Berman, and G. Raithel, 2005, “Atom counting statistics in ensembles of interacting Rydberg atoms,” *Phys. Rev. Lett.* **95**, 253002; **98**, 109903(E) (2007).
- Cummins, H. K., G. Llewellyn, and J. A. Jones, 2003, “Tackling systematic errors in quantum logic gates with composite rotations,” *Phys. Rev. A* **67**, 042308.
- Cundiff, S. T., and J. Ye, 2003, “*Colloquium*: Femtosecond optical frequency combs,” *Rev. Mod. Phys.* **75**, 325.
- Das, S., G. S. Agarwal, and M. O. Scully, 2008, “Quantum interferences in cooperative Dicke emission from spatial variation of the laser phase,” *Phys. Rev. Lett.* **101**, 153601.
- Day, J. O., E. Brekke, and T. G. Walker, 2008, “Dynamics of low-density ultracold Rydberg gases,” *Phys. Rev. A* **77**, 052712.
- Deiglmayr, J., M. Reetz-Lamour, T. Amthor, S. Westermann, A. L. de Oliveira, and M. Weidemüller, 2006, “Coherent excitation of Rydberg atoms in an ultracold gas,” *Opt. Commun.* **264**, 293.
- DiCarlo, L., J. M. Chow, J. M. Gambetta, L. S. Bishop, B. R. Johnson, D. I. Schuster, J. Majer, A. Blais, L. Frunzio, S. M. Girvin, and R. J. Schoelkopf, 2009, “Demonstration of two-qubit algorithms with a superconducting quantum processor,” *Nature (London)* **460**, 240.
- Diehl, S., A. Micheli, A. Kantian, B. Kraus, H. P. Büchler, and P. Zoller, 2008, “Quantum states and phases in driven open quantum systems with cold atoms,” *Nat. Phys.* **4**, 878.
- DiVincenzo, D., 1998, “The physical implementation of quantum computers,” *Fortschr. Phys.* **48**, 771.
- Duan, L. M., M. D. Lukin, J. I. Cirac, and P. Zoller, 2001, “Long-distance quantum communication with atomic ensembles and linear optics,” *Nature (London)* **414**, 413.
- Dumke, R., M. Volk, T. Mütther, F. B. J. Buchkremer, G. Birkl, and W. Ertmer, 2002, “Micro-optical realization of arrays of selectively addressable dipole traps: A scalable configuration for quantum computation with atomic qubits,” *Phys. Rev. Lett.* **89**, 097903.
- Dür, W., and H.-J. Briegel, 2003, “Entanglement purification for quantum computation,” *Phys. Rev. Lett.* **90**, 067901.
- Dutta, S. K., J. R. Guest, D. Feldbaum, A. Walz-Flannigan, and G. Raithel, 2000, “Ponderomotive optical lattice for Rydberg atoms,” *Phys. Rev. Lett.* **85**, 5551.
- Emmert, A., A. Lupaşcu, G. Nogues, M. Brune, J.-M. Raimond, and S. Haroche, 2009, “Measurement of the trapping lifetime close to a cold metallic surface on a cryogenic atom-chip,” *Eur. Phys. J. D* **51**, 173.
- Fabre, C., and S. Haroche, 1983, in *Rydberg States of Atoms and Molecules*, edited by R. F. Stebbings and F. B. Dunning (Cambridge University Press, Cambridge), Chap. 4, p. 117.
- Fano, U., and A. R. P. Rau, 1986, *Atomic Collisions and Spectra* (Academic, Orlando).
- Farooqi, S. M., D. Tong, S. Krishnan, J. Stanojevic, Y. P. Zhang, J. R. Ensher, A. S. Estrin, C. Boisseau, R. Côté, E. E. Eyler, and P. L. Gould, 2003, “Long-range molecular resonances in a cold Rydberg gas,” *Phys. Rev. Lett.* **91**, 183002.
- Flannery, M. R., D. Vrinceanu, and V. N. Ostrovsky, 2005, “Long-range interaction between polar Rydberg atoms,” *J. Phys. B* **38**, S279.
- Fleischhauer, M., A. Imamoglu, and J. P. Marangos, 2005, “Electromagnetically induced transparency: Optics in coherent media,” *Rev. Mod. Phys.* **77**, 633.
- Fleischhauer, M., and M. D. Lukin, 2000, “Dark-state polaritons in electromagnetically induced transparency,” *Phys. Rev. Lett.* **84**, 5094.
- Förster, T., 1948, “Zwischenmolekulare energiewanderung und fluoreszenz,” *Ann. Phys. (Paris)* **437**, 55.
- Fortágh, J., and C. Zimmermann, 2007, “Magnetic microtraps for ultracold atoms,” *Rev. Mod. Phys.* **79**, 235.
- Frese, D., B. Ueberholz, S. Kuhr, W. Alt, D. Schrader, V. Gomer, and D. Meschede, 2000, “Single atoms in an optical dipole trap: Towards a deterministic source of cold atoms,” *Phys. Rev. Lett.* **85**, 3777.
- Frey, M. T., S. B. Hill, K. A. Smith, F. B. Dunning, and I. I. Fabrikant, 1995, “Studies of electron-molecule scattering at microelectronvolt energies using very-high- n Rydberg atoms,” *Phys. Rev. Lett.* **75**, 810.
- Frey, M. T., X. Ling, B. G. Lindsay, K. A. Smith, and F. B. Dunning, 1993, “Use of the Stark effect to minimize residual electric fields in an experimental volume,” *Rev. Sci. Instrum.* **64**, 3649.
- Friedenauer, A., H. Schmitz, J. T. Glueckert, D. Porras, and T. Schaetz, 2008, “Simulating a quantum magnet with trapped ions,” *Nat. Phys.* **4**, 757.
- Friedler, I., D. Petrosyan, M. Fleischhauer, and G. Kurizki, 2005, “Long-range interactions and entanglement of slow single-photon pulses,” *Phys. Rev. A* **72**, 043803.
- Gaëtan, A., C. Evellin, J. Wolters, P. Grangier, T. Wilk, and A. Browaeys, 2010, “Analysis of the entanglement between two individual atoms using global Raman rotations,” *New J. Phys.* **12**, 065040.
- Gaëtan, A., Y. Miroshnychenko, T. Wilk, A. Chotia, M. Viteau, D. Comparat, P. Pillet, A. Browaeys, and P. Grangier, 2009, “Observation of collective excitation of two individual atoms in the Rydberg blockade regime,” *Nat. Phys.* **5**, 115.

- Gallagher, T. F., 1994, *Rydberg Atoms* (Cambridge University Press, Cambridge).
- Gallagher, T. F., and P. Pillet, 2008, “Dipole-dipole interactions of Rydberg atoms,” *Adv. At., Mol., Opt. Phys.* **56**, 161.
- Gallagher, T. F., P. Pillet, M. P. Robinson, B. Laburthe-Tolra, and M. W. Noel, 2003, “Back and forth between Rydberg atoms and ultracold plasmas,” *J. Opt. Soc. Am. B* **20**, 1091.
- Gallagher, T. F., K. A. Safinya, F. Gounand, J. F. Delpech, W. Sandner, and R. Kachru, 1982, “Resonant Rydberg-atom–Rydberg-atom collisions,” *Phys. Rev. A* **25**, 1905.
- García-Ripoll, J. J., P. Zoller, and J. I. Cirac, 2003, “Speed optimized two-qubit gates with laser coherent control techniques for ion trap quantum computing,” *Phys. Rev. Lett.* **91**, 157901.
- Gerritsma, R., S. Whitlock, T. Fernholz, H. Schlatter, J. A. Luigjes, J.-U. Thiele, J. B. Goedkoop, and R. J. C. Spreeuw, 2007, “Lattice of microtraps for ultracold atoms based on patterned magnetic films,” *Phys. Rev. A* **76**, 033408.
- Gillet, J., G. S. Agarwal, and T. Bastin, 2010, “Tunable entanglement, antibunching, and saturation effects in dipole blockade,” *Phys. Rev. A* **81**, 013837.
- Gorshkov, A. V., T. Calarco, M. D. Lukin, and A. S. Sørensen, 2008, “Photon storage in Lambda-type optically dense atomic media: IV. Optimal control using gradient ascent,” *Phys. Rev. A* **77**, 043806.
- Gorshkov, A. V., L. Jiang, M. Greiner, P. Zoller, and M. D. Lukin, 2008, “Coherent quantum optical control with sub-wavelength resolution,” *Phys. Rev. Lett.* **100**, 093005.
- Gounand, F., 1979, “Calculation of radial matrix elements and radiative lifetimes for highly excited states of alkali atoms using the Coulomb approximation,” *J. Phys. (France)* **40**, 457.
- Grabowski, A., R. Heidemann, R. Löw, J. Stuhler, and T. Pfau, 2006, “High resolution Rydberg spectroscopy of ultracold rubidium atoms,” *Fortschr. Phys.* **54**, 765.
- Grabowski, A., and T. Pfau, 2003, “A lattice of magneto-optical and magnetic traps for cold atoms,” *Eur. Phys. J. D* **22**, 347.
- Grimm, R., M. Weidemüller, and Y. B. Ovchinnikov, 2000, “Optical dipole traps for neutral atoms,” *Adv. At., Mol., Opt. Phys.* **42**, 95.
- Grover, L. K., 1997, “Quantum mechanics helps in searching for a needle in a haystack,” *Phys. Rev. Lett.* **79**, 325.
- Guerlin, C., J. Bernu, S. Deléglise, C. Sayrin, S. Gleyzes, S. Kuhr, M. Brune, J.-M. Raimond, and S. Haroche, 2007, “Progressive field-state collapse and quantum nondemolition photon counting,” *Nature (London)* **448**, 889.
- Hagley, E., X. Maître, G. Nogues, C. Wunderlich, M. Brune, J. M. Raimond, and S. Haroche, 1997, “Generation of Einstein-Podolsky-Rosen pairs of atoms,” *Phys. Rev. Lett.* **79**, 1.
- Hammerer, K., A. S. Sørensen, and E. S. Polzik, 2010, “Quantum interface between light and atomic ensembles,” *Rev. Mod. Phys.* **82**, 1041.
- Han, J., and T. F. Gallagher, 2009, “Millimeter-wave rubidium Rydberg van der Waals spectroscopy,” *Phys. Rev. A* **79**, 053409.
- Heidemann, R., U. Raitzsch, V. Bendkowsky, B. Butscher, R. Löw, and T. Pfau, 2008, “Rydberg excitation of Bose-Einstein condensates,” *Phys. Rev. Lett.* **100**, 033601.
- Heidemann, R., U. Raitzsch, V. Bendkowsky, B. Butscher, R. Löw, L. Santos, and T. Pfau, 2007, “Evidence for coherent collective Rydberg excitation in the strong blockade regime,” *Phys. Rev. Lett.* **99**, 163601.
- Hernández, J. V., and F. Robicheaux, 2006, “Coherence conditions for groups of Rydberg atoms,” *J. Phys. B* **39**, 4883.
- Hernández, J. V., and F. Robicheaux, 2008a, “Simulation of a strong van der Waals blockade in a dense ultracold gas,” *J. Phys. B* **41**, 045301.
- Hernández, J. V., and F. Robicheaux, 2008b, “Simulations using echo sequences to observe coherence in a cold Rydberg gas,” *J. Phys. B* **41**, 195301.
- Hezel, B., I. Lesanovsky, and P. Schmelcher, 2007, “Ultracold Rydberg atoms in a Ioffe-Pritchard trap,” *Phys. Rev. A* **76**, 053417.
- Hinds, E. A., and I. G. Hughes, 1999, “Magnetic atom optics: Mirrors, guides, traps, and chips for atoms,” *J. Phys. D* **32**, R119.
- Hogan, S. D., and F. Merkt, 2008, “Demonstration of three-dimensional electrostatic trapping of state-selected Rydberg atoms,” *Phys. Rev. Lett.* **100**, 043001.
- Hu, Z., and H. J. Kimble, 1994, “Observation of a single atom in a magneto-optical trap,” *Opt. Lett.* **19**, 1888.
- Hyafil, P., J. Mozley, A. Perrin, J. Tailleur, G. Nogues, M. Brune, J. M. Raimond, and S. Haroche, 2004, “Coherence-preserving trap architecture for long-term control of giant Rydberg atoms,” *Phys. Rev. Lett.* **93**, 103001.
- Imamoglu, A., 2002, “High efficiency photon counting using stored light,” *Phys. Rev. Lett.* **89**, 163602.
- Isenhower, L., E. Urban, X. L. Zhang, A. T. Gill, T. Henage, T. A. Johnson, T. G. Walker, and M. Saffman, 2010, “Demonstration of a neutral atom controlled-NOT quantum gate,” *Phys. Rev. Lett.* **104**, 010503.
- Isenhower, L., W. Williams, A. Dally, and M. Saffman, 2009, “Atom trapping in an interferometrically generated bottle beam trap,” *Opt. Lett.* **34**, 1159.
- Jaksch, D., H.-J. Briegel, J. I. Cirac, C. W. Gardiner, and P. Zoller, 1999, “Entanglement of atoms via cold controlled collisions,” *Phys. Rev. Lett.* **82**, 1975.
- Jaksch, D., J. I. Cirac, P. Zoller, S. L. Rolston, R. Côté, and M. D. Lukin, 2000, “Fast quantum gates for neutral atoms,” *Phys. Rev. Lett.* **85**, 2208.
- James, D. F. V., and P. G. Kwiat, 2002, “Atomic-vapor-based high efficiency optical detectors with photon number resolution,” *Phys. Rev. Lett.* **89**, 183601.
- Jessen, P. S., and I. H. Deutsch, 1996, “Optical lattices,” *Adv. At., Mol., Opt. Phys.* **37**, 95.
- Jiang, L., J. M. Taylor, A. S. Sørensen, and M. D. Lukin, 2007, “Distributed quantum computation based on small quantum registers,” *Phys. Rev. A* **76**, 062323.
- Johnson, T. A., E. Urban, T. Henage, L. Isenhower, D. D. Yavuz, T. G. Walker, and M. Saffman, 2008, “Rabi oscillations between ground and Rydberg states with dipole-dipole atomic interactions,” *Phys. Rev. Lett.* **100**, 113003.
- Jones, M. P. A., J. Beugnon, A. Gaëtan, J. Zhang, G. Messin, A. Browaeys, and P. Grangier, 2007, “Fast quantum state control of a single trapped neutral atom,” *Phys. Rev. A* **75**, 040301R.
- Julsgaard, B., J. Sherson, J. I. Cirac, J. Fiurášek, and E. S. Polzik, 2004, “Experimental demonstration of quantum memory for light,” *Nature (London)* **432**, 482.
- Kaplan, A., M. F. Andersen, and N. Davidson, 2002, “Suppression of inhomogeneous broadening in rf spectroscopy of optically trapped atoms,” *Phys. Rev. A* **66**, 045401.
- Karski, M., L. Förster, J. M. Choi, W. Alt, A. Widera, and D. Meschede, 2009, “Nearest-neighbor detection of atoms in a 1D optical lattice by fluorescence imaging,” *Phys. Rev. Lett.* **102**, 053001.

- Karski, M., L. Förster, J.-M. Choi, A. Steffen, W. Alt, D. Meschede, and A. Widera, 2009, “Quantum walk in position space with single optically trapped atoms,” *Science* **325**, 174.
- Kaulakys, B., 1995, “Consistent analytical approach for the quasiclassical radial dipole matrix elements,” *J. Phys. B* **28**, 4963.
- Killian, T. C., M. J. Lim, S. Kulin, R. Dumke, S. D. Bergeson, and S. L. Rolston, 2001, “Formation of Rydberg atoms in an expanding ultracold neutral plasma,” *Phys. Rev. Lett.* **86**, 3759.
- Kim, S., R. R. Mcleod, M. Saffman, and K. H. Wagner, 2008, “Doppler-free multiwavelength acousto-optic deflector for two-photon addressing arrays of Rb atoms in a quantum information processor,” *Appl. Opt.* **47**, 1816.
- Kimble, H. J., 2008, “The quantum internet,” *Nature (London)* **453**, 1023.
- Knill, E., 2005, “Quantum computing with realistically noisy devices,” *Nature (London)* **434**, 39.
- Knoernschild, C., C. Kim, F. P. Lu, and J. Kim, 2009, “Multiplexed broadband beam steering system utilizing high speed MEMS mirrors,” *Opt. Express* **17**, 7233.
- Kok, P., W. J. Munro, K. Nemoto, T. C. Ralph, J. P. Dowling, and G. J. Milburn, 2007, “Linear optical quantum computing with photonic qubits,” *Rev. Mod. Phys.* **79**, 135.
- Kübler, H., J. P. Shaffer, T. Baluktian, R. Löw, and T. Pfau, 2010, “Coherent excitation of Rydberg atoms in micrometre-sized atomic vapor cells,” *Nature Photon.* **4**, 112.
- Kuga, T., Y. Torii, N. Shiokawa, and T. Hirano, 1997, “Novel optical trap of atoms with a doughnut beam,” *Phys. Rev. Lett.* **78**, 4713.
- Kuhr, S., W. Alt, D. Schrader, I. Dotsenko, Y. Miroshnychenko, A. Rauschenbeutel, and D. Meschede, 2005, “Analysis of dephasing mechanisms in a standing-wave dipole trap,” *Phys. Rev. A* **72**, 023406.
- Kuhr, S., W. Alt, D. Schrader, I. Dotsenko, Y. Miroshnychenko, W. Rosenfeld, M. Khudaverdyan, V. Gomer, A. Rauschenbeutel, and D. Meschede, 2003, “Coherence properties and quantum state transportation in an optical conveyor belt,” *Phys. Rev. Lett.* **91**, 213002.
- Kulin, S., S. Aubin, S. Christe, B. Peker, S. L. Rolston, and L. A. Orozco, 2001, “A single hollow-beam optical trap for cold atoms,” *J. Opt. B: Quantum Semiclassical Opt.* **3**, 353.
- Lahaye, T., C. Menotti, L. Santos, M. Lewenstein, and T. Pfau, 2009, “The physics of dipolar bosonic quantum gases,” *Rep. Prog. Phys.* **72**, 126401.
- Langer, C., *et al.*, 2005, “Long-lived qubit memory using atomic ions,” *Phys. Rev. Lett.* **95**, 060502.
- Lee, S. A., J. Helmcke, J. L. Hall, and B. P. Stoicheff, 1978, “Doppler-free two-photon transitions to Rydberg levels: Convenient, useful, and precise reference wavelengths for dye lasers,” *Opt. Lett.* **3**, 141.
- Lengwenus, A., J. Kruse, M. Volk, W. Ertmer, and G. Birkl, 2006, “Coherent manipulation of atomic qubits in optical micropotentials,” *Appl. Phys. B: Lasers Opt.* **86**, 377.
- Lesanovsky, I., and P. Schmelcher, 2005, “Magnetic trapping of ultracold Rydberg atoms,” *Phys. Rev. Lett.* **95**, 053001.
- Li, W., P. J. Tanner, and T. F. Gallagher, 2005, “Dipole-dipole excitation and ionization in an ultracold gas of Rydberg atoms,” *Phys. Rev. Lett.* **94**, 173001.
- Li, W., P. J. Tanner, Y. Jamil, and T. F. Gallagher, 2006, “Ionization and plasma formation in high n cold Rydberg samples,” *Eur. Phys. J. D* **40**, 27.
- Li, X., Y. Wu, D. Steel, D. Gammon, T. H. Stievater, D. S. Katzer, D. Park, C. Piermarocchi, and L. J. Sham, 2003, “An all-optical quantum gate in a semiconductor quantum dot,” *Science* **301**, 809.
- Lin, G.-D., S.-L. Zhu, R. Islam, K. Kim, M.-S. Chang, S. Korenblit, C. Monroe, and L.-M. Duan, 2009, “Large-scale quantum computation in an anharmonic linear ion trap,” *EPL* **86**, 60004.
- Liu, C., Z. Dutton, C. H. Behroozi, and L. V. Hau, 2001, “Observation of coherent optical information storage in an atomic medium using halted light pulses,” *Nature (London)* **409**, 490.
- Löw, R., H. Weimer, U. Raitzsch, R. Heidemann, V. Bendkowsky, B. Butscher, H. P. Büchler, and T. Pfau, 2009, “Universal scaling in a strongly interacting Rydberg gas,” *Phys. Rev. A* **80**, 033422.
- Lu, M., S. H. Youn, and B. L. Lev, 2010, “Trapping ultracold dysprosium: A highly magnetic gas for dipolar physics,” *Phys. Rev. Lett.* **104**, 063001.
- Lugiato, L. A., 1984, in *Progress in Optics XXI*, edited by E. Wolf (Elsevier, New York), pp. 69–216.
- Lukin, M. D., M. Fleischhauer, R. Cote, L. M. Duan, D. Jaksch, J. I. Cirac, and P. Zoller, 2001, “Dipole blockade and quantum information processing in mesoscopic atomic ensembles,” *Phys. Rev. Lett.* **87**, 037901.
- Lukin, M. D., and P. R. Hemmer, 2000, “Quantum entanglement via optical control of atom-atom interactions,” *Phys. Rev. Lett.* **84**, 2818.
- Lundblad, N., J. M. Obrecht, I. B. Spielman, and J. V. Porto, 2009, “Field-sensitive addressing and control of field-insensitive neutral-atom qubits,” *Nat. Phys.* **5**, 575.
- Mandel, O., M. Greiner, A. Widera, T. Rom, T. W. Hänsch, and I. Bloch, 2003, “Controlled collisions for multiparticle entanglement of optically trapped atoms,” *Nature (London)* **425**, 937.
- Mandilara, A., V. M. Akulin, and P. Pillet, 2009, “Population dynamics in cold gases resulting from the long-range dipole-dipole interaction,” *J. Phys. B* **42**, 215301.
- Marinescu, M., H. R. Sadeghpour, and A. Dalgarno, 1994, “Dispersion coefficients for alkali-metal dimers,” *Phys. Rev. A* **49**, 982.
- Mayle, M., I. Lesanovsky, and P. Schmelcher, 2009a, “Exploiting the composite character of Rydberg atoms for cold-atom trapping,” *Phys. Rev. A* **79**, 041403R.
- Mayle, M., I. Lesanovsky, and P. Schmelcher, 2009b, “Magnetic trapping of ultracold Rydberg atoms in low angular momentum states,” *Phys. Rev. A* **80**, 053410.
- Mazets, I. E., and G. Kurizki, 2007, “Multiatom cooperative emission following single-photon absorption: Dicke-state dynamics,” *J. Phys. B* **40**, F105.
- McClelland, J. J., and J. L. Hanssen, 2006, “Laser cooling without repumping: A magneto-optical trap for erbium atoms,” *Phys. Rev. Lett.* **96**, 143005.
- Mei, F., M. Feng, Y.-F. Yu, and Z.-M. Zhang, 2009, “Scalable quantum information processing with atomic ensembles and flying photons,” *Phys. Rev. A* **80**, 042319.
- Metcalf, H. J., and P. van der Straten, 1999, *Laser Cooling and Trapping* (Springer-Verlag, New York).
- Miller, J. D., R. A. Cline, and D. J. Heinzen, 1993, “Far-off-resonance optical trapping of atoms,” *Phys. Rev. A* **47**, R4567.
- Minns, R. S., M. R. Kutteruf, H. Zaidi, L. Ko, and R. R. Jones, 2006, “Preserving coherence in Rydberg quantum bits,” *Phys. Rev. Lett.* **97**, 040504.

- Mohapatra, A. K., M. G. Bason, B. Butscher, K. J. Weatherill, and C. S. Adams, 2008, “A giant electro-optic effect using polarizable dark states,” *Nat. Phys.* **4**, 890.
- Mohapatra, A. K., T. R. Jackson, and C. S. Adams, 2007, “Coherent optical detection of highly excited Rydberg states using electromagnetically induced transparency,” *Phys. Rev. Lett.* **98**, 113003.
- Møller, D., L. B. Madsen, and K. Mølmer, 2008, “Quantum gates and multiparticle entanglement by Rydberg excitation blockade and adiabatic passage,” *Phys. Rev. Lett.* **100**, 170504.
- Mølmer, K., 2009, unpublished.
- Mompert, J., K. Eckert, W. Ertmer, G. Birkl, and M. Lewenstein, 2003, “Quantum computing with spatially delocalized qubits,” *Phys. Rev. Lett.* **90**, 147901.
- Mourachko, I., D. Comparat, F. de Tomasi, A. Fioretti, P. Nosbaum, V. M. Akulin, and P. Pillet, 1998, “Many-body effects in a frozen Rydberg gas,” *Phys. Rev. Lett.* **80**, 253.
- Mozley, J., P. Hyafil, G. Nogues, M. Brune, J.-M. Raimond, and S. Haroche, 2005, “Trapping and coherent manipulation of a Rydberg atom on a microfabricated device: A proposal,” *Eur. Phys. J. D* **35**, 43.
- Mudrich, M., N. Zahzam, T. Vogt, D. Comparat, and P. Pillet, 2005, “Back and forth transfer and coherent coupling in a cold Rydberg dipole gas,” *Phys. Rev. Lett.* **95**, 233002.
- Mülken, O., A. Blumen, T. Amthor, C. Giese, M. Reetz-Lamour, and M. Weidemüller, 2007, “Survival probabilities in coherent exciton transfer with trapping,” *Phys. Rev. Lett.* **99**, 090601.
- Müller, M., I. Lesanovsky, H. Weimer, H. P. Büchler, and P. Zoller, 2009, “Mesoscopic Rydberg gate based on electromagnetically induced transparency,” *Phys. Rev. Lett.* **102**, 170502.
- Müller, M., L. Liang, I. Lesanovsky, and P. Zoller, 2008, “Trapped Rydberg ions: From spin chains to fast quantum gates,” *New J. Phys.* **10**, 093009.
- Nägerl, H. C., D. Leibfried, H. Rohde, G. Thalhammer, J. Eschner, F. Schmidt-Kaler, and R. Blatt, 1999, “Laser addressing of individual ions in a linear ion trap,” *Phys. Rev. A* **60**, 145.
- Nascimento, V. A., L. L. Caliri, A. Schwettmann, J. P. Shaffer, and L. G. Marcassa, 2009, “Electric field effects in the excitation of cold Rydberg-atom pairs,” *Phys. Rev. Lett.* **102**, 213201.
- Nelson, K. D., X. Li, and D. S. Weiss, 2007, “Imaging single atoms in a three-dimensional array,” *Nat. Phys.* **3**, 556.
- Neukammer, J., H. Rinneberg, K. Vietzke, A. König, H. Hieronymus, M. Kohl, H. J. Grabka, and G. Wunner, 1987, “Spectroscopy of Rydberg atoms at $n \approx 500$: Observation of quasi-Landau resonances in low magnetic fields,” *Phys. Rev. Lett.* **59**, 2947.
- Nielsen, A. E. B., and K. Mølmer, 2010, “Deterministic multimode photonic device for quantum-information processing,” *Phys. Rev. A* **81**, 043822.
- Nielsen, M. A., and I. L. Chuang, 2000, *Quantum Computation and Quantum Information* (Cambridge University Press, Cambridge).
- Nunn, J., K. Reim, K. C. Lee, V. O. Lorenz, B. J. Sussman, I. A. Walmsley, and D. Jaksch, 2008, “Multimode memories in atomic ensembles,” *Phys. Rev. Lett.* **101**, 260502.
- Ohlsson, N., R. K. Mohan, and S. Kröll, 2002, “Quantum computer hardware based on rare-earth-ion-doped inorganic crystals,” *Opt. Commun.* **201**, 71.
- Olmos, B., R. González-Férez, and I. Lesanovsky, 2009a, “Collective Rydberg excitations of an atomic gas confined in a ring lattice,” *Phys. Rev. A* **79**, 043419.
- Olmos, B., R. González-Férez, and I. Lesanovsky, 2009b, “Fermionic collective excitations in a lattice gas of Rydberg atoms,” *Phys. Rev. Lett.* **103**, 185302.
- Olmos, B., R. González-Férez, and I. Lesanovsky, 2010, “Creating collective many-body states with highly excited atoms,” *Phys. Rev. A* **81**, 023604.
- Olmos, B., M. Müller, and I. Lesanovsky, 2010, “Thermalization of a strongly interacting 1D Rydberg lattice gas,” *New J. Phys.* **12**, 013024.
- Osterwalder, A., and F. Merkt, 1999, “Using high Rydberg states as electric field sensors,” *Phys. Rev. Lett.* **82**, 1831.
- Overstreet, K. R., A. Schwettmann, J. Tallant, D. Booth, and J. P. Shaffer, 2009, “Observation of Cs Rydberg atom macrorodimers,” *Nat. Phys.* **5**, 581.
- Ozeri, R., L. Khaykovich, and N. Davidson, 1999, “Long spin relaxation times in a single-beam blue-detuned optical trap,” *Phys. Rev. A* **59**, R1750; **65**, 069903(E) (2002).
- Pedersen, L. H., and K. Mølmer, 2009, “Few qubit atom-light interfaces with collective encoding,” *Phys. Rev. A* **79**, 012320.
- Peik, E., 1999, “Electrodynamic trap for neutral atoms,” *Eur. Phys. J. D* **6**, 179.
- Peil, S., J. V. Porto, B. L. Tolra, J. M. Obrecht, B. E. King, M. Subbotin, S. L. Rolston, and W. D. Phillips, 2003, “Patterned loading of a Bose-Einstein condensate into an optical lattice,” *Phys. Rev. A* **67**, 051603R.
- Pellizzari, T., S. A. Gardiner, J. I. Cirac, and P. Zoller, 1995, “Decoherence, continuous observation, and quantum computing: A cavity QED model,” *Phys. Rev. Lett.* **75**, 3788.
- Perets, H. B., Y. Lahini, F. Pozzi, M. Sorel, R. Morandotti, and Y. Silberberg, 2008, “Realization of quantum walks with negligible decoherence in waveguide lattices,” *Phys. Rev. Lett.* **100**, 170506.
- Petrosyan, D., G. Bensky, G. Kurizki, I. Mazets, J. Majer, and J. Schmiedmayer, 2009, “Reversible state transfer between superconducting qubits and atomic ensembles,” *Phys. Rev. A* **79**, 040304R.
- Petrosyan, D., and M. Fleischhauer, 2008, “Quantum information processing with single photons and atomic ensembles in microwave coplanar waveguide resonators,” *Phys. Rev. Lett.* **100**, 170501.
- Petrus, J. A., P. Bohlouli-Zanjani, and J. D. D. Martin, 2008, “ac electric-field-induced resonant energy transfer between cold Rydberg atoms,” *J. Phys. B* **41**, 245001.
- Petta, J., A. Johnson, J. Taylor, E. Laird, A. Yacoby, M. Lukin, C. Marcus, M. P. Hanson, and A. Gossard, 2005, “Coherent manipulation of coupled electron spins in semiconductor quantum dots,” *Science* **309**, 2180.
- Pohl, T., and P. R. Berman, 2009, “Breaking the dipole blockade: Nearly resonant dipole interactions in few-atom systems,” *Phys. Rev. Lett.* **102**, 013004.
- Pohl, T., E. Demler, and M. D. Lukin, 2010, “Dynamical crystallization in the dipole blockade of ultracold atoms,” *Phys. Rev. Lett.* **104**, 043002.
- Porras, D., and J. I. Cirac, 2007, “Quantum engineering of photon states with entangled atomic ensembles,” e-print [arXiv:0704.0641](https://arxiv.org/abs/0704.0641).
- Porras, D., and J. I. Cirac, 2008, “Collective generation of quantum states of light by entangled atoms,” *Phys. Rev. A* **78**, 053816.
- Potvliege, R. M., and C. S. Adams, 2006, “Photo-ionization in

- far-off-resonance optical lattices,” *New J. Phys.* **8**, 163.
- Poulsen, U. V., and K. Mølmer, 2010, unpublished.
- Preskill, J., 1998, in *Introduction to Quantum Computation*, edited by H. Lo, S. Popescu, and T. Spiller (World Scientific, Singapore), pp. 213–269.
- Pritchard, J. D., A. Gauguier, K. J. Weatherill, M. P. A. Jones, and C. S. Adams, 2009, “Cooperative optical nonlinearity due to dipolar interactions in an ultracold Rydberg ensemble,” e-print [arXiv:0911.3523](https://arxiv.org/abs/0911.3523).
- Protsenko, I. E., G. Reymond, N. Schlosser, and P. Grangier, 2002, “Operation of a quantum phase gate using neutral atoms in microscopic dipole traps,” *Phys. Rev. A* **65**, 052301.
- Pupillo, G., A. Micheli, M. Boninsegni, I. Lesanovsky, and P. Zoller, 2009, “Mesoscopic phases of dipolar ensembles with polar molecules and Rydberg atoms,” e-print [arXiv:0904.2735](https://arxiv.org/abs/0904.2735).
- Pupillo, G., A. Micheli, M. Boninsegni, I. Lesanovsky, and P. Zoller, 2010, “Strongly correlated gases of Rydberg-dressed atoms: Quantum and classical dynamics,” *Phys. Rev. Lett.* **104**, 223002.
- Qian, J., Y. Qian, M. Ke, X.-L. Feng, C. H. Oh, and Y. Wang, 2009, “Breakdown of the dipole blockade with a zero-area phase-jump pulse,” *Phys. Rev. A* **80**, 053413.
- Rabl, P., A. J. Daley, P. O. Fedichev, J. I. Cirac, and P. Zoller, 2003, “Defect-suppressed atomic crystals in an optical lattice,” *Phys. Rev. Lett.* **91**, 110403.
- Rabl, P., and P. Zoller, 2007, “Molecular dipolar crystals as high-fidelity quantum memory for hybrid quantum computing,” *Phys. Rev. A* **76**, 042308.
- Raimond, J. M., M. Brune, and S. Haroche, 2001, “Manipulating quantum entanglement with atoms and photons in a cavity,” *Rev. Mod. Phys.* **73**, 565.
- Raimond, J. M., G. Vitrant, and S. Haroche, 1981, “Spectral line broadening due to the interaction between very excited atoms: The dense Rydberg gas,” *J. Phys. B* **14**, L655.
- Raitzsch, U., V. Bendkowsky, R. Heidemann, B. Butscher, R. Löw, and T. Pfau, 2008, “Echo experiments in a strongly interacting Rydberg gas,” *Phys. Rev. Lett.* **100**, 013002.
- Raitzsch, U., R. Heidemann, H. Weimer, B. Butscher, P. Kollmann, R. Löw, H. P. Büchler, and T. Pfau, 2009, “Investigation of dephasing rates in an interacting Rydberg gas,” *New J. Phys.* **11**, 055014.
- Rauschenbeutel, A., G. Nogues, S. Osnaghi, P. Bertet, M. Brune, J. M. Raimond, and S. Haroche, 1999, “Coherent operation of a tunable quantum phase gate in cavity QED,” *Phys. Rev. Lett.* **83**, 5166.
- Raussendorf, R., and H. J. Briegel, 2001, “A one-way quantum computer,” *Phys. Rev. Lett.* **86**, 5188.
- Raussendorf, R., D. E. Browne, and H. J. Briegel, 2003, “Measurement-based quantum computation on cluster states,” *Phys. Rev. A* **68**, 022312.
- Reetz-Lamour, M., T. Amthor, J. Deiglmayr, and M. Weidemüller, 2008, “Rabi oscillations and excitation trapping in the coherent excitation of a mesoscopic frozen Rydberg gas,” *Phys. Rev. Lett.* **100**, 253001.
- Reetz-Lamour, M., J. Deiglmayr, T. Amthor, and M. Weidemüller, 2008, “Rabi oscillations between ground and Rydberg states and van der Waals blockade in a mesoscopic frozen Rydberg gas,” *New J. Phys.* **10**, 045026.
- Reinhard, A., T. C. Liebisch, B. Knuffman, and G. Raithel, 2007, “Level shifts of rubidium Rydberg states due to binary interactions,” *Phys. Rev. A* **75**, 032712.
- Reinhard, A., K. C. Younge, T. C. Liebisch, B. Knuffman, P. R. Berman, and G. Raithel, 2008, “Double-resonance spectroscopy of interacting Rydberg-atom systems,” *Phys. Rev. Lett.* **100**, 233201.
- Reinhard, A., K. C. Younge, and G. Raithel, 2008, “Effect of Förster resonances on the excitation statistics of many-body Rydberg systems,” *Phys. Rev. A* **78**, 060702R.
- Remacle, F., E. W. Schlag, H. Selzle, K. L. Kompa, U. Even, and R. D. Levine, 2001, “Logic gates using high Rydberg states,” *Proc. Natl. Acad. Sci. U.S.A.* **98**, 2973.
- Reynaud, S., M. Himbert, J. Dalibard, J. Dupont-Roc, and C. Cohen-Tannoudji, 1982, “Compensation of Doppler broadening by light shifts in two photon absorption,” *Opt. Commun.* **42**, 39.
- Robicheaux, F., and J. V. Hernández, 2005, “Many-body wave function in a dipole blockade configuration,” *Phys. Rev. A* **72**, 063403.
- Roos, I., and K. Mølmer, 2004, “Quantum computing with an inhomogeneously broadened ensemble of ions: Suppression of errors from detuning variations by specially adapted pulses and coherent population trapping,” *Phys. Rev. A* **69**, 022321.
- Rosenband, T., *et al.*, 2008, “Frequency ratio of Al^+ and Hg^+ single-ion optical clocks; Metrology at the 17th decimal place,” *Science* **319**, 1808.
- Ryabtsev, I. I., D. B. Tretyakov, and I. I. Beterov, 2003, “Stark-switching technique for fast quantum gates in Rydberg atoms,” *J. Phys. B* **36**, 297.
- Ryabtsev, I. I., D. B. Tretyakov, and I. I. Beterov, 2005, “Applicability of Rydberg atoms to quantum computers,” *J. Phys. B* **38**, S421.
- Ryabtsev, I. I., D. B. Tretyakov, I. I. Beterov, and V. M. Entin, 2007, “Effect of finite detection efficiency on the observation of the dipole-dipole interaction of a few Rydberg atoms,” *Phys. Rev. A* **76**, 012722; **76**, 049902(E) (2007).
- Ryabtsev, I. I., D. B. Tretyakov, I. I. Beterov, and V. M. Entin, 2010, “Observation of the Stark-tuned Förster resonance between two Rydberg atoms,” *Phys. Rev. Lett.* **104**, 073003.
- Saffman, M., 2004, “Addressing atoms in optical lattices with Bessel beams,” *Opt. Lett.* **29**, 1016.
- Saffman, M., and L. Isenhower, 2009, unpublished.
- Saffman, M., and K. Mølmer, 2008, “Scaling the neutral-atom Rydberg gate quantum computer by collective encoding in holmium atoms,” *Phys. Rev. A* **78**, 012336.
- Saffman, M., and K. Mølmer, 2009, “Efficient multiparticle entanglement via asymmetric Rydberg blockade,” *Phys. Rev. Lett.* **102**, 240502.
- Saffman, M., and T. G. Walker, 2002, “Creating single-atom and single-photon sources from entangled atomic ensembles,” *Phys. Rev. A* **66**, 065403.
- Saffman, M., and T. G. Walker, 2005a, “Analysis of a quantum logic device based on dipole-dipole interactions of optically trapped Rydberg atoms,” *Phys. Rev. A* **72**, 022347.
- Saffman, M., and T. G. Walker, 2005b, “Entangling single- and N-atom qubits for fast quantum state detection and transmission,” *Phys. Rev. A* **72**, 042302.
- Saffman, M., F. W. Wilhelm, and R. F. McDermott, 2009, “Quantum gates between superconducting and atomic qubits,” *Bull. Am. Phys. Soc.* **54**, E1.103.
- Safinya, K. A., J. F. Delpuch, F. Gounand, W. Sandner, and T. F. Gallagher, 1981, “Resonant Rydberg-atom-Rydberg-atom collisions,” *Phys. Rev. Lett.* **47**, 405.
- Safronova, M. S., C. J. Williams, and C. W. Clark, 2003, “Optimizing the fast Rydberg quantum gate,” *Phys. Rev. A* **67**, 040303(R).

- Scheunemann, R., F. S. Cataliotti, T. W. Hänsch, and M. Weitz, 2000, "Laser cooling in a CO₂-laser optical lattice," *Phys. Rev. A* **62**, 051801(R).
- Schlosser, N., G. Reymond, I. Protchenko, and P. Grangier, 2001, "Sub-Poissonian loading of single atoms in a microscopic dipole trap," *Nature (London)* **411**, 1024.
- Schmidt, U., I. Lesanovsky, and P. Schmelcher, 2007, "Ultracold Rydberg atoms in a magnetoelectric trap," *J. Phys. B* **40**, 1003.
- Schmidt-Kaler, F., H. Häffner, S. Gulde, M. Riebe, G. P. T. Lancaster, T. Deuschle, C. Becher, W. Hänsel, J. Eschner, C. F. Roos, and R. Blatt, 2003, "How to realize a universal quantum gate with trapped ions," *Appl. Phys. B: Lasers Opt.* **77**, 789.
- Schmitz, H., R. Matjeschk, C. Schneider, J. Glueckert, M. Enderlein, T. Huber, and T. Schaetz, 2009, "Quantum walk of a trapped ion in phase space," *Phys. Rev. Lett.* **103**, 090504.
- Schrader, D., I. Dotsenko, M. Khudaverdyan, Y. Miroshnychenko, A. Rauschenbeutel, and D. Meschede, 2004, "Neutral atom quantum register," *Phys. Rev. Lett.* **93**, 150501.
- Schwettmann, A., J. Crawford, K. R. Overstreet, and J. P. Shaffer, 2006, "Cold Cs Rydberg-gas interactions," *Phys. Rev. A* **74**, 020701R.
- Seaton, M. J., 1958, "The quantum defect method," *Mon. Not. R. Astron. Soc.* **118**, 504.
- Seidelin, S., *et al.*, 2006, "Microfabricated surface-electrode ion trap for scalable quantum information processing," *Phys. Rev. Lett.* **96**, 253003.
- Singer, K., M. Reetz-Lamour, T. Amthor, S. Fölling, M. Tschernerneck, and M. Weidemüller, 2005, "Spectroscopy of an ultracold Rydberg gas and signatures of Rydberg-Rydberg interactions," *J. Phys. B* **38**, S321.
- Singer, K., M. Reetz-Lamour, T. Amthor, L. G. Marcassa, and M. Weidemüller, 2004, "Suppression of excitation and spectral broadening induced by interactions in a cold gas of Rydberg atoms," *Phys. Rev. Lett.* **93**, 163001.
- Singer, K., J. Stanojevic, M. Weidemüller, and R. Cote, 2005, "Long-range interactions between alkali Rydberg atom pairs correlated to the ns - ns , np - np , and nd - nd asymptotes," *J. Phys. B* **38**, S295.
- Sørensen, A. S., and K. Mølmer, 2001, "Entanglement and extreme spin squeezing," *Phys. Rev. Lett.* **86**, 4431.
- Sørensen, A. S., C. H. van der Wal, L. I. Childress, and M. D. Lukin, 2004, "Capacitive coupling of atomic systems to mesoscopic conductors," *Phys. Rev. Lett.* **92**, 063601.
- Stanojevic, J., and R. Côté, 2009, "Many-body Rabi oscillations of Rydberg excitation in small mesoscopic samples," *Phys. Rev. A* **80**, 033418.
- Stanojevic, J., R. Côté, D. Tong, E. E. Eyler, and P. L. Gould, 2008, "Long-range potentials and $(n-1)d+ns$ molecular resonances in an ultracold Rydberg gas," *Phys. Rev. A* **78**, 052709.
- Stanojevic, J., R. Côté, D. Tong, S. Farooqi, E. E. Eyler, and P. Gould, 2006, "Long-range Rydberg-Rydberg interactions and molecular resonances," *Eur. Phys. J. D* **40**, 3.
- Stebbing, R. F., and F. B. Dunning, 1983, Eds., *Rydberg States of Atoms and Molecules* (Cambridge University Press, Cambridge).
- Sun, B., and F. Robicheaux, 2008, "Numerical study of two-body correlation in a 1D lattice with perfect blockade," *New J. Phys.* **10**, 045032.
- Takekoshi, T., and R. J. Knize, 1996, "CO₂ laser trap for cesium atoms," *Opt. Lett.* **21**, 77.
- Tannian, B. E., C. L. Stokely, F. B. Dunning, C. O. Reinhold, S. Yoshida, and J. Burgdörfer, 2000, "Kicked Rydberg atom: Response to trains of unidirectional and bidirectional impulses," *Phys. Rev. A* **62**, 043402.
- Tauschinsky, A., C. S. E. van Ditzhuijzen, L. D. Noordam, and H. B. van Linden van den Heuvell, 2008, "Radio-frequency-driven dipole-dipole interactions in spatially separated volumes," *Phys. Rev. A* **78**, 063409.
- Teo, B. K., D. Feldbaum, T. Cubel, J. R. Guest, P. R. Berman, and G. Raithel, 2003, "Autler-Townes spectroscopy of the $5S_{1/2}$ - $5P_{3/2}$ - $44D$ cascade of cold ⁸⁵Rb atoms," *Phys. Rev. A* **68**, 053407.
- Terraciano, M. L., M. Bashkansky, and F. K. Fatemi, 2008, "Faraday spectroscopy of atoms confined in a dark optical trap," *Phys. Rev. A* **77**, 063417.
- Tey, M. K., Z. Chen, S. A. Aljunid, B. Chng, F. Huber, G. Maslennikov, and C. Kurtsiefer, 2008, "Strong interaction between light and a single trapped atom without the need for a cavity," *Nat. Phys.* **4**, 924.
- Thoumany, P., T. Germann, T. Hänsch, G. Stania, L. Urbonas, and T. Becker, 2009, "Spectroscopy of rubidium Rydberg states with three diode lasers," *J. Mod. Opt.* **56**, 2055.
- Thoumany, P., T. Hänsch, G. Stania, L. Urbonas, and T. Becker, 2009, "Optical spectroscopy of rubidium Rydberg atoms with a 297 nm frequency-doubled dye laser," *Opt. Lett.* **34**, 1621.
- Tong, D., S. M. Farooqi, J. Stanojevic, S. Krishnan, Y. P. Zhang, R. Côté, E. E. Eyler, and P. L. Gould, 2004, "Observation of electric quadrupole transitions to Rydberg nd states of ultracold rubidium atoms," *Phys. Rev. Lett.* **93**, 063001.
- Tong, D., S. M. Farooqi, E. G. M. van Kempen, Z. Pavlovic, J. Stanojevic, R. Côté, E. E. Eyler, and P. L. Gould, 2009, "Local blockade of Rydberg excitation in an ultracold gas," *Phys. Rev. A* **79**, 052509.
- Tordrup, K., A. Negretti, and K. Mølmer, 2008, "Holographic quantum computing," *Phys. Rev. Lett.* **101**, 040501.
- Tóth, G., C. Knapp, O. Gühne, and H. J. Briegel, 2007, "Optimal spin squeezing inequalities detect bound entanglement in spin models," *Phys. Rev. Lett.* **99**, 250405.
- Treutlein, P., P. Hommelhoff, T. Steinmetz, T. W. Hänsch, and J. Reichel, 2004, "Coherence in microchip traps," *Phys. Rev. Lett.* **92**, 203005.
- Turchette, Q. A., C. S. Wood, B. E. King, C. J. Myatt, D. Leibfried, W. M. Itano, C. Monroe, and D. J. Wineland, 1998, "Deterministic entanglement of two trapped ions," *Phys. Rev. Lett.* **81**, 3631.
- Unanyan, R. G., and M. Fleischhauer, 2002, "Efficient and robust entanglement generation in a many-particle system with resonant dipole-dipole interactions," *Phys. Rev. A* **66**, 032109.
- Urban, E., T. Henage, L. Isenhower, T. Johnson, T. G. Walker, and M. Saffman, 2009, "ac Stark shifts in two-photon excitation of Rydberg levels," *Bull. Am. Phys. Soc.* **54**, T1.23.
- Urban, E., T. A. Johnson, T. Henage, L. Isenhower, D. D. Yavuz, T. G. Walker, and M. Saffman, 2009, "Observation of Rydberg blockade between two atoms," *Nat. Phys.* **5**, 110.
- Vaishnav, B., and D. S. Weiss, 2008, "Site-resolved Bragg scattering," *Opt. Lett.* **33**, 375.
- Vala, J., A. V. Thapliya, S. Myrgren, U. Vazirani, D. S. Weiss, and K. B. Whaley, 2005, "Perfect pattern formation of neutral atoms in an addressable optical lattice," *Phys. Rev. A* **71**, 032324.
- Vala, J., K. B. Whaley, and D. S. Weiss, 2005, "Quantum error correction of a qubit loss in an addressable atomic system," *Phys. Rev. A* **72**, 052318.

- van Ditzhuijzen, C. S. E., A. F. Koenderink, J. V. Hernández, F. Robicheaux, L. D. Noordam, and H. B. van Linden van den Heuvell, 2008, “Spatially resolved observation of dipole-dipole interaction between Rydberg atoms,” *Phys. Rev. Lett.* **100**, 243201.
- van Ditzhuijzen, C. S. E., A. Tauschinsky, and H. B. van Linden van den Heuvell, 2009, “Observation of Stückelberg oscillations in dipole-dipole interactions,” *Phys. Rev. A* **80**, 063407.
- van Enk, S. J., N. Lütkenhaus, and H. J. Kimble, 2007, “Experimental procedures for entanglement verification,” *Phys. Rev. A* **75**, 052318.
- Varada, G. V., and G. S. Agarwal, 1992, “Two-photon resonance induced by the dipole-dipole interaction,” *Phys. Rev. A* **45**, 6721.
- Verstraete, F., M. M. Wolf, and J. I. Cirac, 2009, “Quantum computation and quantum-state engineering driven by dissipation,” *Nat. Phys.* **5**, 633.
- Vogt, T., M. Viteau, A. Chotia, J. Zhao, D. Comparat, and P. Pillet, 2007, “Electric-field induced dipole blockade with Rydberg atoms,” *Phys. Rev. Lett.* **99**, 073002.
- Vogt, T., M. Viteau, J. Zhao, A. Chotia, D. Comparat, and P. Pillet, 2006, “Dipole blockade at Förster resonances in high resolution laser excitation of Rydberg states of cesium atoms,” *Phys. Rev. Lett.* **97**, 083003.
- Vuletic, V., 2006, “Quantum networks: When superatoms talk photons,” *Nat. Phys.* **2**, 801.
- Walker, T. G., and M. Saffman, 2005, “Zeros of Rydberg-Rydberg Förster interactions,” *J. Phys. B* **38**, S309.
- Walker, T. G., and M. Saffman, 2008, “Consequences of Zeeman degeneracy for the van der Waals blockade between Rydberg atoms,” *Phys. Rev. A* **77**, 032723.
- Walther, H., B. T. H. Varcoe, B.-G. Englert, and T. Becker, 2006, “Cavity quantum electrodynamics,” *Rep. Prog. Phys.* **69**, 1325.
- Wang, T., S. F. Yelin, R. Côté, E. E. Eyler, S. M. Farooqi, P. L. Gould, M. Kostrun, D. Tong, and D. Vranceanu, 2007, “Superradiance in ultracold Rydberg gases,” *Phys. Rev. A* **75**, 033802.
- Weatherill, K. J., J. D. Pritchard, R. P. Abel, A. K. Mohapatra, M. G. Bason, and C. S. Adams, 2008, “Electromagnetically induced transparency of an interacting cold Rydberg ensemble,” *J. Phys. B* **41**, 201002.
- Weimer, H., R. Löw, T. Pfau, and H. P. Büchler, 2008, “Quantum critical behavior in strongly interacting Rydberg gases,” *Phys. Rev. Lett.* **101**, 250601.
- Weimer, H., M. Müller, I. Lesanovsky, P. Zoller, and H. P. Büchler, 2010, “A Rydberg quantum simulator,” *Nat. Phys.* **6**, 382.
- Weinstein, J. D., and K. G. Libbrecht, 1995, “Microscopic magnetic traps for neutral atoms,” *Phys. Rev. A* **52**, 4004.
- Weiss, D. S., J. Vala, A. V. Thapliyal, S. Myrgren, U. Vazirani, and K. B. Whaley, 2004, “Another way to approach zero entropy for a finite system of atoms,” *Phys. Rev. A* **70**, 040302(R).
- Wesenberg, J. H., A. Ardavan, G. A. D. Briggs, J. J. L. Morton, R. J. Schoelkopf, D. I. Schuster, and K. Mølmer, 2009, “Quantum computing with an electron spin ensemble,” *Phys. Rev. Lett.* **103**, 070502.
- Wesenberg, J. H., K. Mølmer, L. Rippe, and S. Kröll, 2007, “Scalable designs for quantum computing with rare-earth-ion-doped crystals,” *Phys. Rev. A* **75**, 012304.
- Westermann, S., T. Amthor, A. L. de Oliveira, J. Deiglmayr, M. Reetz-Lamour, and M. Weidemüller, 2006, “Dynamics of resonant energy transfer in a cold Rydberg gas,” *Eur. Phys. J. D* **40**, 37.
- Wilk, T., A. Gaëtan, C. Evellin, J. Wolters, Y. Miroshnychenko, P. Grangier, and A. Browaeys, 2010, “Entanglement of two individual neutral atoms using Rydberg blockade,” *Phys. Rev. Lett.* **104**, 010502.
- Windpassinger, P. J., D. Oblak, U. B. Hoff, J. Appel, N. Kjaergaard, and E. S. Polzik, 2008, “Inhomogeneous light shift effects on atomic quantum state evolution in nondestructive measurements,” *New J. Phys.* **10**, 053032.
- Wineland, D. J., J. J. Bollinger, W. M. Itano, and D. J. Heinzen, 1994, “Squeezed atomic states and projection noise in spectroscopy,” *Phys. Rev. A* **50**, 67.
- Würtz, P., T. Langen, T. Gericke, A. Koglbauer, and H. Ott, 2009, “Experimental demonstration of single-site addressability in a two-dimensional optical lattice,” *Phys. Rev. Lett.* **103**, 080404.
- Wüster, S., J. Stanojevic, C. Ates, T. Pohl, P. Deuar, J. F. Corneey, and J. M. Rost, 2010, “Correlations of Rydberg excitations in an ultracold gas after an echo sequence,” *Phys. Rev. A* **81**, 023406.
- Xu, P., X. He, J. Wang, and M. Zhan, 2010, “Trapping a single atom in a blue detuned optical bottle beam trap,” *Opt. Lett.* **35**, 2164.
- Yavuz, D. D., P. B. Kulatunga, E. Urban, T. A. Johnson, N. Proite, T. Henage, T. G. Walker, and M. Saffman, 2006, “Fast ground state manipulation of neutral atoms in microscopic optical traps,” *Phys. Rev. Lett.* **96**, 063001.
- Yavuz, D. D., and N. A. Proite, 2007, “Nanoscale resolution fluorescence microscopy using electromagnetically induced transparency,” *Phys. Rev. A* **76**, 041802.
- You, L., and M. S. Chapman, 2000, “Quantum entanglement using trapped atomic spins,” *Phys. Rev. A* **62**, 052302.
- Younge, K. C., and G. Raithel, 2009, “Rotary echo tests of coherence in Rydberg-atom excitation,” *New J. Phys.* **11**, 043006.
- Younge, K. C., A. Reinhard, T. Pohl, P. R. Berman, and G. Raithel, 2009, “Mesoscopic Rydberg ensembles: Beyond the pairwise-interaction approximation,” *Phys. Rev. A* **79**, 043420.
- Zhang, C., S. L. Rolston, and S. D. Sarma, 2006, “Manipulation of single neutral atoms in optical lattices,” *Phys. Rev. A* **74**, 042316.
- Zhao, J., X. Zhu, L. Zhang, Z. Feng, C. Li, and S. Jia, 2009, “High sensitivity spectroscopy of cesium Rydberg atoms using electromagnetically induced transparency,” *Opt. Express* **17**, 15821.
- Zuo, Z., M. Fukusen, Y. Tamaki, T. Watanabe, Y. Nakagawa, and K. Nakagawa, 2009, “Single atom Rydberg excitation in a small dipole trap,” *Opt. Express* **17**, 22898.
- Zwierz, M., and P. Kok, 2009, “High-efficiency cluster-state generation with atomic ensembles via the dipole-blockade mechanism,” *Phys. Rev. A* **79**, 022304.